NEWPORT

Projects in Fiber Optics

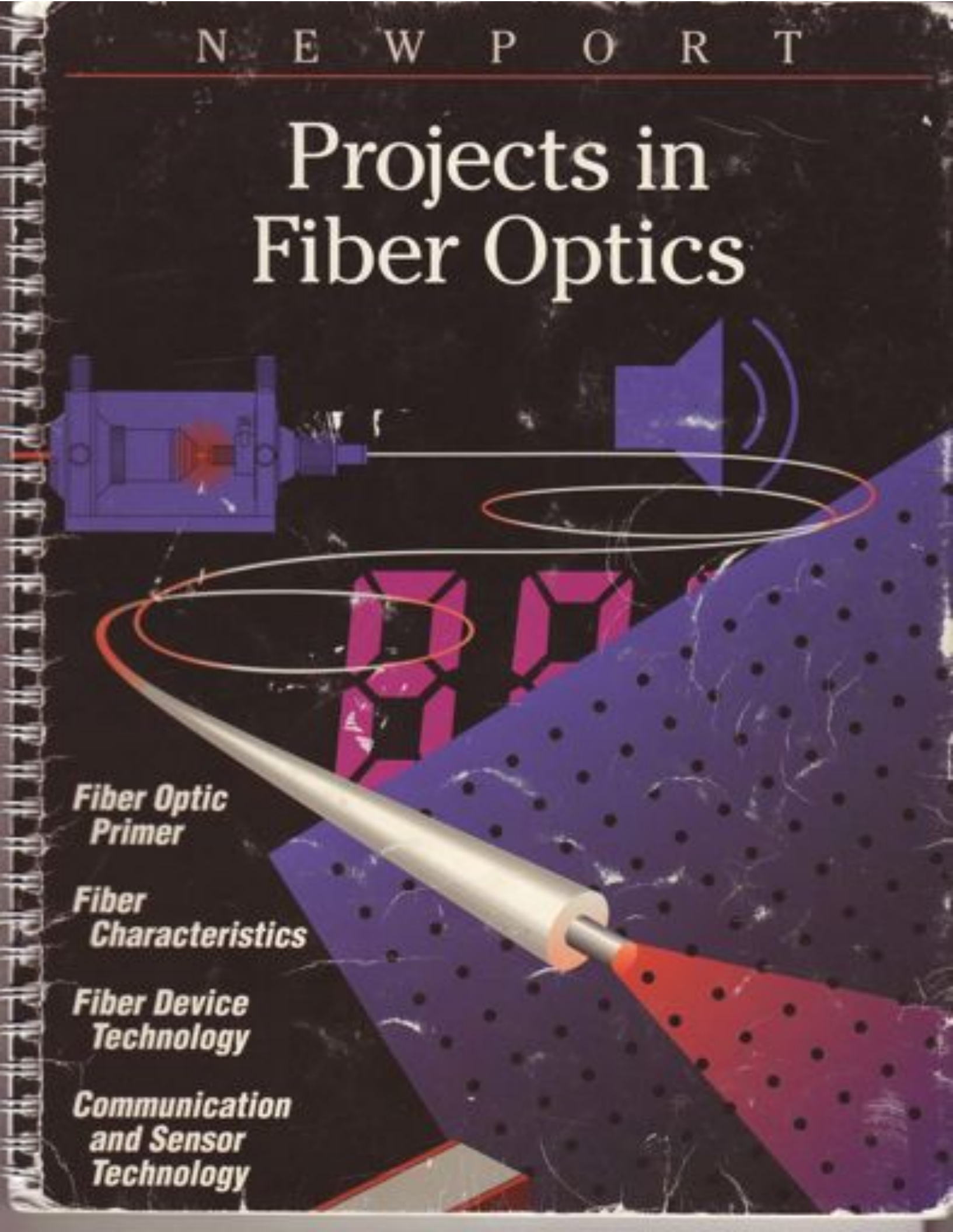

Fiber Optic Primer

Fiber Characteristics

Fiber Device Technology

Communication and Sensor Technology

PROJECTS IN FIBER OPTICS
Applications Handbook

Newport Corporation

18235 Mt. Baldy Circle, P.O. Box 8020, Fountain Valley, CA 92728-8020
Phone (714) 963-9811 Telex 685535

Project #8: Building a two-channel fiber optics communications link

Start with the basics, or explore today's most advanced applications with Newport's Projects in Fiber Optics

Model FKP-STD (see Equipment List on page 90) contains a complete set of research-quality equipment for performing ten educational, applications-oriented projects

By project completion, you will be able to use the same equipment with other compatible Newport components to explore new areas of interest. What better way to start a fiber optics lab?

TABLE OF CONTENTS

PROJECTS IN FIBER OPTICS

PREFACE

Projects in Fiber Optics (Newport Model "FKP") is a set of laboratory equipment containing the hardware needed to complete a series of projects which will provide students, engineers and scientists with an introduction to the hands-on experience needed to master the basic concepts and laboratory techniques of optical fiber technology. The projects cover a wide range of applications in both communications and sensors and cover the use of both multimode and single-mode fibers. Because this is a new and rapidly expanding technology, the education of most engineers does not include courses in fiber optics. **Projects in Fiber Optics** has been developed by the technical staff of Newport Corporation in order to bridge the gap between current college course offerings and today's rapidly expanding technology.

This companion applications handbook begins with a Primer in Fiber Optics which outlines, at an elementary level, the physics and optics background required to understand the field of fiber optics. The handbook then gives a complete description of each of the projects which are to be performed with the equipment in **Projects in Fiber Optics.** (A complete list of the projects is given in **Table I.**) At the end of the handbook is a list of references which may be considered for classroom use. This handbook will serve as a supplement to the material covered in a comprehensive classroom or independent study of fiber optics.

Each project description contains a statement of purpose outlining what is to be accomplished in that project, a section reviewing the related background and theory, suggested references, and a complete step-by-step instruction set which will guide the experimenter through the laboratory exercise. The material contained in each project description will allow the student to focus on "what's happening" in each laboratory exercise.

These projects can be used in structuring a course at either the sophomore or upper-division level for engineering or physical science students. A knowledge of ray optics from high-school physics or from a college freshman physics course (not requiring calculus) will be a sufficient background for a sophomore course using **Projects in Fiber Optics**. A simplified description of the propagation of modes at the level of the Primer in Fiber Optics may be used in Projects #3, #4, and #10.

For an upper-division course for engineering and physical science majors at a four-year school, the instructor may want to give a more complete theoretical development of the propagation of electromagnetic waves in optical fiber waveguides. The background for such a course might include a knowledge of Maxwell's equations, wave equations, propagation of electromagnetic waves in dielectric media, and an introduction to waveguides. However, the instructor may choose to include an introduction to some of this material in the fiber optics course itself.

TABLE I
LIST OF PROJECTS

1. Handling fibers, numerical aperture
2. Fiber attenuation
3. Single-mode fibers I
4. Single-mode fibers II
5. Coupling fibers to semiconductor sources
6. Connectors and splices
7. Components for fiber communication
8. Fiber optic communication link
9. Multimode intensity sensors
10. Single-mode interferometric sensors

Although many of the students in these courses will be electrical engineering or electronic technician students, the intent of the projects is to concentrate on the properties of the optical fibers and optical components being studied and to keep the amount of electrical equipment used and the amount of wiring done in the laboratory to a minimum. The problems of designing and building transmitters and receivers for optical fiber systems is best left to another course.

These **Projects in Fiber Optics** will provide a well-grounded introduction to fiber optic technology. The technical staff of Newport Corporation is available to provide technical advice in implementing these projects.

ACKNOWLEDGEMENTS

The technical staff of Newport Corporation would like to thank Dr. Donald C. O'Shea, School of Physics, Georgia Institute of Technology, for co-authoring the Primer in Fiber Optics. Thanks also to Dr. O'Shea and to Dr. Rick Feinberg, Department of Physics, Western Washington University, for their comments on the instruction sets in this manual.

PRIMER IN FIBER OPTICS

0.1 HISTORY OF FIBER OPTICS

The concept of optical communications goes far back into history. The sending of messages by light is certainly as old as the first signal fires or smoke signals, and has continued, in more recent history, in the use of signal lamps for communication between ships at sea. However, the first patents for an optical communications system were filed in 1880. At that time, Alexander Graham Bell obtained patents on the photophone and demonstrated communication on a beam of light at a distance of 200 meters. The photophone, shown in **Fig.0.1**, used a photosensitive selenium cell to detect variations in the intensity of a beam of light. However, all of these methods mentioned here depend on the atmosphere as the transmission medium, and anyone who has ever driven on a foggy day knows how unreliable that is.

A waveguide made of a non-conducting material which transmits light (a dielectric), such as glass or plastic, would provide a much more reliable transmission medium, because it is not subject to the variations of the atmosphere. The guiding of light by a dielectric medium is also not a new idea. In 1870, John Tyndall showed that light could be guided within a stream of water. Tyndall's experiment is illustrated in **Fig.0.2**. By 1910, Hondros and Debye had developed a theory of dielectric waveguides.

The breakthrough which has made the optical fiber waveguide the leading contender as the transmission medium of choice for current and future communications systems was triggered by two events. The first was the demonstration of the first operating laser in 1960. The second was a calculation, in 1966, by a pair of scientists, Charles Kao and George A. Hockham, speculating that optical fiber waveguides could compete with the existing coaxial cables used for communications if fibers could be made that would transmit 1% of the light in them over a distance of 1 kilometer (km). It is important to note that at that time the light energy which was transmitted would be down to 1% of its initial value after only 20 meters in the best existing fibers and that no materials expert was on record predicting that the required high-quality transmission could be achieved.

Many research groups began to actively pursue this possibility, however. In 1970, Corning Glass Works investigated high-silica glasses for fibers and was the first to report a transmission greater than 1% over a distance of 1 km. This group later increased the transmission to greater than 40% over 1 km. Today, transmissions in the range of 95-96% over 1 km are being achieved. For comparison, if ocean water had an optical transmission of ~ 79% through each km of depth, one could see to the bottom of the world's deepest oceans with the naked eye. The progress in high-transmission fibers is traced in **Fig.0.3**.

The achievement of low-loss transmission, along with the additional advantages of large information carrying capacity, immunity from electromagnetic interference, and small size and weight, has created a new technology. Optical

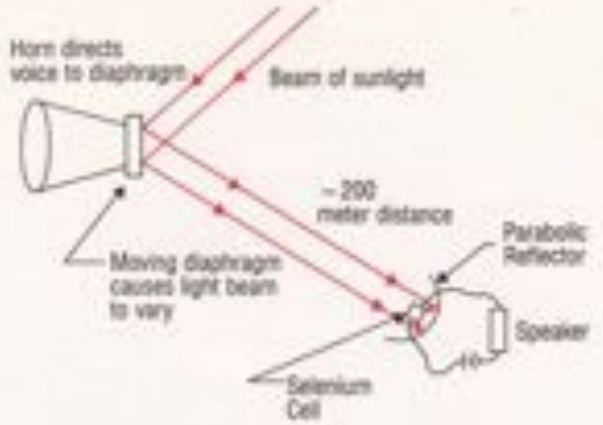

Figure 0.1. Schematic diagram of Alexander Graham Bell's photophone.

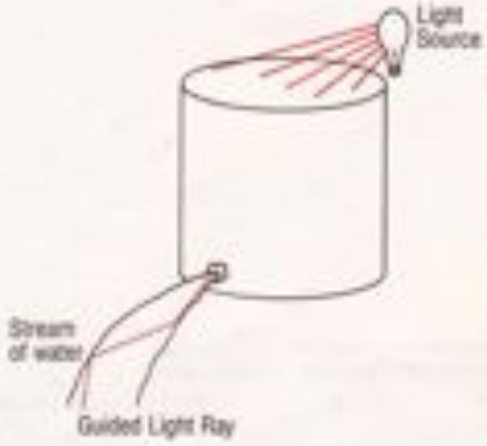

Figure 0.2. Tyndall's experiment showing that a stream of water will guide a beam of light.

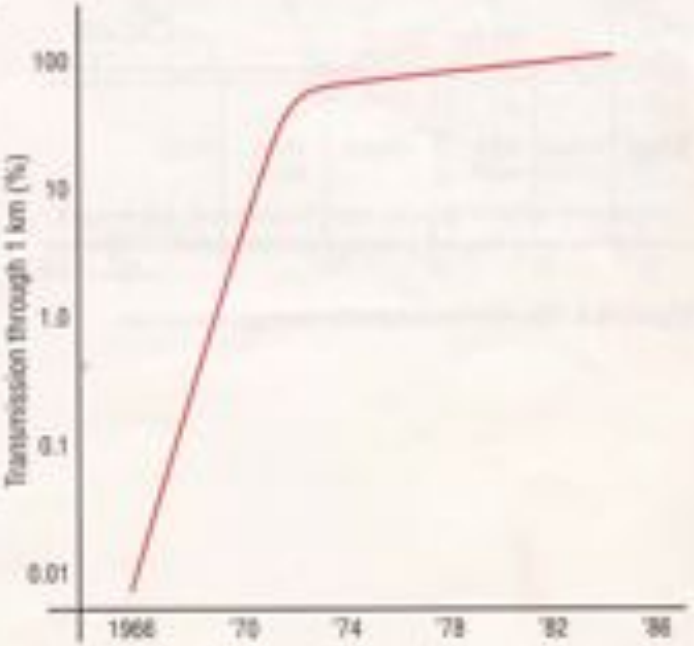

Figure 0.3. Progress in optical fiber transmission. The last two data points represent results near the theoretical limits at 0.85 and 1.55 μm.

fiber has become the medium of choice for communications applications. For example, the TAT-8 (Trans-Atlantic Telephone #8) system, scheduled for completion in 1988, will be a 6500-km all-fiber link which will bring trans-Atlantic telephone capacity to the equivalent of 20,000 voice channels. Compare this with TAT-1, completed in 1955, which carried 50 voice channels over coaxial cable. Also, Pacific Bell has announced plans to convert all of its cables to optical fiber. They plan to have all long-distance calls carried by fiber by 2005 and plan to have fully converted to an all-fiber system by 2025. Optical fiber is also being used extensively in Local Area Networks (LAN's), which are used for voice or data communications within or between buildings. Many new buildings are now being built with fiber installed in their framework for future LAN use.

Optical fiber is also used in sensor applications, where the high sensitivity, low loss, and electromagnetic interference immunity of the fibers can be exploited. Optical fibers are versatile and sensors can be designed to detect many physical parameters, such as temperature, pressure, strain, and electrical and magnetic fields, using either the power transmission properties of multimode fibers or the phase sensitive properties of single-mode fibers. Another application of optical fiber is beam delivery for medical uses. Lasers are now being investigated for use in surgery and diagnostics and optical fiber is being used to deliver beams to sites within the human body.

0.2 GEOMETRICAL OPTICS AND FIBER OPTICS

To understand what is occurring in these projects in fiber optics, it is necessary to understand some basic concepts of optics and physics. This section is intended to introduce these ideas for those who may not have studied the field and to review these ideas for those who have. The student-experimenter is urged to seek additional information in the references at the end of this handbook.

0.2.1 LIGHT AS AN ELECTROMAGNETIC FIELD

The light by which we see the world around us is a part of the range, or spectrum, of electromagnetic waves that extends from radio frequencies to high power gamma radiation. (**Fig. 0.4**) These waves, a combination of electric and magnetic fields, which can propagate through a vacuum, have as their most distinguishing features their wavelength and frequency of oscillation. The range of wavelengths for visible light is from about 400 nanometers (nm) to about 700 nm. (A nanometer is one billionth of a meter.) In most of the work done in the field of fiber optics, the most useful sources of electromagnetic radiation emit just outside the visible in the near infrared with wavelengths in the vicinity of 800 to 1500 nm.

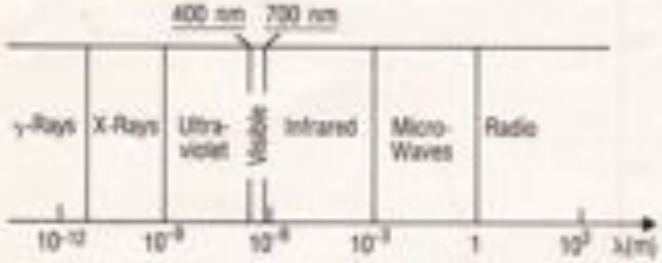

Figure 0.4. The electromagnetic energy spectrum.

It can be difficult to follow what happens in an optical fiber system if the progress of light through the system is depicted in terms of the wave motion of the light. For the simplest cases it is easier to think of light traveling as a series of rays propagating through space. The experience of seeing the sun's rays streaming through the clouds on a partially cloudy day provides a familiar example of light as a collection of rays.

In a vacuum, light travels at approximately 3×10^8 meters per second. In material media, such as air or water or glass, the speed is reduced. For air, the reduction is very small; for water, the reduction is about 25%; in glass, the reduction can vary from 30% to nearly 50%.

0.2.2 LIGHT IN MATERIALS

In most cases, the results of the interaction of an electromagnetic wave with a material medium can be expressed in terms of a single number, the index of refraction of the medium. The **refractive index** is the ratio of the speed of light in a vacuum, c, to the speed of light in the medium, v,

$$n = c/v \qquad (0\text{-}1)$$

Since the speed of light in a medium is always less than it is in a vacuum, the refractive index is always greater than one. In air, the value is very close to one; in water, it is about 4/3 (n = 1.33); in glasses, it varies from about 1.44 to about 1.9.

There are some qualifications to the simple picture presented here. First, the refractive index varies with the wavelength of the light. This is called **wavelength dispersion**, which will be discussed in **Project #8**. Second, not only can the medium slow down the light, but it can also absorb some of the light as it passes through.

In a homogeneous medium, that is, one in which the refractive index is constant in space, light travels in a straight line. Only when the light meets a variation or a discontinuity in the refractive index will the light rays be bent from their initial direction.

In the case of a variation in the refractive index within a material, the behavior of the light is governed by the way in which the index changes in space. For example, the air just above a road heated by the sun will be less dense than the air further from the road. Since the refractive index increases with density, the refractive index of the air increases with height. This is called a **refractive index gradient** and is, in this case, equivalent to having an extended prism above the road with its vertex pointing downwards (see **Fig.0.5**). Light coming from an object down the road will not only travel directly to the observer's eye, but some of the light from the

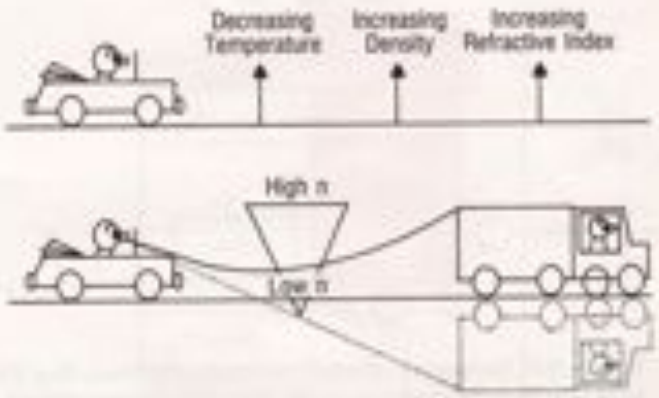

Figure 0.5. Bending of light rays by a refractive index gradient, using the mirage on a heated road as an example.

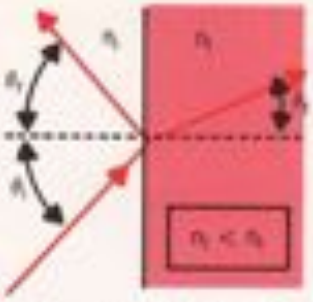

Figure 0.6. Geometry of reflection and refraction.

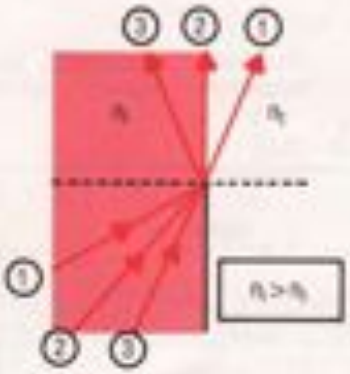

Figure 0.7. Geometry of total internal reflection. Ray #1 is at less than the critical angle. Ray #2 is at the critical angle. Ray #3 is totally internally reflected.

object that would normally be absorbed by the road is bent toward the observer. The result is that someone looking down the road will see a reflection, called a mirage, of a distant object on the road, as if it were reflected in a pool of water. This gradual bending of light by a refractive index gradient is used in fiber optics to increase the information carrying capacity of fibers and to provide a very compact lens for fiber optic systems.

If the change in refractive index is not gradual, as in the case of the refractive index gradient, but is, instead, an abrupt change like that between glass and air, the direction of light is governed by the Laws of Geometrical Optics. If the angle of incidence, θ_i, of a ray is angle between an incident ray and a line perpendicular to the interface at the point where the light ray strikes the interface (**Fig. 0.6**), then:

1. The angle of reflection, θ_r, also measured with respect to the same perpendicular, is equal to the angle of incidence:

$$\theta_r = \theta_i \qquad (0\text{-}2)$$

2. The angle of the transmitted light is given by the relation:

$$n_i \sin(\theta_i) = n_t \sin(\theta_t) \qquad (0\text{-}3)$$

The first of these relations is known as the **Law of Reflection**; the second as the **Law of Refraction** or **Snell's Law**.

It is useful to refer to a material whose refractive index is greater than another as being optically denser and one whose refractive index is less as being rarer. Thus, light travelling into an optically denser medium would be bent toward the normal, while light entering an optically rarer medium would be bent away from the normal. In **Fig.0.7**, a series of rays in a dense medium are incident on an interface at different angles of incidence. Ray #1 is refracted at the interface to a rarer medium according to Snell's Law. Ray #2 is incident at an angle such that the refracted angle is 90°. Ray #3 is incident at an even larger angle. If the angle of incidence of Ray #3 in inserted into Snell's Law, the sine of the angle of transmission will be found to be greater than one! This can not happen. Instead, all of the light is reflected back into the incident medium. There is no light transmitted into the second medium. The light is said to be **totally internally reflected**. For all angles of incidence greater than a critical angle, total internal reflection will occur. This **critical angle** occurs at the angle of incidence at which the transmitted ray is refracted along the surface of the interface (the case illustrated by Ray #2). Setting the angle of transmission equal to 90°, the critical angle, θ_{crit}, is found from Eq. 0-3 to be:

$$\sin(\theta_{crit}) = n_t/n_i \qquad (0\text{-}4)$$

In the ray picture, the concept of total internal reflection makes the interface look like a perfect mirror. If this process is examined in terms of wave propagation, theory predicts and experiment confirms that a weak electromagnetic field exists in the rarer medium, but it decays rapidly with distance from the interface and no light energy is transmitted to the rarer medium. This field is called an **evanescent field**. However, if another optically dense material were located very close to the material in which the total internal reflection were occurring (within a wavelength or so) some of the light energy could be coupled out of the first medium across the small gap and into the second dense medium. This process is called **frustrated total internal reflection** since the usual reflection is frustrated by the location of the material next to the interface. Frustrated total internal reflection is responsible for the operation of a component in fiber optic systems called a bidirectional coupler. This component is studied in **Project #7** and used in subsequent projects.

0.2.3 LIGHT IN OPTICAL FIBERS

Once you understand total internal reflection, you understand the illuminated stream shown in **Fig 0.2** of **Section 0.1**. Light traveling through the water is reflected off of the surface of the water-air interface and trapped inside the stream. The same thing will happen to a glass rod or thread. Optical fibers are a little more complicated than this, however.

If one were to use a fiber consisting of only a single strand of glass or plastic, light could be lost at any point where the fiber touched a surface for support. Thus, the amount of light that could be transmitted would be dependent on the methods used for holding the fiber. The output of the fiber would also be affected by any movement of the fiber during its use. To eliminate these problems, the central light-carrying portion of the fiber, called the **core**, is surrounded by a cylindrical region, called the **cladding (Fig 0.8)**. The cladding is then covered with a protective plastic jacket. Since the refractive index difference between the core and the cladding is less than in the case of a core in air, the critical angle is much bigger for the clad fiber. The index of the cladding, n_{cl}, is still less than the index of the core, n_{co}, because total internal reflection will occur only when $n_{co} > n_{cl}$. Looking at a cross-section of the fiber in **Fig.0.8**, one sees that the cone of rays that will be accepted by the fiber is determined by the difference between the refractive indices of the core and cladding. The **fractional refractive index difference** is given by

$$\Delta = (n_{co} - n_{cl})/n_{co} \qquad (0\text{-}5)$$

Because the refractive index of the core is a constant and the index changes abruptly at the core-cladding interface, the type of fiber in **Fig. 0.8** is called a **step-index fiber**.

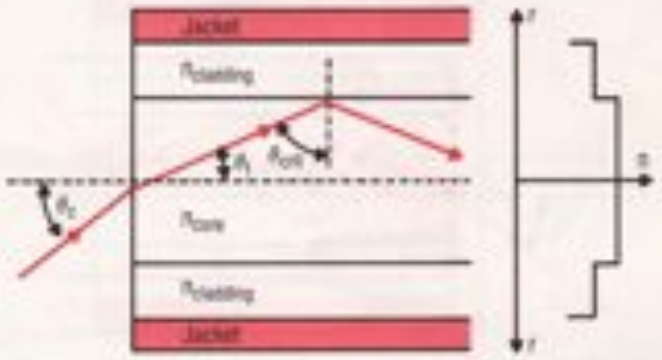

Figure 0.8. Step-index fiber. The refractive index profile is shown at the right. The geometry for derivation of the numerical aperture is given.

The definition of the critical angle can be used to find the size of the cone of light that will be accepted by an optical fiber with a fractional index difference, Δ. In **Fig. 0.8** a ray is drawn that is incident on the core-cladding interface at the critical angle. If the cone angle is θ_c, then by Snell's Law,

$$\begin{aligned} n_c \sin\theta_c &= n_{core} \sin\theta_c = n_{core} \sin(90°-\theta_{crit}) \\ &= n_{core} \cos(\theta_{crit}) \\ &= n_{core} \sqrt{1-\sin^2(\theta_{crit})} \end{aligned}$$

From Eq. 0-4, $\sin(\theta_{crit}) = n_{cl}/n_{core}$, so

$$n_c \sin\theta_c = \sqrt{n_{core}^2 - n_{cl}^2}. \qquad (0\text{-}6)$$

The **numerical aperture**, NA, is a measure of how much light can be collected by an optical system, whether it is an optical fiber or a microscope objective lens or a photographic lens. It is the product of the refractive index of the incident medium and the sine of the maximum ray angle.

$$NA = n_c \sin(\theta_{max}) \qquad (0\text{-}7)$$

In most cases, the light is incident from air and $n_c = 1$. In this case, the numerical aperture of a step-index fiber is, from Eqs. 0-6 and 0-7,

$$NA = \sqrt{n_{core}^2 - n_{cl}^2}. \qquad (0\text{-}8)$$

When $\Delta << 1$, Eq. 0-8 can be approximated by

$$\begin{aligned} NA &= \sqrt{(n_{core} + n_{cl})(n_{core} - n_{cl})} \\ &= \sqrt{(2\,n_{core})(n_{core}\,\Delta)} = n_{core}\sqrt{2\Delta}. \end{aligned} \qquad (0\text{-}9)$$

The condition in which $\Delta << 1$ is referred to as the **weakly-guiding approximation**. The NA of a fiber will be measured in **Project #1**.

In **Fig.0.9**, two rays are shown. One, the **axial ray**, travels along the axis of the fiber; the other, the **marginal ray**, travels along a path near the critical angle for the core-cladding interface and is the highest-angle ray which will be propagated by the fiber. At the point where the marginal ray hits the interface the ray has traveled a distance L_c, while the axial ray has traveled a distance L_z. From the geometry, it can be seen that

$$\sin\theta = n_{cl}/n_{core} = L_z/L_c \qquad (0\text{-}10)$$

The length L_c is a factor n_{cl}/n_{core} larger than L_z in the case shown in the figure. For any length of fiber L, the additional distance traveled by a marginal ray is

$$\delta L = (n_{core} - n_{cl})\,L/n_{cl} \qquad (0\text{-}11)$$

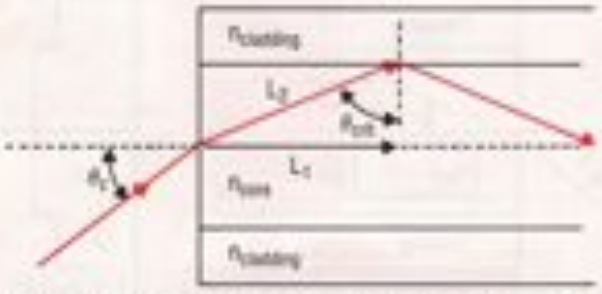

Figure 0.9. The geometry for derivation of the differential delay of a step-index fiber.

Eq. 0-11 can be simplified to $\delta L = L\Delta$. The additional time it takes light to travel along this marginal ray is

$$\delta t = \delta L/v = L\Delta\, n_{cl}/c. \qquad (0\text{-}12)$$

Therefore, a pulse with a length t representing one bit of information will be lengthened to $t + \delta t$. This **differential time** between axial and marginal rays will cause a pulse to smear and thereby limit the number of pulses per second that could be sent through a fiber and distinguished at the far end. In such a case, the system may be limited not by how fast the source can be turned on and off or by the speed of response of the detector, but by the differential time delay of the fiber. This smearing of pulses can be remedied through the use of graded-index or single-mode fibers.

Earlier, it was noted that light rays can be deflected by variations in the refractive index of a medium as well as by encountering an abrupt interface between two indices. There are a number of methods of creating controlled index gradients. Some involve introducing impurities into thin layers of glass as they are laid down on a substrate. This is not a continuous process since the refractive index within each layer is nearly constant. The resulting variation of refractive index in a fiber resembles that of a series of concentric tree rings rather than a smooth change in the index. Other techniques involve the removal of material from the base glass by some type of chemical method. Fibers whose cores have such an index gradient are called **graded-index fibers**. In our discussion, we will not make a distinction between these processes, but instead assume that the graded-index profiles are smooth and exactly conform to theory. In real graded-index optical fibers this may not be correct and such departures from the ideal gradient will affect their performance.

Once the refractive index gradient can be controlled through manufacturing processes, it is up to the designer of optical fibers to determine the most useful **refractive index profiles**, $n(r)$, the variation of index with radial distance in the core. This usually fits a power law profile given by

$$n(r) = n_1' [1 - 2\Delta (r/a)^\alpha], \qquad (0\text{-}13)$$

where n_1 is the index of refraction at the center of the core, and Δ is the fractional index difference defined earlier in Eq. 0-5, but with n_1 now substituting for n_{co}. The parameter, α, is the exponent of the power law and determines the shape of the graded-index profile. When $\alpha = \infty$, the profile is that of a step-index fiber. For $\alpha = 2$, the profile is parabolic (**Fig. 0.10**). This is the profile found in most telecommunications graded-index fibers, because this profile eliminates the differential time delay between axial and marginal rays. The numerical aperture of a graded-index fiber is the same as that of a step-index fiber only for rays entering on the fiber axis. For rays entering at other points on the core, the local numerical aperture is less because the local index, $n(r)$, must be used in Eq. 0-8. In the case of the parabolic graded-index fiber, the total amount of light which can be collected is one half of that which can be collected by a step-index fiber with the same Δ.

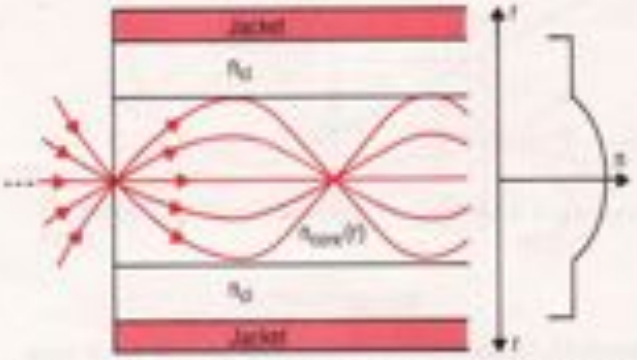

Figure 0.10. Graded-index fiber. The refractive index profile is shown at the right. Diverging rays are refocused at a point further down the fiber.

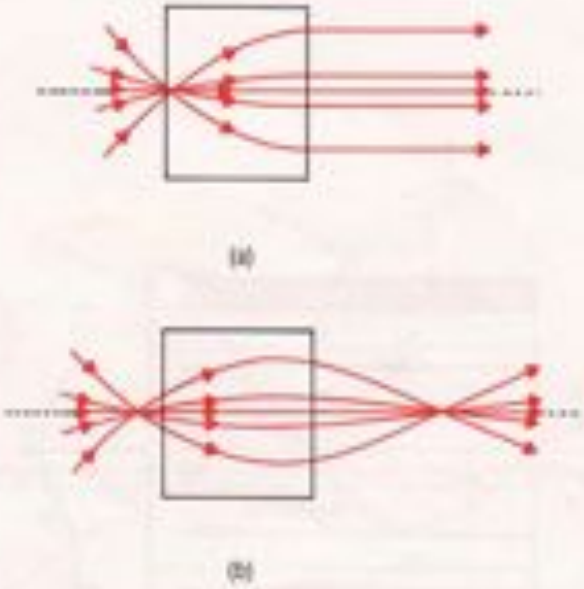

Figure 0.11. Graded-index (GRIN) lens. (a) 0.25 pitch lens. (b) 0.29 pitch lens.

Without plunging into the mathematics needed to prove that graded-index fibers with a parabolic profile remove differential delay, it is possible to get a qualitative feel of why the smearing of light pulses in such a fiber would be reduced. Instead of the rays bouncing off of the core-cladding interface as in step-index fibers, rays follow a gently curving path in graded-index fibers. In those with a parabolic profile, this path is sinusoidal. That is, the path can be described as a sine function in space. It would seem that light paths which have a large radial amplitude are still longer than the path down the axis of the fiber. But because of the refractive index gradient, the velocity of the light at the center of the fiber is smaller than the velocity of the light near the edge of the core. Although the light that travels near the edge of the fiber has to go farther, it travels faster and arrives at the end of the fiber at the same time as the light travelling down the center of the fiber. If the length of the fiber is L and the speed of light down the center of the fiber is $v = c/n_o$, then the time for a pulse to travel to the end of the fiber is $t = L/v = n_oL/c$. For light travelling a sinusoidal path, the length traveled will be L'' and the time to travel to the end of the fiber is $t = n(r,x)L''/c$. The product of the geometrical path and the refractive index is called the optical path length. If the optical path length, $n(r)L$, is the same for all paths, there will be no differential delay in the time the rays take to travel through a fiber. For all optical path lengths to be equal, the profile must be parabolic ($a = 2$).

0.2.4 GRADED-INDEX LENSES

One thing to note in **Fig.0.10** is that a fan of rays injected at a point in a graded-index fiber spreads out and then recrosses the axis at a common point just as rays from a small object are reimaged by a lens. The distance it takes for a ray to traverse one full sine path is called the pitch of the fiber. The length of the pitch is determined by Δ, the fractional index difference.

If a parabolic graded-index fiber is cut to a length of one quarter of the pitch of the fiber, it can serve as an extremely compact lens (sometimes called a **GRIN lens**, for GRaded-INdex) for fiber applications (**Fig.0.11**). By positioning the output of a fiber at the face of the short fiber length, light from the lens will be collimated, just as diverging light at the focal point of a lens is collimated. Because its properties are set by its length, this graded-index lens is referred to as a **quarter-pitch or 0.25 pitch lens**.

In some cases, it is not collimation of light which is required, but focusing of the fiber output onto a small detector or focusing of the output of a source onto the core of a fiber. The easiest way of accomplishing this is to increase the length of the GRIN lens slightly to 0.29 of a pitch (**Fig.0.11**). This enables the fiber optic system designer to move the source back from the lens and have the transmitted light refocus at some point beyond the lens. This is particularly useful for coupling sources to fibers and fibers to detectors. Both 0.25 and 0.29 pitch GRIN lenses will be used in **Projects #5, 7, 8, 9, and 10**.

0.3 WAVE OPTICS AND MODES IN OPTICAL FIBERS

Although the ray picture of light propagation through a fiber is easy to depict, it does not reveal some of the interesting properties of light in optical fibers, particularly in those fibers where the core size is on the order of the wavelength of light.

0.3.1 WAVE FIELDS IN A FIBER

The laws governing the propagation of light in optical fibers are Maxwell's equations, the same laws that describe the propagation of light in a vacuum or any medium. When information about the material constants, such as the refractive indices, and the boundary conditions for the cylindrical geometry of core and cladding is incorporated into the equations, they may be combined to produce a wave equation that can be solved for those electromagnetic field distributions that will propagate through the fiber. These allowed distributions of the electromagnetic field across the fiber are referred to as the **modes** of the fiber. They are similar to the modes found in microwave cavities and laser cavities. When the number of allowed modes becomes large, as is the case with large-diameter-core fibers, the ray picture we have used gives an adequate description of light propagation in fibers.

The description of the modes that propagate in a fiber is found by solving the wave equation in cylindrical coordinates for the electric field of the light in the fiber. The cylindrical coordinate system for a fiber is illustrated in **Fig.0.12**. The solutions, which are found to be harmonic (consisting of sine and cosine functions) in space and time, are of the form

$$E(r,\Phi,z) = l(r)\cos(\omega t - \beta z + \gamma)\cos(q\Phi), \qquad (0\text{-}14)$$

where ω is the frequency of light in radians/sec ($\omega = 2\pi\nu$, where ν is the linear frequency in Hertz, cycles/sec), β is the **propagation constant**, expressed in radians per unit distance, γ is a phase constant to provide the correct amplitude at time $t = 0$ and position $z = 0$, and q is an integer. The

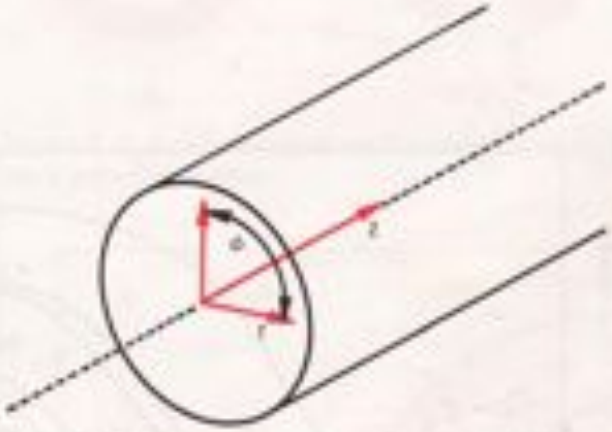

Figure 0.12. Coordinate system for modes in an optical fiber.

parameter, β, is important for specifying how light propagates in a fiber. In the ray optics description, β is the projection of the propagation vector on the z axis, where the magnitude of the propagation vector is $k = 2\pi n/\lambda_o$, λ_o being the wavelength of light in vacuum. It is important to make the distinction between the magnitude of the propagation vector, k, and the propagation constant, β, which is the z-component of the propagation vector, in order to avoid later confusion.

Solutions for β, f(r), and q are obtained by substituting **Eq. 0-14** into the wave equation. The solutions will depend on the particular fiber geometry and index profile, including both the core and the cladding, under consideration. The step-index profile is one of the few refractive index profiles for which exact solutions may be obtained. For this case the solutions for f(r) are Bessel functions. (Many people are unfamiliar with Bessel functions, since most rarely get beyond trigonometric functions or, perhaps, hyperbolic functions. While trig functions are familiar from high school mathematics, it is hard to find a sine wave in everyday life. The motion of a guitar string is fairly sinusoidal but hard to see because of the high frequency of vibration. However, Bessel functions are easily found. All that is required is a surface that can move freely and a cylindrical boundary to that surface. Anyone's morning cup of coffee will suffice. Just tap the side of the cup and watch the circular waves generated on the surface: Bessel functions!)

An important quantity in determining which modes of an electromagnetic field will be supported by a fiber is a parameter called the **characteristic waveguide parameter** or the **normalized wavenumber**, or, simply, the **V-number** of the fiber. It is written as

$$V = k_o \cdot a \cdot NA, \qquad (0\text{-}15)$$

where k_o is the free space wavenumber, $2\pi/\lambda_o$, a is the radius of the core, and NA is the numerical aperture of the fiber.

When the propagation constants (β's) of the fiber modes are plotted as a function of the V-number (remember, each V-number represents a particular wavenumber-core diameter-NA product), it is easy to determine the number of modes that can propagate in a particular fiber. In **Fig. 0.13**, such a plot is given for some of the lowest order modes. The number of propagating modes is determined by the number of curves that cross a vertical line drawn at the V-number of the fiber. Note that for fibers with V<2.405, only a single mode will propagate in the fiber. This is the single-mode region. The wavelength at which V = 2.405 is called the **cut-off wavelength**, denoted by λ_c, because, for a particular product of core diameter and NA, as the wavelength of radiation is increased, this is the wavelength at which all higher-order modes are cut off and only a single mode will propagate in the fiber. A fiber which propagates only the HE_{11} mode is said to be a **single-mode fiber**. For example, the Newport F-SV fiber has a core diameter of 4 μm and an NA of 0.11. According to Eq. 0-14, this fiber has a V-number of 2.19 for 633 nm light, putting it well inside the single-mode region. An experiment with this fiber will be done in **Project #3**.

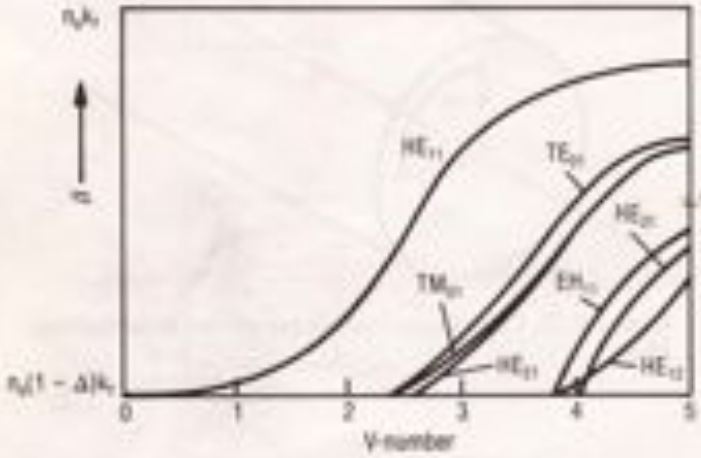

Figure 0.13. Low order modes of an optical fiber. Plot of the propagation constant in a fiber (β) as a function of V-number of a fiber. Each V-number represents a different fiber configuration or a different wavelength of light in a given fiber configuration. [after D.B. Keck in Fundamentals of Optical Fiber Communication, 2nd Edition, M. K. Barnoski, ed. see references, Copyright © Academic Press, 1981]

In the weakly-guiding approximation ($\Delta << 1$), the exact solutions of waveguide theory, HE_{mn}, can be replaced by a set of modes which are linearly polarized, called the LP modes. (The details of polarization of waves in fibers will be discussed in Section 0.3.2.) These LP modes are combinations of the modes found from the exact theory of the waveguide. These linearly-polarized modes may be characterized by two subscripts, m and n. The first subscript, m, gives the number of azimuthal, or angular, nodes (zeroes) that occur in the electric field distribution of the mode; the second subscript, n, gives the number of radial nodes that occur. They can be identified by pattern in the output of the fiber as it illuminates a screen. The patterns are symmetric about the center of the beam and show bright regions separated by dark regions (the nodes that determine the order numbers m and n). Some of these are shown in **Fig. 0.14**. It is assumed that the zero field at the outer edge of the field distribution is counted as a node, so $n \geq 1$. For the azimuthal nodes, $m \geq 0$. The lowest order HE_{11} mode consists of two LP_{01} modes with polarizations at right angles to one another. **Fig. 0.15** shows the propagation constants of these modes as a function of V-number. (Compare this figure with the exact solutions in **Fig. 0.13**.)

When the V number is greater than 2.405 (the value at which the first zero of the zero-order Bessel function occurs), the next linearly-polarized mode, LP_{11}, can be supported by the fiber, so that both the LP_{01} and LP_{11} modes will propagate. For a fiber with a V-number of 3.832 (corresponding to the first zero of the first-order Bessel function), two more linearly-polarized modes can propagate: the LP_{11} and the LP_{02} modes. By changing the position and angle of the input beam incident on a low-V number multimode fiber, individual linearly-polarized modes can be launched in the fiber and observed at the output. The propagation of individual modes in such a fiber will be observed in **Project #4**. This will help overcome one of the difficulties of the concept of modes in optical fibers, which is understanding what they are and how they differ from one another.

0.3.2 MODES IN MULTIMODE FIBERS

The multimode fibers used for telecommunications may have $a = 25\ \mu m$ and $NA = 0.20$ or $a = 50\ \mu m$ and $NA = 0.30$, so that for 633 nm light, the V-number will be about 50 or 150, respectively. This means that a large number of modes will be supported by the fiber. The amount of light carried by each mode will be determined by the input, or launch, conditions. For example, if the angular spread of the rays from the source is greater than the angular spread that can be accepted by the fiber (the NA of the input radiation is greater than the NA of the fiber) and the radius of the input beam is greater than the core radius of the fiber, then the fiber is said to be **overfilled (Fig. 0.16 (a))**. That is, some of the light which the source will be putting into the fiber cannot be propagated by the fiber. Conversely, when the input beam NA is less than the fiber NA and the input beam radius is less

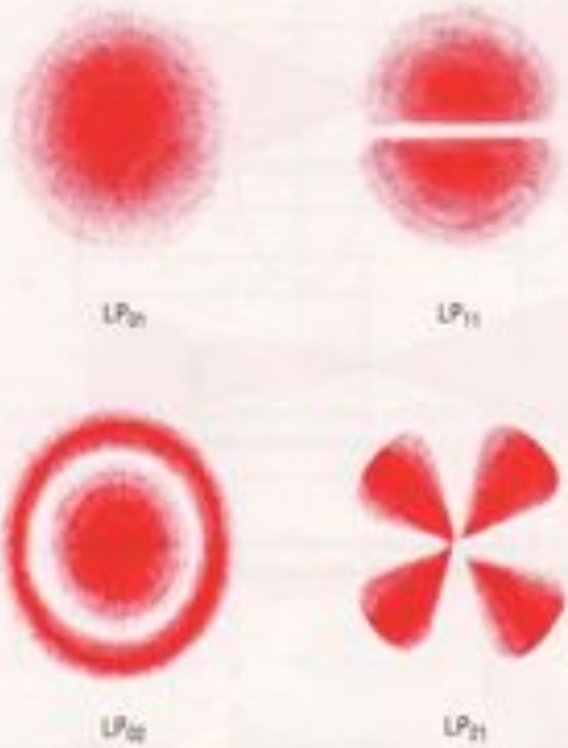

Figure 0.14. Irradiance patterns for some low order linearly polarized modes.

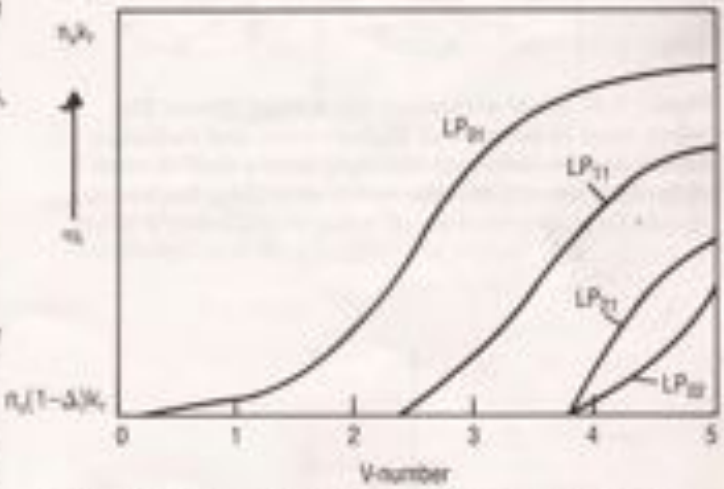

Figure 0.15. Low order linearly polarized modes of an optical fiber. Compare with Figure 0.13.

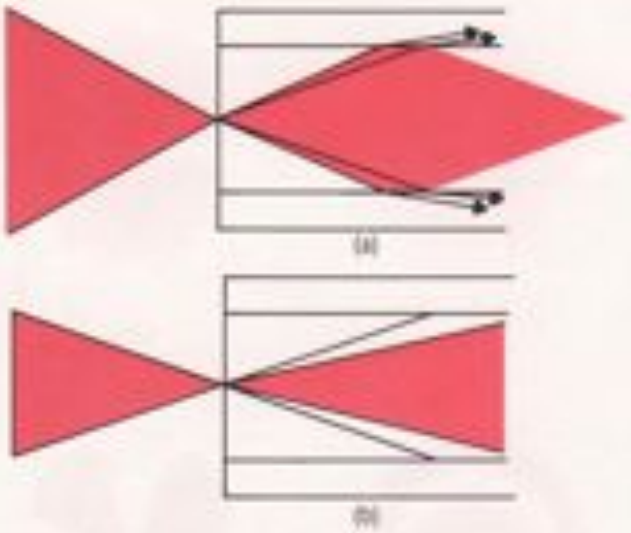

Figure 0.16. Launching conditions in a multimode optical fiber. (a) Overfilled. (b) Underfilled.

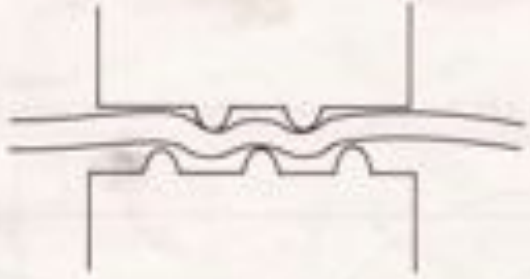

Figure 0.17. Mode scrambler for optical fibers. The bends tend to couple out higher-order and radiation modes and to distribute the light into a distribution of modes that will remain stable over long distances.

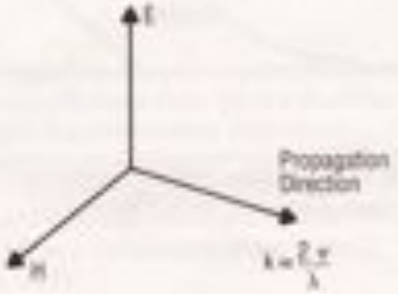

Figure 0.18. Components of an electromagnetic field.

than that of the fiber, the fiber is **underfilled (Fig. 0.16 (b))** and only low-order modes (low-angle rays in the ray picture) will be excited in the fiber. These two distributions will yield different measured attenuations, with the overfilled case having a higher loss than the underfilled case. In the ray picture, the higher-order rays will spend more of the time near the core-cladding interface and will have more of their evanescent field extending into the fiber cladding, resulting in higher attenuation. Also, if the fiber undergoes bending, the rays at high angles to the fiber axis may no longer satisfy the critical angle condition and not be totally internally reflected. Since power from these modes will radiate into the cladding and increase the attenuation, they are referred to as **radiation modes**. There is another class of modes called **leaky modes**. These modes have part of their electromagnetic energy distribution inside the core and part of their energy distribution in the cladding, but none of their energy distribution is actually at the core-cladding interface. The energy in the core "leaks" into the cladding by a process known, from quantum mechanics, as tunneling. Leaky modes are not true guided modes, but may not be fully attenuated until the light has traveled long distances.

After light has been launched into a fiber and has propagated a considerable distance (which may be several kilometers), a distribution of power within the core of the fiber develops that is essentially independent of further propagation distance. This is called a **stable mode distribution**. To generate an approximation of a stable mode distribution that will not be sensitive to small bends and twists in the fiber orientation, even with only a short length of fiber, a technique called **mode filtering** is used. Mode filtering may be accomplished through the use of **mode scrambling**. Mode scrambling is done by bending the fiber in a series of corrugations, as shown in **Fig. 0.17**. The effect of these bends is to couple out the light in the radiation and leaky modes and a portion of the light in the higher-order allowed modes and distribute the remaining light among the guided modes of the fiber, producing an approximation of the stable mode distribution. Mode scrambling permits repeatable, accurate measurements of fiber attenuation to be made in the laboratory, even with short lengths of fiber. It will be used in several of the projects in this manual.

0.3.3 POLARIZATION OF WAVES

The electromagnetic field is a vector quantity. Both the electric and magnetic field components are vectors at right angles to each other and both are, in most cases, mutually perpendicular to the propagation vector of the light, as shown in **Fig. 0.18**. Once the propagation vector whose z-component is β and whose direction along the light ray is known, information about the electric field is all that is required to fully define the field in the medium (the magnetic field can then be determined from this information). The direction of the electric field determines the polarization of the wave.

In many light sources, the polarization of the light varies in a random manner and these sources are said to be **randomly polarized**. Other sources, such as the output of many lasers, are linearly polarized. When light is **linearly polarized**, the electric field vector maintains a constant orientation in space, as depicted in **Fig. 0.19a**. Since the light field is a vector, it can be resolved into its components along two perpendicular axes. If there is a time lag between the two components, which can be translated into a phase delay, then other forms of polarization are created. For example, if the time difference between two orthogonal polarizations is 1/4 of a cycle (which corresponds to 1/4 of a wavelength), the phase difference between the two components is 90°. The electric field vector of the wave is the resultant of the two components, and the electric field vector traces out an ellipse in space (**Fig. 0.19b**). For this reason, it is called **elliptically polarized** light. As a special case, if the the two components are equal and out of phase by 90°, the wave would be **circularly polarized** as shown in **Fig. 0.19c**. In the case of optical fibers the polarization of light transmitted through them may be preserved or it may be scrambled to yield randomly polarized light, depending on the fiber that is used.

When light interacts with a material, the electrons in the material are set in motion. While most of the light is transmitted by the medium, a small portion of the light is scattered by the electrons and by defects in the medium. In randomly polarized light, the light is scattered in all directions. When the light in the medium is linearly polarized, however, there is little light scattered along the direction of the polarization vector. Most of the light is scattered in or near the plane perpendicular to the polarization direction, as shown in **Fig. 0.20**. This means that if we send linearly polarized light through a medium that changes the polarization direction, but does not scramble it, we can follow the orientation of the polarization through the medium (**Fig. 0.21**). This is done as part of **Project #4**.

In a perfectly symmetric, circular fiber, the two polarized components of the HE_{11} mode (the LP_{01} modes with orthogonal polarizations) travel at the same velocity, since they have identical propagation constants. If the fiber is not perfectly symmetric, then the fiber will be **birefringent**, since the two polarization components have different propagation constants. For example, fibers with elliptical cores will create a birefringence in which the slow and fast axes are along the major and minor axes of the ellipse, respectively. This ellipticity can be either accidental, due to errors in manufacture, or intentional, as part of the fiber design. If the birefringence is to be controlled, it is most often created by building stress regions into the fiber, as shown in the **"bow-tie" birefringent fiber** illustrated in **Fig. 0.22**. Here the slow axis is parallel to the high stress axis of the bow tie (parallel to the bow tie) and the fast axis is perpendicular to the high stress axis.

If light is launched with a linear component along each of the optical axes, the difference in propagation constants causes the resultant vector of the two polarizations to vary

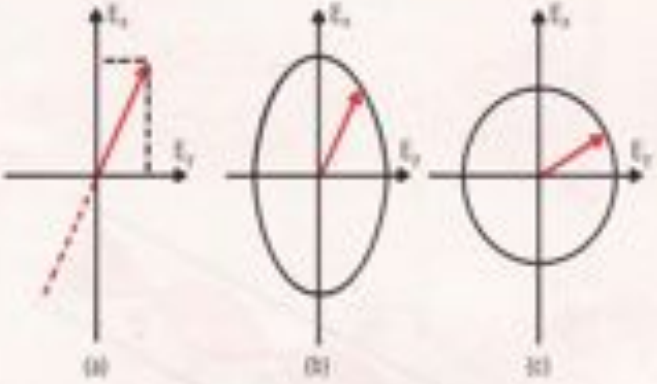

Figure 0.19. Forms of polarization of light. (a) Linear polarization. (b) Elliptical polarization. (c) Circular polarization.

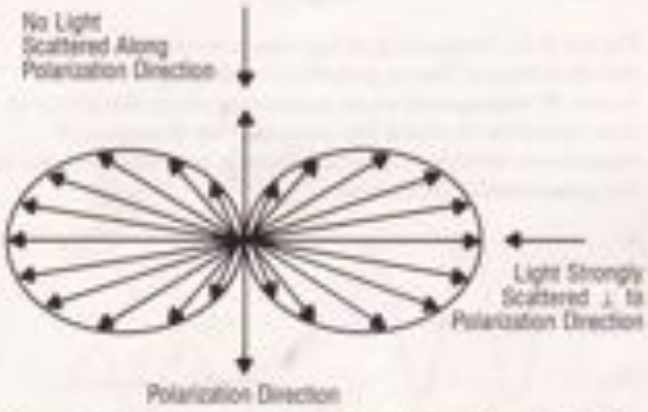

Figure 0.20. Scattering of light by a linearly-polarized field (dipole). Light is scattered strongly at right angles to the dipole direction, but is not scattered at all along the direction of the electric field vector.

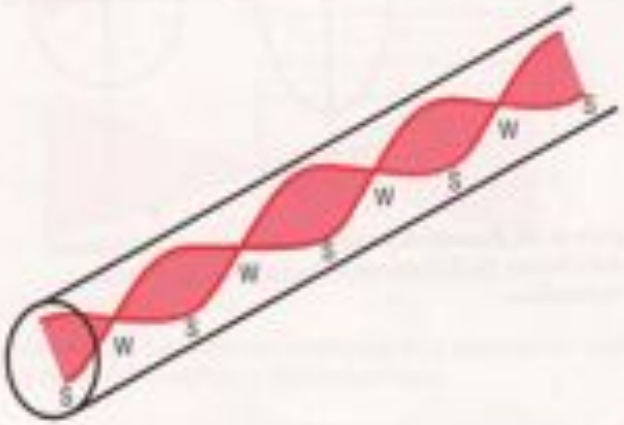

Figure 0.21. Scattering of light by a medium in which the direction of linear polarization changes with distance. W represents weak scattering since the observation direction is along the polarization direction; S represents strong scattering since it is perpendicular to the polarization direction.

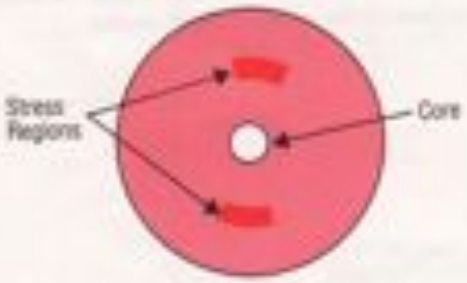

Figure 0.22. Cross section of a polarization-preserving fiber. Stress regions outside the core provide an asymmetry that causes birefringence in the fiber core. Elliptical fibers will also have the same effect.

periodically with distance along the fiber. When the two components are in phase, the light is linearly polarized. As the light propagates and the components go out of phase, the polarization state goes from linear to elliptical and back to linear at a phase difference of 180°. When the two polarization components are made equal in amplitude by launching linearly polarized light at 45° to the optical axes, the polarization progresses from linear, to elliptical, to circular, to elliptical, and back to linear in a plane that is at an angle of 90° to the plane of the original linear polarization. This sequence of alternating polarization states continues along the entire length of the fiber. The distance, L_p, over which the polarization rotates through an entire 360° is known as the **beat length** of the fiber. (Just as the alternate defocusing and refocusing by a graded-index fiber gives rise to a pitch length, a birefringent fiber causes a beat length.) The beat length is related to the birefringence, $\delta n = n_{max} - n_{min}$, by

$$L_p = 2\pi/\delta\beta, \qquad (0\text{-}16)$$

where $\delta\beta = 2\pi\delta n/\lambda_o$. This beat length can be observed visually when light from a helium-neon laser is launched into the fiber with its direction of polarization oriented at 45° to the fast axis of the fiber. As was discussed earlier in this section, scattering from centers illuminated by linearly polarized light varies from zero to a maximum as the angle of observation varies from along the polarization direction to perpendicular to it. Thus, as light progresses through a birefringent fiber, the amount of light scattered out at right angles will vary with the state of polarization at each point. In the case of a polarization-preserving fiber with the launch condition described above, the polarization goes from linear to circular and back again. This is slightly different from what was illustrated in **Fig. 0.21**, since that was for the case of rotating linear polarization. However, at points where the polarization is linear, the scattered light is weaker or stronger (depending on the direction of observation) than at the circular polarization positions. By measuring the repetition distances for scattered light variation, the beat length of the fiber can be determined. This will be done as part of **Project #4**.

When linearly-polarized light is launched with the polarization vector parallel to either the fast or slow axis of a high birefringence fiber, the output polarization will still be linearly polarized despite fiber bending. This "polarization-preserving" fiber provides reduced sensitivity to environmental effects. For other launch conditions, however, this will not be true. Instead, the fiber will act to change the polarization of the light; the actual effect on the input polarized light will be determined by the launch conditions, the beat length, and the fiber length. Polarization-preserving fibers have applications wherever the polarization of the transmitted light must be stable and well-defined. These application include fiber interferometric sensors (studied in **Project #10**), fiber gyroscopes, and heterodyne detection systems.

0.3.4 COHERENCE OF WAVES

The output of many lasers is highly monochromatic. Ideally, the light from the laser is a single color; in actuality, it consists of light within a small band of wavelengths, $\Delta\lambda$. There are a number of ways of describing the degree of monochromaticity in addition to the wavelength bandwidth, $\Delta\lambda$. It can be characterized as a frequency bandwidth, $\Delta\nu$. The two are related by

$$\Delta\nu = \Delta\lambda c/\lambda^2 \text{ or } \Delta\lambda = \Delta\nu c/\nu^2. \qquad (0\text{-}17)$$

The smaller the bandwidth, the more monochromatic the light source.

Another way of describing the monochromaticity of the source is through its **coherence length**. If a source were totally monochromatic, the output would consist of an electromagnetic field of constant amplitude that oscillates for an infinitely long time with a single output frequency and wavelength. Any deviation in the amplitude or shortening of the length of oscillation results in an increase in the bandwidth of the source or, alternatively, a decrease in the coherence length of the radiation. One may think of this description as trains of waves whose lengths represent the monochromaticity of the source. The relation between the coherence length and the bandwidth is

$$l_c = c/\Delta\nu = \lambda^2/\Delta\lambda. \qquad (0\text{-}18)$$

0.3.5 INTERFERENCE OF WAVES

When two electromagnetic fields are present in the same place at the same time, their result may be added vectorially, since the fields are vectors. If two fields are linearly polarized in the same direction, the fields may be added point-by-point as scalars. If two electric fields with the same amplitude are in phase the sum will be twice as large; if they are 180° out of phase, the fields will cancel point by point and resultant field is zero, as shown in **Fig. 0.23**. The phenomenon of two or more electromagnetic fields summing to give a resultant is called **interference**. When the fields are in phase, it is called **constructive interference,** and when the fields are 180° out of phase, it is called **destructive interference**. In many optics arrangements the path lengths alternatively vary through constructive and destructive interference, producing a series of dark and light fringes. From the fringe patterns and their changes as physical conditions in the interfering paths are changed, it is possible to measure extremely small changes in distances and refractive indices. In all of this we have the same polarization direction. If the fields have polarizations at right angles to each other, the resultant would be the vector addition of the two fields, but no constructive or destructive interference would occur and no fringes would be visible. A fuller explanation of interference and interference fringes is available in a number of elementary optics texts.

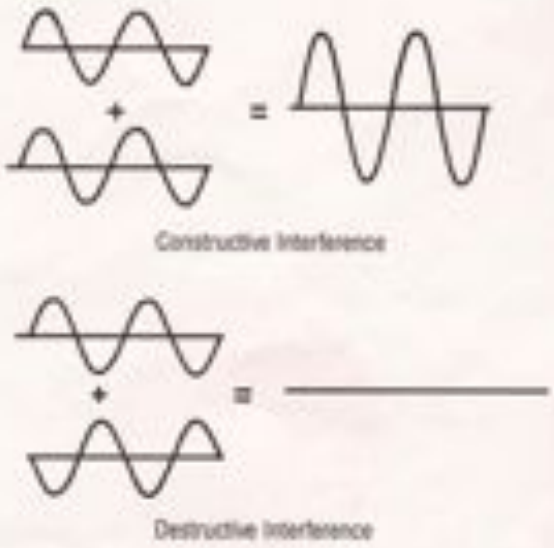

Figure 0.23. Illustrations of the interference of two waves.

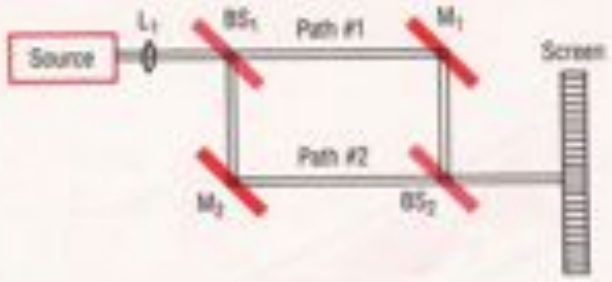

Figure 0.24. Mach-Zehnder interferometer. L: collimating lens; BS: beamsplitter; M: mirror.

One geometry that exhibits interference is the **Mach-Zehnder interferometer**, shown in **Fig. 0.24**. The source is collimated by lens L_1 and the collimated beam is divided by beamsplitter BS_1. A **beamsplitter** is a component that transmits a fraction of the light incident on it and reflects the rest, assuming that there is no absorption by it. In most cases, the ratio of transmission to reflection is 50/50. The split beams are then redirected by mirrors M_1 and M_2 to be recombined at a second beamsplitter BS_2. Their interference is seen on the screen S. If there is any change in optical path length introduced into either path, or arm, of the interferometer, the fringe pattern will change in a manner that will, in most cases, enable an observer to measure that change. In **Project #10**, a fiber optics version of the Mach-Zehnder interferometer will be constructed and examined. In this device, the mirrors will be replaced by optical fibers and beamsplitter BS_2 will be replaced with a component called a bidirectional coupler.

0.4 TRANSMITTING POWER THROUGH OPTICAL FIBERS

0.4.1 LOSSES IN FIBERS

In all of the above discussion, it has been assumed that the light travels down the fiber without any losses beyond those from radiation and leaky modes and some higher-order modes that are coupled out into the cladding.

When light is transmitted through an absorbing medium, the irradiance falls exponentially with the distance of transmission. This relation, called **Beer's Law**, can be expressed as

$$I(z) = I(0)\exp(-\Gamma z) \qquad (0\text{-}19)$$

where $I(z)$ is the irradiance at a distance z from a point $z = 0$, and Γ is the **attenuation coefficient**, expressed in units reciprocal to the units of z. In some fields of physics and chemistry, where absorption by a material has been carefully measured, the amount of absorption at a particular wavelength for a specific path length, such as 1 cm, can be used to measure the concentration of the absorbing material in a solution.

Although the absorption coefficient can be expressed in units of reciprocal length for exponential decay, in the field of fiber optics, as well as in most of the communications field, the absorption is expressed in units of dB/km (dB stand for decibels, tenths of a logarithmic unit). In this case, exponential decay is expressed using the base 10 instead of the base e ($= 2.7182818\ldots$) as

$$I(z) = I(0)\,10^{-\alpha z/10}, \qquad (0\text{-}20)$$

where z is in kilometers and Γ' – is now expressed in decibels per kilometer (dB/km). Thus, a fiber of one kilometer length with an absorption coefficient of 10 dB/km permits $I(z)/I(0) = 10^{-(10 \times 1)} = 0.10$ or 10% of the input power to be transmitted through the fiber. **Project #2** involves the measurement of the attenuation in an optical fiber.

The losses in fibers are wavelength dependent. That is, light of different wavelengths introduced into the same fiber will suffer different amounts of loss. **Fig. 0.25** shows the attenuation in dB/km of a typical optical fiber as a function of wavelength.

Although the exponential dependence was described for absorption losses, the same mathematics can be used for other sources of losses in fibers. Optical transmission losses in fibers are due to several mechanisms. First, optical fibers are limited in the short wavelength region (toward the visible and ultraviolet) by absorption bands of the material and by scattering from inhomogeneities in the refractive index of the fiber. These inhomogeneities are due to thermal fluctuations when the fiber is in the molten state. As the fiber solidifies, these fluctuations cause refractive index variations on a scale smaller than the parabolic variation that is imposed upon graded-index fibers. Scattering off of the inhomogeneities is known as **Rayleigh scattering** and is proportional to λ^{-4}, where λ is the wavelength of the light. (This same phenomenon is responsible for the color of the sky. The stronger scattering of light at shorter wavelengths gives the sky its blue color.)

In the long wavelength region, infrared absorption bands of the material limit the long wavelength end of the radiation spectrum to about 1600 nm. These two mechanisms are the ultimate limit for fiber losses. The highest quality fibers are sometimes characterized by how closely they approach the Rayleigh scattering limit, which is about 0.17 dB/km at 1550 nm.

At one time metal ions were the major source of absorption by impurities in optical fibers. It was the elimination of these ions that produced low-loss optical fibers. Today, the only impurity of consequence in optical fibers is water in the form of the hydroxyl ion (OH^-), whose absorption bands at 950, 1250, and 1380 nm dominate the excess loss in today's fibers. They are evident in the absorption spectrum shown in **Fig. 0.25**.

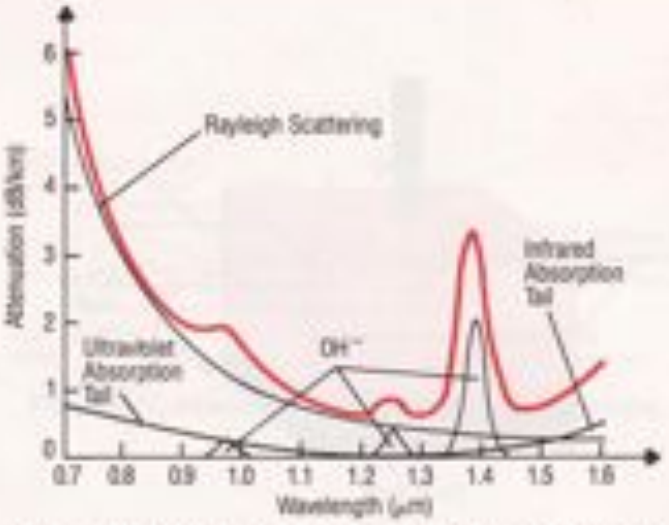

Figure 0.25. Attenuation of an optical fiber as a function of wavelength.

0.4.2 LIGHT SOURCES FOR OPTICAL FIBERS

Although light of many wavelengths and degrees of coherence may be transmitted by an optical fiber, there are a number of sources that are fairly convenient and efficient in coupling light into a fiber.

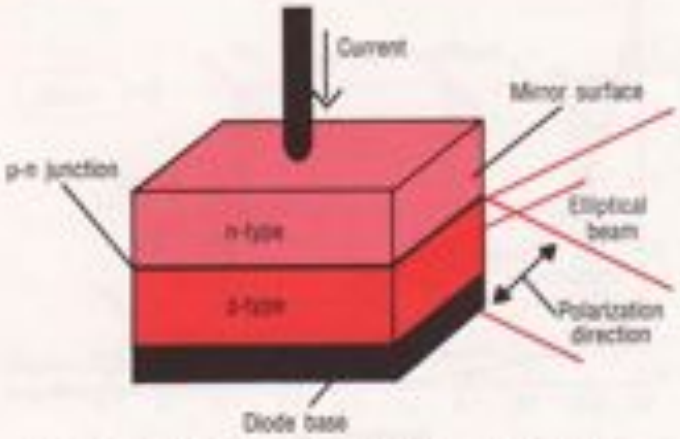

Figure 0.26. Construction of a simple semiconductor diode. Light emitting diodes and injection laser diodes have a similar basic construction, although the actual structure of the laser device is considerably more complicated.

The small red indicator lights that we see in smoke detectors and electronic panel lights are **light emitting diodes** (LED's). The name is quite descriptive, since these devices are nothing more than special semiconductor diodes that emit light. They are made of semiconductors, such as gallium arsenide, to which small amounts of atomic impurities have been added to raise the conductivity. The carrier of electrical current is either an electron or a hole (the absence of an electron). The material in which electrons are the major carrier of current is called n-type material and the material in which holes are the major carrier is called p-type. A diode is created when pieces of n-type and p-type material are constructed next to one another, as in **Fig. 0.26**. The interface plane between them is called the junction. When a voltage is applied across the diode junction so that the diode conducts, it emits light which is radiation resulting from the recombination of electrons and holes. This radiation is called, appropriately, **recombination radiation**. The amount of light output is proportional to the number of electron-hole pairs that recombine in the diode and this is proportional to the diode current. Therefore, the optical power-current curve of an LED will be a straight line. The wavelength of the emitted radiation in an LED depends on the differences between the energies of the electrons in the n-type material and holes in the p-type material. The bandwidth of the radiation is broad compared to that of laser sources.

Although the construction of **current injection laser diodes** (ILD's) is much more elaborate than LED's the two are shown in **Fig. 0.26** as being similar. Both in the simplest illustration and in the basic principles of operation, these two devices are similar. Current is injected into the diode by applying a voltage across the diode. However, the current densities are considerably greater in an ILD than those in an LED. Instead of electron-hole pairs recombining spontaneously as in an LED, in an ILD this enormous current flow stimulates the pairs to emit coherently, creating a more powerful output with a narrower bandwidth. This process is called **stimulated emission**. The optical power-current curve of the ILD is different from that of the LED in that the current must reach a threshold value before lasing can occur. The output then increases rapidly in proportion to the current in excess of the threshold current. The stimulated process just described is enhanced by the surfaces of the semiconductor crystal that serve as partially reflecting mirrors to redirect part of the laser output back into the junction region. These mirrors also cause the output of the ILD to be partially collimated, although diffraction of the light by the edges of the junction region causes the light to be directed into a fan-shaped beam with a divergence which is typically about 15° by 30°. The larger divergence angle is in the direction perpendicular to the junction plane, as shown in **Fig. 0.26**.

In contrast to the solid state semiconductor medium of the ILD, the lasing medium of the helium-neon (HeNe) laser is a mixture of helium and neon gases which is excited by an electrical current, creating a light-emitting discharge similar to those seen in neon signs. The difference between the neon sign and the HeNe laser is the proportions of the gas mixture, a narrow discharge path in the glass tube, and reflecting end mirrors, as shown in **Fig. 0.27**. The output wavelength of the HeNe laser is usually in the red at 633 nm, although outputs at other wavelengths in the visible and infrared can be obtained by using different sorts of mirrors with higher reflectivities at the allowed wavelengths. The output is more highly collimated than the output of the ILD. For a typical HeNe laser, the beam divergence is about 1 milliradian (mrad) or 0.06°.

The polarization of radiation in a fiber optics system depends on the type of source that is used. Some HeNe lasers possess a high degree of linear polarization; others are randomly polarized. Their polarization is usually determined by the details of the laser construction. The output of an LED is randomly polarized, while that of an ILD is polarized parallel to the plane of the p-n junction. The polarization of a source can be checked by observing the variation in power on a detector as a polarizer is rotated in front of the source. A linearly polarized source will show large variations in the transmitted power as the polarizer is rotated, while randomly polarized or circularly polarized light will show little or no variation. Separating circularly from randomly polarized light requires the use of an optical component known as a waveplate.

There are other sources that might be considered for use in fiber optics system: the sun, tungsten lamps, fluorescent light neon lamps, electric arcs, etc. However, most of these sources are extended sources. That is, they have a large emission area compared to the sources already discussed. To introduce light from these sources into a fiber requires that some optical system be constructed to refocus the source onto the fiber end. The larger and more divergent the source, the more difficult it is to couple light into the system.

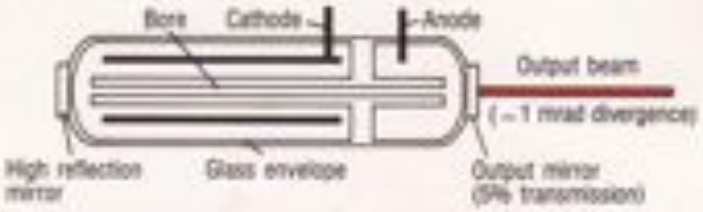

Figure 0.27. Construction of a Helium-Neon laser tube.

0.4.3 COUPLING SOURCES TO FIBERS

One objective in any fiber optics system is to insert as much power into the system with as little loss as possible. This allows the use of lower power sources in a system, reducing the cost and enhancing the reliability, since the source does not have to be operated near its maximum rated power. Attention paid to coupling a source to a fiber or a fiber to other components will be repaid in a more reliable and cheaper system. (Losses which occur in fiber-to-fiber coupling and splicing will be discussed and measured in **Project #6**.)

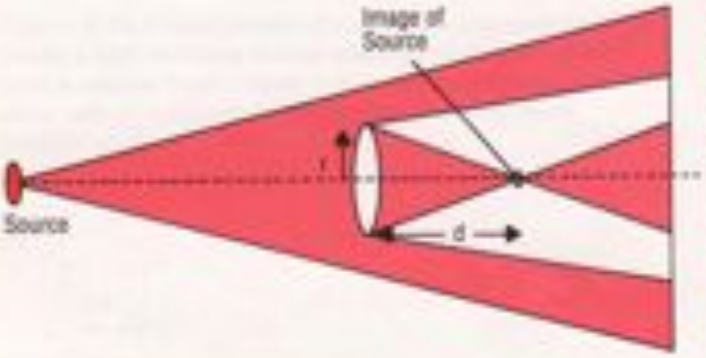

Figure 0.28. Calculation of the NA of an extended source.

The direction of the radiation that is emitted from a source must be considered in the field of fiber optics, since that radiation has to be collected and focused onto a fiber end. Sources can range from isotropic (emitting in all directions) to collimated (emitting in only one direction). In general, the angular distribution of the source can be expressed as

$$B(\theta) = B_o (\cos\theta)^m, \quad \theta < \theta_{max} \qquad (0\text{-}22)$$

where θ_{max} is the maximum angle from the normal at which the light is emitted and is determined by the geometry of the source. If m = 1 in Eq. 0-22, the source is called a **Lambertian source**. Many non-laser sources closely approximate Lambertian sources. For a collimated source, m is very large. For intermediate cases, the source may be considered to be a partially collimated source. The angular distribution of an LED and and ILD will be measured in **Project #5**.

The ability of a fiber to accept radiation can be characterized by its NA. We can describe the range of angles into which a source emits by a similar NA. The definition of the maximum angle of the source is not as easily determined as the maximum angle of a fiber with its critical angle, since the light may be emitted into a distribution of angles that does not have a precisely defined cut off.

In some cases, the light from the source is so divergent and the source is so large that the source must be reimaged on the fiber end face by a short focal length lens. For such a source, the lens is overfilled and the marginal rays, those at the edge of the cone of light, are determined by the size of the lens that is used. In that case, the NA of the source is given by

$$NA_{source} = n \sin\theta. \qquad (0\text{-}23)$$

where $\theta = \tan^{-1} r/d$, with r = radius of the lens and d = image distance, as shown in **Fig. 0.28**.

For collimated laser sources, the lens is usually underfilled if it is placed close to the source. The light comes to a focus at the focal point of the lens. The beam then has a divergence half-angle that is approximately equal to the ratio of the beam waist radius before the lens, r_w, to the focal length of the lens. Thus, the NA of the beam is given by

$$NA_{beam} = n \sin (r_w/f). \qquad (0\text{-}24)$$

There are four parameters which affect the efficiency of source-fiber coupling, the NAs of the source and the fiber and the dimensions of the source and the fiber core. It is possible to show that the product of the source diameter and the NA of the source is a constant no matter what the focal length of the imaging lens may be. By comparing this value to the product of the fiber core diameter times the fiber NA, it is possible to determine whether a lens may be chosen that can image the

source onto the fiber core without overfilling the fiber. Overfilling is marked by a source NA which is larger than the fiber NA. If the diameter-NA product of the source is larger than that of its fiber counterpart, reducing a source NA to fit a fiber NA will not increase the coupling since that action enlarges the diameter of the source image on the fiber face. Thus, a careful consideration of the diameter-NA products will keep someone from trying to do the impossible. This same approach can be applied also to coupling between fibers of different sizes and NA's. Further details of coupling will be discussed and illustrated in **Project #5**.

0.5 APPLICATIONS

Most of the applications of fiber optics systems fall into one of three categories: communications, sensors, and power distribution. In this section, each will be described briefly.

By far the most extensive use of fiber optics is in the field of communications. It encompasses short links between computers and telecommunications devices, the so-called local area networks (LAN's) and longer distance connections that include those between the metropolitan areas of the Northeastern United States and those between America and the European continent. A fiber optics communication link will be constructed in **Project #8**.

When information is sent through a fiber optics system, it is encoded on the light wave by changing the light irradiance as a function of time. This process of varying the light level with time is called **modulation**. There are two types of modulation: analog and digital. Analog modulation consists of changing the light level in a continuous manner, while with digital modulation, the information is encoded through a series of pulses separated by spaces, as shown in **Fig. 0.29**. The absence or presence of a pulse at some point on the stream of pulses represents one element, or bit, of information.

The performance of a system using analog modulation is determined by how faithfully it reproduces the signal and by the smallest signal that can be transmitted, which is limited by random or extraneous noise in the system. Part of this is due to the type of detector that is used to convert the modulated light signal back into an electrical signal and part is due to the system itself. The ratio of the detected signal to the smallest signal which can be distinguished from the noise is called the **signal-to-noise ratio** (SNR). This will be discussed as part of **Project #8**. In the case of digital systems, the faithful reproduction of signal level is not required, which makes such systems superior in the presence of noise sources. All that is required is that pulses be transmitted with sufficient power for the detector and electronics to determine the presence or absence of the pulse. Performance in digital systems is given in terms of the **bit error rate** (BER), the fraction of bits sent that are determined to be in error when compared with the original digital information. BER's of less than 10^{-9} are generally required for a fiber optic digital communication link to be considered a high-quality system.

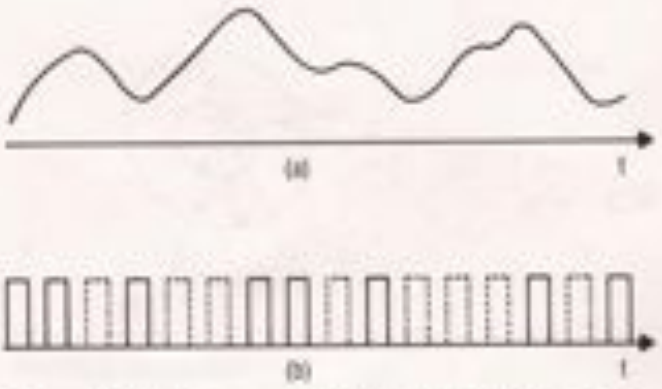

Figure 0.29. Two types of signal modulation. (a) analog. (b) digital.

Another application involves the use of optical fiber sensors to measure physical parameters. Because of their small diameter, sensors made of optical fibers can be fit into tight geometries where conventional sensors would be too large. Also, because the fiber medium is non-conducting, fiber sensors can be used in dangerous circumstances, such as explosive atmospheres. Sensors can be used to measure physical parameters such as temperature and pressure and engineering information such as liquid levels and distances. Four different types of multimode intensity sensors will be explored in **Project #9** and in **Project #10** a single mode interferometric sensor will be constructed.

Persons who have not studied fiber optics tend to think of them as optical water hoses. But as we have seen, the launching conditions, the fiber NA, the mode distribution in the fiber, and the fiber absorption and scattering losses all can contribute to reducing the usefulness of a fiber as a conductor of optical power. There are, however, certain fields where the transmission of optical power by optical fibers has proved useful.

In the field of medicine, the ability to insert optical fibers inside small hollow tubes that are pushed through small incisions in the body has provided a number of successful surgical procedures that do not call for massive cutting of tissues and yet still provide treatment for diseased parts of the body from the output of the optical fiber. Parallel to the power carrying optical fiber there is usually a second tube with many strands of optical fiber arranged in a precise manner that conduct illuminating light to the location of the treatment and carry an image of the treatment site back to the surgeon. Many of the treatments are still in the experimental phase. One of the most sought after products is an optical fiber that would carry large amounts of long wavelength infrared radiation from a carbon dioxide laser. The focused output of this laser makes an ideal surgical scalpel, but in the near term there are no fibers of sufficient flexibility, low cost, and low absorption at the CO_2 laser wavelength that this specific application will become widespread.

There are a number of applications in the field of material processing where the delivery of laser power to a location would be an ideal method of operation. In dusty and difficult environments, the replacement of multiple lens-based optical power delivery systems with fiber-based systems is useful because of the reduction in down time and maintenance. Usually, the divergent output of the fiber must be refocused by a lens to produce the required irradiance to heat treat, melt, or vaporize an area of the material being processed. Depending on the wavelength of the radiation being used and the type of fiber employed, there are maximum values of power that can be delivered by such systems.

1.0 PROJECT #1: HANDLING FIBERS, NUMERICAL APERTURE

In this first project, you will learn how to prepare fiber ends for use in the laboratory. You will be able to observe the geometry of a fiber and you will measure the numerical aperture (NA) of a telecommunications-grade fiber.

The method which is presented for determining the NA of a fiber is especially illustrative of what is to be learned. Another technique for measuring a fiber's NA, which is one often used in standard practice, will be used in **Project #3**.

1.1 FIBER GEOMETRY

An optical fiber is illustrated in **Fig. 1.1**. It consists of a core, with refractive index n_{core}, of circularly-symmetric cross section of radius a, and diameter 2a, and a cladding, with refractive index n_{cl}, which surrounds the core and has an outer diameter of d. Typical core diameters range from 4-8 μm (1 μm = 1 micrometer = 10^{-6} m) for single-mode fibers to 50-100 μm for multimode fibers used for communications to 200-1000 μm for large-core fibers used in power transmission applications. (See **Section 0.5** for a discussion of these applications.) Communications-grade fibers will have d in the range of 125-140 μm, with some single-mode fibers as small as 80 μm. In high-quality communications fibers, both the core and the cladding are made of silica glass, with small amounts of impurities added to the core to slightly raise the index of refraction. There are also lower-quality fibers available which have a glass core surrounded by a plastic cladding, as well as some all-plastic fibers. The latter have very high attenuation coefficients (**Section 0.4.1**) and are used only in applications requiring short lengths of fiber.

Surrounding the fiber will generally be a protective jacket. This jacket may be made from a plastic and have an outside diameter of 500-1000 μm. However, the jacket may also be a very thin layer of varnish or acrylate material.

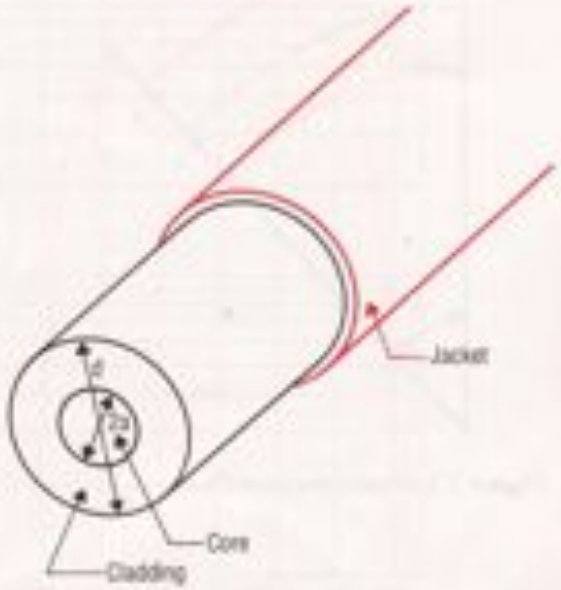

Figure 1.1. Geometry of an optical fiber, showing core, cladding, and jacket.

1.2 FIBER MECHANICAL PROPERTIES

Before measuring the NA of a fiber, it will be necessary to prepare the ends of the fiber so that light can be efficiently coupled in and out of the fiber. This is done by using a scribe-and-break technique to cleave the fiber. A carbide or diamond blade is used to start a small crack in the fiber, as illustrated in **Fig. 1.2**. Evenly applied stress, applied by pulling the fiber, causes the crack to propagate through the fiber and cleave it across a flat cross section of the fiber perpendicular to the fiber axis.

In theory, the breaking strength of glass fibers can be very large, up to about 725 kpsi (where 1 kpsi = 1000 pounds/sq. inch) or 5 GPa (where 1 Pa = 1 Newton/sq. meter and 1 GPa = 10^9 Pa). However, because of inhomogeneities and flaws, fibers do not exhibit strengths anywhere near that

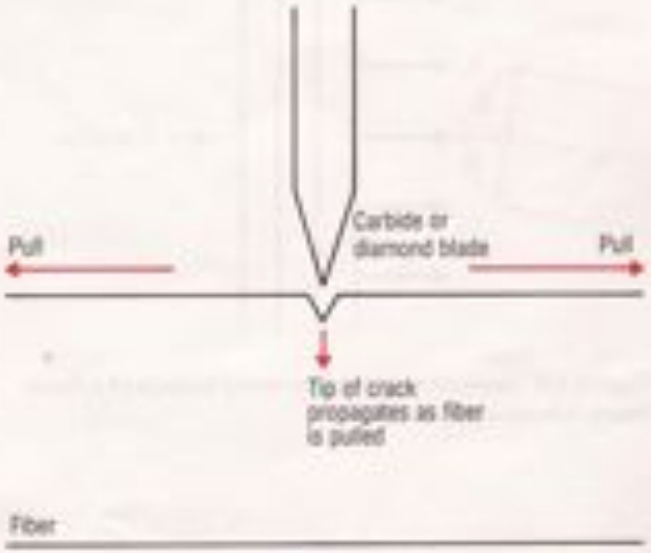

Figure 1.2. Scribe-and-break technique of fiber cleaving. A carbide blade makes a small scribe, or nick, in the fiber. The fiber is pulled to propagate the scribe through the fiber.

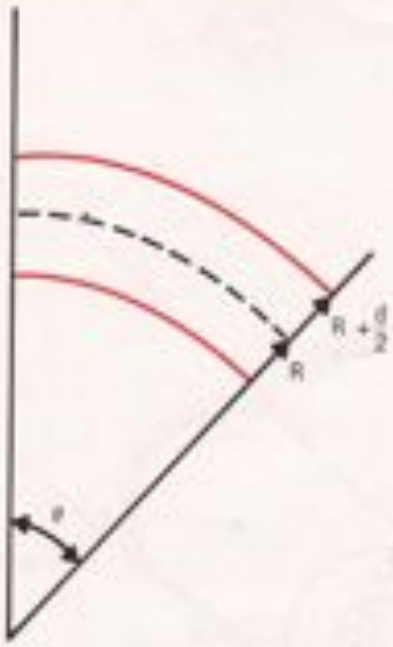

Figure 1.3. Strain of a bent fiber.

value. Before being wound on a spool, a fiber is stretched over a pair of pulleys, which apply a fixed amount of strain (stretching per unit length). This process is called proof-testing. Typical commercial fibers may be proof-tested to about 50 kpsi (345 MPa), which is equivalent to about a one pound load on a 125-μm OD fiber. When a crack is introduced, this is reduced even further in the neighborhood of the crack. Fracture occurs when the stress at the tip of the crack equals the theoretical breaking strength, even while the average stress in the body of the fiber is still very low.[1] The crack causes sequential fracturing of the atomic bonds only at the tip of the crack. This is the reason that a straight crack will yield a flat, cleaved, fiber face.

Optical fibers are required to have high strength while maintaining flexibility. Fiber fracture usually occurs at points of high strain when the fiber is bent. For a fiber of radius d/2, bent to a radius of curvature R, as shown in **Fig. 1.3**, the surface strain on the fiber is the elongation of the fiber surface, $(R + d/2)\theta - R\theta$, divided by the length of the arc, $R\theta$. The strain is, then, $d/2R$. Although silica fibers have been prepared which can withstand strains of several percent, an upper strain limit of a fraction of 1% has been found to be necessary to guarantee fiber survival in a cable installed in the field.[1] If a strain limit of 0.5% is used as a reasonably conservative value, a 125-μm diameter fiber will be able to survive a bend radius of 1.25 cm.

1.3 MEASURING NUMERICAL APERTURE

A detailed derivation of the expression for the NA of a fiber was given in **Section 0.2.3**. Recalling Eq. 0-9, the NA of a fiber, in the weakly-guiding approximation, was found to be

$$NA = n_{co}\sqrt{2\Delta} \qquad (1\text{-}1)$$

where n_{co} is the refractive index of the core of a step-index fiber or the refractive index at the center of the core of a graded-index fiber, and Δ is the fractional index difference,

$$\Delta = (n_{co} - n_{cl})/n_{co}.$$

As an example, a typical multimode communications fiber may have Δ=0.01, in which case the weakly-guiding approximation, which assumes $\Delta \ll 1$, is certainly justified. For silica-based fibers, n_{co} will be approximately 1.46. Using Eq. 1-1, these values of Δ and n_{co} give NA = 0.2. This gives a value of 11.5° for the maximum incident angle in **Fig. 0.8** and a total cone angle of 23°. Values of NA range from about 0.1 for single-mode fibers to 0.2-0.3 for multimode communications fibers up to about 0.5 for large-core fibers.

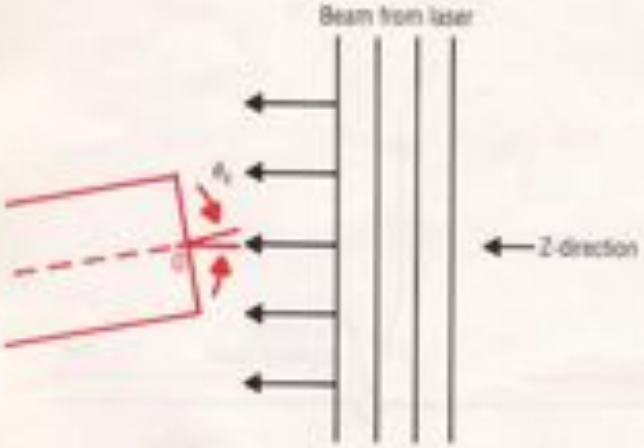

Figure 1.4. Geometry of a plane-wave launch of a laser beam into an optical fiber.

The way in which light is launched into the fiber in the method used here to measure the fiber NA is shown in **Fig. 1.4**. The light from the laser represents a wave front propagating in the z-direction. The width of the laser beam, ~1 mm, is much larger than the diameter of the fiber core, 100 μm in this case. In the neighborhood of the fiber core, the wave front of the laser light takes on the same value at all points having the same z, so we say that we have a plane wave prop-

agating parallel to the z-axis. When a plane wave is incident on the end face of a fiber, then we can be sure that all of the light launched into the fiber has the same incident angle, θ_i in **Fig.1.4**.

If the fiber end face is then rotated about the point O in **Fig. 1.4**, we can then measure the amount of light accepted by the fiber as a function of the incident angle, θ_i.

Fig. 1.5 shows the light accepted by a Newport F-MLD fiber as a function of acceptance angle using the method just described. The point where the accepted radiation has fallen to a specified value is then used to define the maximum incident angle for the acceptance cone. The Electronic Industries Association uses the angle at which the accepted power has fallen to 5% of the peak accepted power as the definition of the experimentally determined NA.[3] The 5% intensity points are chosen as a compromise to reduce requirements on the power level which has to be distinguished from background noise.[4]

Note that in **Fig. 1.5**, the radiation levels were measured for both positive and negative rotations of the fiber and the NA was determined using one half of the full angle between the two 5%-intensity points. This eliminates any small errors resulting from not perfectly aligning $\theta_i = 0$ to the plane wave laser beam. The NA obtained in this test case was 0.29, which compares well with the manufacturer's specification of NA = 0.30.

1.4 REFERENCES

1. D. Kalish, et al., "Fiber Characterization-Mechanical", in *Optical Fiber Communications*, S. E. Miller and A. G. Chynoweth, eds., Academic Press (New York) 1979, p. 406

2. D. Gloge and W. B. Gardner, "Fiber Design Considerations", in *Optical Fiber Communications*, S. E. Miller and A. G. Chynoweth, eds., Academic Press (New York) 1979, p. 152

3. EIA Standard RS-455-47, Section 4.3.2, EIA, Engineering Dept. (Washington D.C.) 1983

4. D. L. Franzen and E. M. Kim, "Interlaboratory measurement comparison to determine the radiation angle (NA) of graded-index optical fibers", Applied Optics 20, p. 1220 (1981)

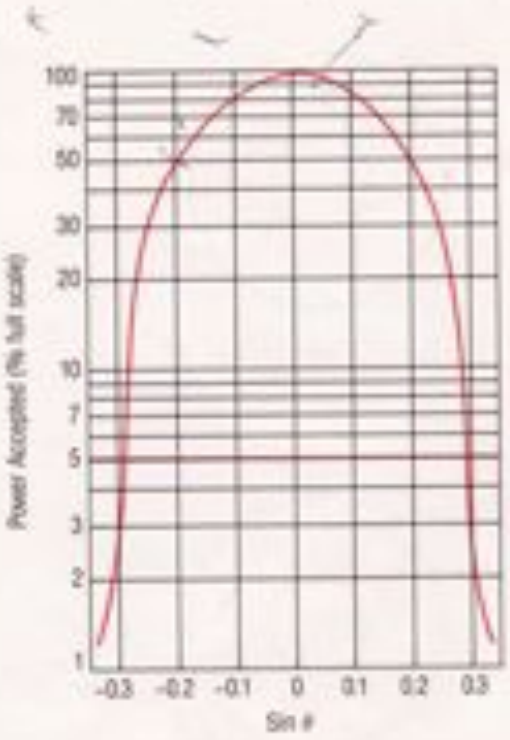

Figure 1.5. Plot of the data taken in the measurement of the NA of the Newport F-MLD fiber.

1.5 PARTS LIST

Cat#	Description	Qty.
F-MLD-50	100/140 MM fiber, 50 meters	1
XSN-22	2x2 Breadboard	1
U-1301P	1 mw HeNe laser	1
807	Laser mount	1
340C	Clamp	1
41	Short rod	1
815	Power meter	1
F-CL1	Fiber cleaver	1
FK-BLX	Ballddriver set	1
SK-25	¼-20 Screw kit	1
SK-08	8-32 Screw kit	1
RSX-2	Rotation stage	1
MPH-1	Micro-series holder	1
MSP-1	Micro-series post	1
VPH-2	Post holder	1
SP-2	Post	1
FP-1	Fiber positioner	2

Additional equipment required:

Methylene chloride for stripping fiber jacket. (Many commercially available paint thinners contain methylene chloride and work well for this purpose. Methylene chloride is toxic and can be absorbed through the skin. Any methylene chloride which gets on your skin should be immediately washed off.) Single-edge razor blades may also be used to strip fiber jackets.

A microscope for viewing the cleaved ends of fibers is essential. If your laboratory is not already equipped with an adequate high-power microscope, you may wish to consider using the Newport F-ML1 Inspection Microscope for inspecting fiber ends. You may also wish to use the F-BC2 fiber breaker in place of the F-CL1 fiber cleaver.

1.6 INSTRUCTION SET

1.6.1 PREPARING FIBER ENDS

1. Remove ~1-1/2 inches of fiber jacket from a ~2 meter segment of F-MLD fiber, by dipping the fiber end in methylene chloride and letting it soak for ~3 minutes. (Some people prefer to use a single-edge razor blade held at a low angle to do the stripping of the fiber jacket. This requires some practice, but goes much faster once you are used to it.)

2. Use the F-CL1 Fiber Cleaver to cleave the stripped end of the fiber. The cleaver should be placed on the top of the table with the blade pointing up. Draw the fiber over the blade with a light motion. Be sure that the fiber is normal to the blade. You should not attempt to cut the fiber with the cleaver. You are only starting a small nick which will propagate through the fiber when you pull it. Gently, but firmly, pull the fiber to cleave it.

3. Check the quality of the cleave by examining it under a high-power microscope. Carefully examine the end face of the fiber. The end face should appear flat and should be free of defects, as in **Fig. 1.6a**. However, chips or cracks which appear near the periphery of the fiber are acceptable if they do not extend into the central region of the fiber. Some poorly cleaved fiber ends are illustrated in **Fig. 1.6b** and **c**. The problems associated with the poor cleaves are discussed in Step 4.

4. If the inspection of the fiber end face in Step 3 does not show that the end face has been properly cleaved, you should consider the following common sources of error:

There are two principal reasons for obtaining a bad cleave, 1) a poor scribe and 2) a non-uniform pull of the fiber.

A scribe which is too deep may cause an irregular cleave and may cause multiple cracks to propagate through the fiber (**Fig.1.6b**). A scribe which is too shallow will be the same as no scribe at all and the fiber will break randomly.

If the pull which propagates the crack through the fiber is not uniform, and especially if it includes twisting of the fiber, irregularities may show up on the fiber end face or a lip may be formed on the end of the fiber, as in **Fig.1.6c**.

If the fiber end is cleaved at an angle, the fiber was probably scribed at an angle other than 90° across the fiber axis, although this, too, can be caused by a non-uniform pull of the fiber. (This will not be a problem if you have chosen to use the F-BK2 Fiber Breaker, but will have to be considered if you are using the F-CL1 Fiber Cleaver. See the note after Step 5.)

5. Once you have a fiber segment with two well-cleaved ends, you may look at the geometry of the fiber, as it was described in the introduction. View a fiber end as you did in Step 3. Use an incandescent lamp to illuminate the far end of the fiber. You will be able to see the light shining through the central portion of the fiber. This is the fiber core. The region surrounding the core is the fiber cladding. You will not be able to see the fiber jacket, because you have stripped that away from the end of the fiber.

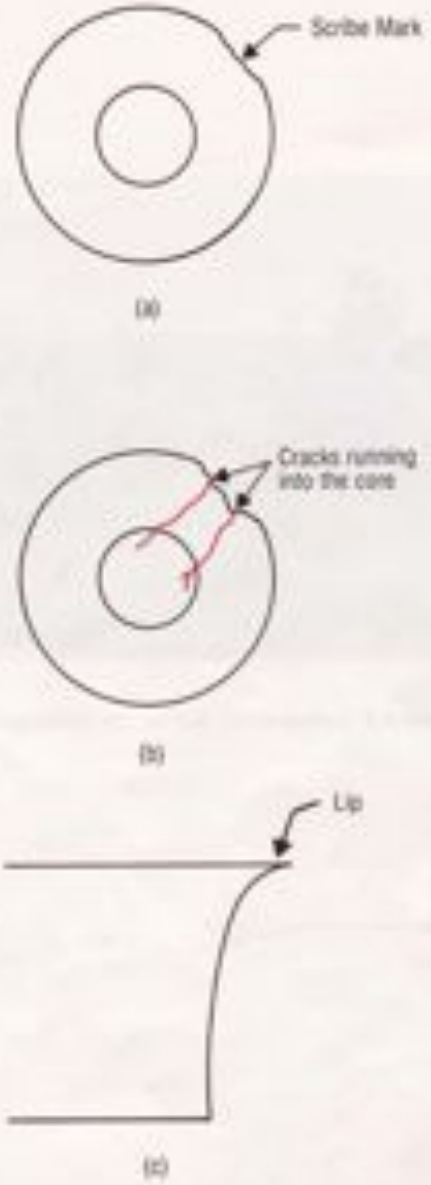

Figure 1.6. Cleaved fiber ends. (a) good cleave. (b) cracked fiber. (c) Side view of a lip on the end of a fiber.

Figure 1.7. Laboratory set-up for determination of fiber NA.

NOTE: The F-CL1 Fiber Cleaver is much more dependent on operator skill than is the F-BK2 which you may choose to use as an option in place of the F-CL1. In that case, follow the directions that are included with the F-BK2 Fiber Breaker and cleave the ends of the fiber. (You will still need to use the F-CL1 in Project #4, so you may want to gain some experience with it at this time.

1.6.2 MEASURING NUMERICAL APERTURE

1. Bolt the Model 807 Laser Mount to the Model 340C Clamp, using 1/4-20 bolts from the SK-25 Screw Kit. Place the 340C Clamp on the Model 41 Short Rod. Mount this on the LS-22 Breadboard. Place the Model U-1301P HeNe Laser into the 807 Mount. Tighten the set screw. Do not overtighten as this will damage the laser. Plug the laser power supply into a 110V wall outlet. Plug the cord from the laser head into the power supply. Note that the plug from the laser head to its power supply can only be inserted one way. The laser is turned on at the key switch on the front of the power supply. The combination of the 807 Mount and the 340C Clamp will align the laser parallel to a line of bolt holes on the table if the Model 41 Short Rod is properly mounted on the table. Check the laser alignment with the line of bolt holes and adjust the Model 41 Short Rod, if necessary.

2. Mount the RSX-2 Rotation Stage to the breadboard so that the beam from the HeNe laser passes over the center hole of the rotation stage. The RSX-2 Rotation Stage will have to be placed at an angle to the line of bolt holes in order to bolt it into place as instructed, as shown in **Fig 1.7**. Mount the MPH-1 Micro-Series Post Holder on the rotation stage. Use an 8-32 screw to mount the MPH-1. The 1/4-20 threaded hole in the bottom of the MPH-1 is used only as a through hole. Place the MSP-1 Micro-Series Post in the MPH-1, as shown in **Fig. 1.7**.

3. Prepare a fiber segment, ~2 meters long, with a good cleave at each end face. The FPH-5 Fiber Holder comes as part of the FP-1 Fiber Positioner. Insert one end of the fiber into an FPH-5 Fiber Holder (you will need to have stripped at least 3" of the jacket from the fiber in order to do this and the following step) and place this holder into its FP-1 Fiber Posi-

tioner, which has been post-mounted on the RSX-2 rotation stage, using the MPH series post holder and the MSP series post.

4. Extend the tip of the fiber and orient the FP-1 Positioner so that the fiber tip is at the center of rotation of the stage. This is a critical step if an accurate value for the fiber NA is to be obtained.

5. Re-check the alignment of your light-launching system by making sure that the tip of the fiber remains at the center of the laser beam as the stage is rotated. This set up achieves plane-wave launching into the end of your fiber.

6. Mount the far end of the fiber in an FPH-S Fiber Holder (taken from an FP-1 Fiber Positioner) and the FP-1 Fiber Positioner. You can get a quick approximate measure of the fiber's NA with a 3x5 card placed a distance, L, away from the laser in a darkened room, as shown in **Fig. 1.8**. Measure the width, w, on the card of the spot out of the fiber and the distance, L, from the fiber to the card. The NA of the fiber is approximately $\sin^{-1}(\frac{1}{2}w/L)$. This is a quick method which is used when only an approximate measurement of a fiber's NA is needed.

7. Mount the detector head of the Model 815 Power Meter so that the output beam from the fiber is incident on the detector head, as shown in **Fig.1.7**. Make a hood of aluminum foil to keep stray room light off of the detector. You will find this to be necessary, because the power levels obtained in plane-wave launching are low. Block the laser beam and note the power measured by the power meter. This determines the stray light seen by the meter. You will need to subtract this amount from all of your data.

8. Measure the power accepted by the fiber as a function of the incident angle of the plane-wave laser beam. Use both positive and negative rotation directions to compensate for any remaining error in laser-fiber alignment.

9. Plot the power received by the detector as a function of the sine of the acceptance angle. Semi-log paper is recommended. Measure the full width of the curve at the points where the received power is at 5% of the maximum intensity. The half-width at this intensity is the experimentally determined numerical aperture of the fiber. Compare your results with the results of Step 6 and Fig 1.5.

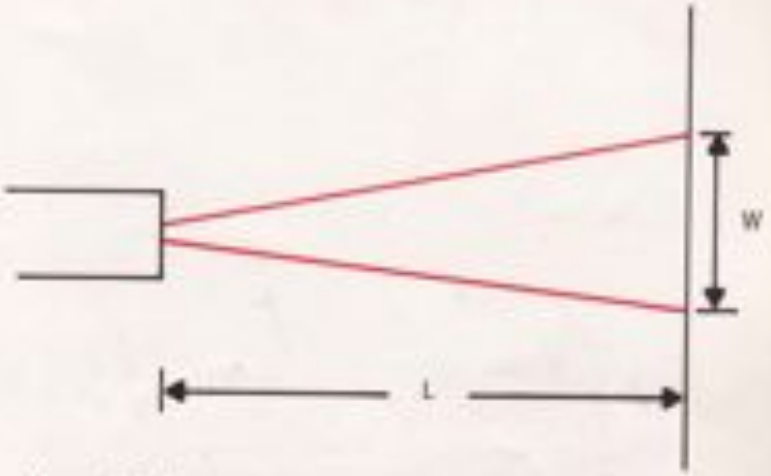

Figure 1.8. Approximate measure of the NA of a fiber.

2.0 PROJECT #2: FIBER ATTENUATION

In this exercise, you will measure one of the most important fiber parameters, the attenuation per unit length, of a multimode communications-grade optical fiber. The technique demonstrated here is called the "cutback method" and is generally used for this measurement.

You will also be introduced to the way that the conditions under which light is launched into the fiber can affect this measurement. You learn about mode scrambling and how to generate a desirable distribution of light in the fiber.

2.1 MEASUREMENT OF OPTICAL FIBER ATTENUATION

Section 0.4.1 contained a detailed description of the loss mechanisms in optical fibers. An expression for the amount of optical power which still remains in a fiber after it has propagated a distance, z, was given in Eq. 0-20 as

$$I(z) = I(0)\, 10^{-\Gamma z/10} \tag{2-1}$$

The length of the fiber, z, is given in kilometers, and the attenuation coefficient, Γ, is given in decibels per kilometer (dB/km).

Because the designers of fiber optic systems need to know how much light will remain in a fiber after propagating a given distance, one of the most important specifications of an optical fiber is the fiber's attenuation. In principle, the fiber attenuation is the easiest of all fiber measurements to make. The method which is generally used is called the **"cutback method."** All that is required is to launch power from a source into a long length of fiber, measure the power at the far end of the fiber using a detector with a linear response, and then, after cutting off a length of the fiber, measure the power transmitted by the shorter length. The reason for leaving a short length of fiber at the input end of the system is to make sure that the loss that is measured is due solely to the loss of the fiber and not to loss which occurs when the light source is coupled to the fiber. **Fig. 2.1** shows a schematic illustration of the measurement system. (The mode scrambler shown in the figure was discussed in **Section 0.3.2.**)

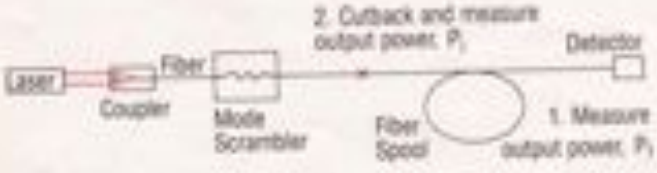

Figure 2.1. Schematic of laboratory set-up for cutback method of determining fiber attenuation.

The transmission through the fiber is written as

$$T = P_2/P_1 \tag{2-2}$$

where we have substituted P_1 (initial power) and P_2 (final power) for I(0) and I(z), respectively. A logarithmic result for the loss in decibels (dB), is given by

$$L\ (dB) = -10 \log (P_2/P_1) \tag{2-3}$$

The minus sign causes the loss to be expressed as a positive number. This allows losses to be summed and then

subtracted from an initial power when it is also expressed logarithmically. [In working with fiber optics, you will often find powers expressed in dBm, which means "dB with respect to 1 mW of optical power." Thus, e.g., 0 dBm = 1 mW, 3 dBm ≈ 2 mW, and −10 dBm = 100 μW. Note that when losses in dB are subtracted from powers in dBm, the result is in dBm. For example, an initial power of +3 dBm minus a loss of 3 dB results in a final power of 0 dBm. This is a shorthand way of saying "An initial power of 2 mW with a 50% loss results in a final power of 1 mW."]

The attenuation coefficient, Γ, in dB/km is found by dividing the loss, L, by the length of the fiber, z. The attenuation coefficient is then given by

$$\Gamma(\text{dB/km}) = (1/z)\,[-10 \log (P_t/P_i)]. \qquad (2\text{-}4)$$

The total attenuation can then be found by multiplying the attenuation coefficient by the fiber length, giving a logarithmic result, in decibels (dB), for the fiber loss.

2.2 PRACTICAL PROBLEMS

The cutback method works well for high-loss fibers, with Γ on the order of 10 to 100 dB/km. However, meaningful measurements on low-loss fibers are more difficult. The highest-quality fibers will have losses which are on the order of 1 dB/km or less, so that cutting a full 1 km from the fiber will result in a transmitted power decrease of less than 20%, putting greater demands on the measurement system's resolution and accuracy.

There is also an uncertainty due to the fact that the measured loss will depend on the characteristics of the way in which light is launched into the fiber. The launch conditions which result in an overfilled or underfilled fiber were discussed in **Section 0.3.2**. When a fiber is overfilled, many high-order and radiation modes are launched. These modes are more highly attenuated than are low-order modes. When a fiber is underfilled, mostly low-order modes are launched and lower losses occur.

The solution to this problem is to attempt to generate what is known as the stable mode distribution (also discussed in **Section 0.3.2**) as quickly as possible after launching. **Fig. 2.2** compares the transmission characteristics of the stable distribution with those of the overfilled and underfilled launch conditions. The stable mode distribution may be achieved, even in a short length of fiber, by using mode scrambling (**Section 0.3.2**) to induce coupling between the modes shortly after the the light is launched.

Mode scrambling generates an approximation of a stable distribution immediately after launch and allows repeatable measurements, which approximate those that would be found in the field, to be made in the laboratory. **Fig. 2.2** compares the optical power in a fiber as a function of propagation distance for the three types of launch conditions: overfilled, underfilled, and stable distribution. The slope of the curve at large distances is equal to the attenua-

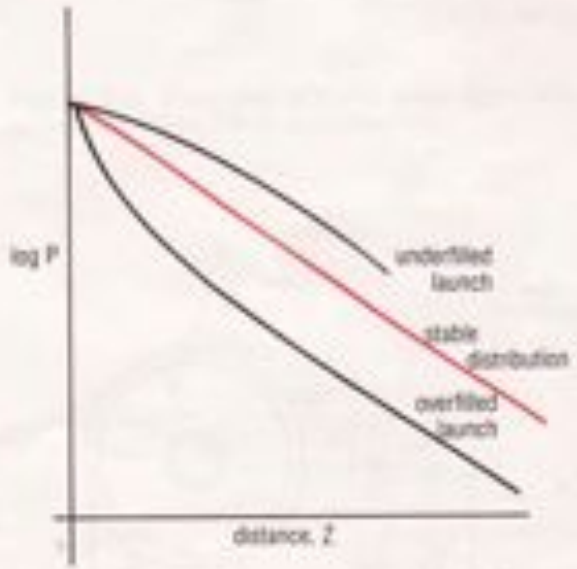

Figure 2.2. Comparison of attenuation characteristics of various launch conditions.

tion coefficient. It is the fact that the mode scrambling generates a stable distribution immediately after the source that allows a short cutback length to be used in the cutback method of measuring attenuation.

2.3 REFERENCE

1. D. Marcuse, *Principles of Optical Fiber Measurements*, Academic Press (New York) 1981, p. 226-236

2.4 PARTS LIST

Cat#	Description	Qty.
XSN-22	2x2 Breadboard	1
U-1301P	1 mw HeNe laser	1
807	Laser mount	1
340C	Clamp	1
41	Short rod	1
815	Power meter	1
F-916	Fiber coupler (w/o lens)	1
M-20X	20X Objective lens	1
F-CL1	Fiber cleaver	1
FK-BLX	Balldriver set	1
SK-25	¼-20 Screw kit	1
VPH-2	Post holder	1
SP-2	Post	1
FP-1	Fiber positioner	1
FM-1	Mode scrambler	1
F-MLD-500	100/140 MM fiber, 500 meters	1

Additional equipment required: Methylene chloride for stripping the jacket from the fiber. (Many commercially available paint thinners contain methylene chloride and work well for this purpose. Methylene chloride is toxic and can be absorbed through the skin. Any methylene chloride which gets on your skin should be washed off immediately.) Microscope slide cover glass for monitoring the positioning of the fiber in the F-916 Fiber Coupler.

2.5 INSTRUCTION SET

1. Prepare both ends of the 500 meter fiber spool which has been provided, as you learned to do in Project #1 **(Section 1.6.1, Steps 1–3)**. This fiber is the Newport F-MLD-500 fiber with a 100-μm core and a 140-μm OD. You may have to use some care in freeing the end of the fiber which was the start of the winding onto the spool. (This end will be referred to as the far end of the fiber.)

2. Place the cleaved far end of the fiber in an FPH-S holder which has been removed from an FP-1 Fiber Positioner and insert this into the post-mounted FP-1. Also, post mount the detector head of the Model 815 power meter. Align the detector head with the fiber end so that you will be able to measure the output power. The laboratory set-up for this project is shown in **Fig. 2.3**.

3. The use of the F-916 Fiber Coupler to couple light from a HeNe laser into a fiber is illustrated in **Fig. 2.4**. Align the coupler and the HeNe laser so that the laser beam shines along the axis of the F-916 Fiber Coupler. Mount a 20X microscope objective in the F-916. Place the cleaved front end of the fiber into the fiber chuck from the F-916 and insert this into the coupler. Carefully align the fiber to maximize the light launched into the fiber, using the power meter to monitor the launched power. Use a microscope slide cover glass in the path of the laser beam to look at the Fresnel reflection from the fiber end face. Focus the Fresnel reflected beam by adjusting the z component of the fiber position, as defined in **Fig. 2.4**; this is done by turning the z adjustment knob on the fiber positioner. When this reflection is focused, the fiber end face is in the focal plane of the coupler's microscope objective lens.

4. Position the FM-1 Mode Scrambler at a convenient place near the launch end of the fiber, as shown in **Fig. 2.3**.

5. Rotate the knob of the FM-1 counter-clockwise to fully separate the two corrugated surfaces. The FM-1 Mode Scrambler is illustrated in **Fig. 2.5**. Place the fiber between the two corrugated surfaces of the Mode Scrambler. Leave the fiber jacket on to protect the fragile glass fiber. Rotate the knob clockwise until the corrugated surfaces just contact the fiber. Examine the far-field distribution of the output of the fiber. Rotate the knob further clockwise and notice the changes in the distribution as the amount of bending of the fiber is changed. Since a narrow, collimated HeNe beam is being used to launch light into the fiber, the original launched distribution will be underfilled. When the distribution of the output just fills the NA of the fiber, an approximation of the stable distribution has been achieved. Do not add any more bending than is necessary to accomplish this, since that will result in excess loss. This launching and mode scrambling set-up should not be changed

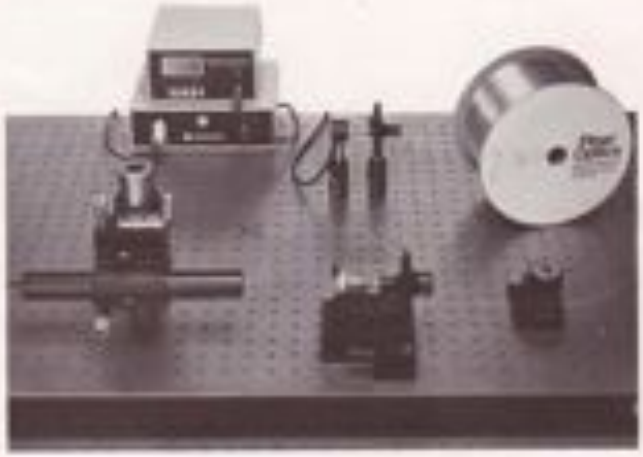

Figure 2.3. Laboratory set-up for determining fiber attenuation using the cutback method.

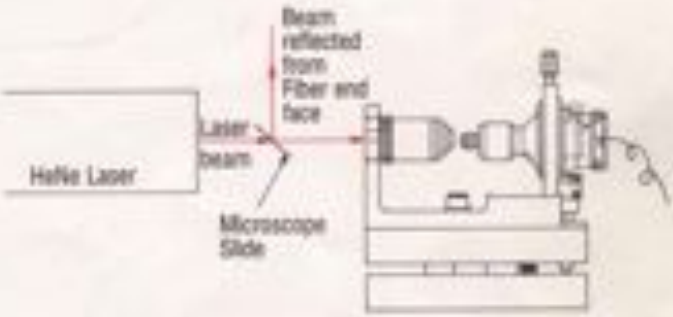

Figure 2.4. Coupling of HeNe laser light into a fiber using the F-916 Fiber Coupler.

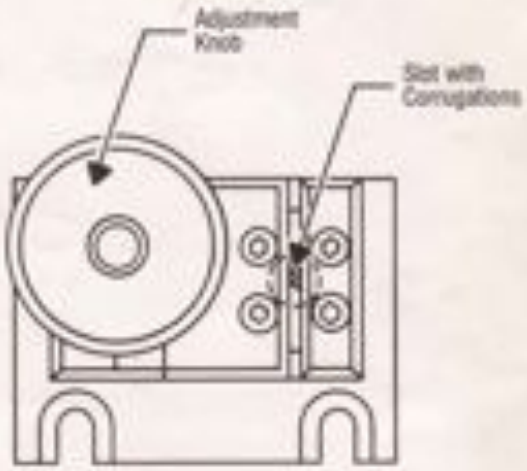

Figure 2.5. Model FM-1 Mode Scrambler.

again during the remainder of the exercise.

6. Measure the power out of the far end of the fiber. Note the exact length of the fiber. It will be part of the information on the label of the spool.

7. Break off the fiber ~2 meters after the mode scrambler (see **Fig. 2.1**) from the launching set-up. (Be sure to note on the spool how much fiber you have removed, so that other people using the same spool in the future will be able to obtain accurate results.) Cleave the broken end of the fiber and measure the output from the cutback segment.

8. Calculate the fiber attenuation, using Eq. 2-4, and compare this with the attenuation written in the fiber specification on the spool. Your value is probably somewhat higher than the specification. Why? (**HINT**: Go back and look at **Fig. 0.25**. Remember, the HeNe laser operates at a wavelength of 633 nm.)

3.0 PROJECT #3: SINGLE-MODE FIBERS I

In this project you will begin the first of two exercises which consider the modal properties of fibers and the properties of single-mode fibers. You will learn to couple laser light into a 4-μm diameter core single-mode fiber. You will then measure the far-field power distribution of the fiber as a function of angle and determine how well it fits a theoretical model which will be described in the following discussion.

3.1 SINGLE-MODE FIBERS

In the first two projects, some of the properties of multimode fibers were explored. The properties of multimode fibers are easily described in terms of the paths of light rays propagating down the fibers. This ray picture of light propagation is adequate for describing large-core-diameter fibers with many propagating modes, but it fails for small-core-diameter fibers with only a few modes or with only a single mode. For fibers of this type, it is necessary to describe the allowed modes of propagation of light in the fibers.

A detailed description of the propagation characteristics of an optical fiber can be obtained by solving Maxwell's equations for the cylindrical fiber waveguide. This leads to knowledge of the allowed modes which may propagate in the fiber. When the number of allowed modes is very large, the mathematics becomes very complex; this is when the ray picture is used to describe the waveguide properties. The solution of Maxwell's equations for the allowed modes of a fiber was outlined in **Section 0.3.1**.

In that section, it was found that an important quantity in characterizing a fiber waveguide is a quantity which is called the V-number of the fiber. Recalling Eq. 0-15, it was written as

$$V = k_0 \cdot a \cdot NA \qquad (3\text{-}1)$$

where k_0 is the free-space wavenumber, $2\pi/\lambda_0$ (λ_0 is the wavelength of the light in free space), a is the radius of the core, and NA is the numerical aperture of the fiber. The V-number can be used to characterize which guided modes are allowed to propagate in a particular waveguide structure. When $V < 2.405$, only a single mode, the HE_{11} mode, may propagate in the waveguide. This is the single-mode regime. The wavelength at which V is equal to 2.405 is called the **"cut-off wavelength,"** (denoted by λ_c) because that is the wavelength at which the next higher-order mode is cut off and no longer propagates.

The Newport F-SV fiber has a core diameter of 4 μm and an NA of 0.11. Therefore, according to Eq. 3-1, this fiber has a V-number of 2.19 for 633 nm light, putting it well within the single-mode regime. This is the fiber which you will be using in this project.

3.2 GAUSSIAN APPROXIMATION

In waveguides in which the diameter of the core is extremely large compared to the wavelength of the light

Figure 3.1. Irradiance of a Gaussian beam.

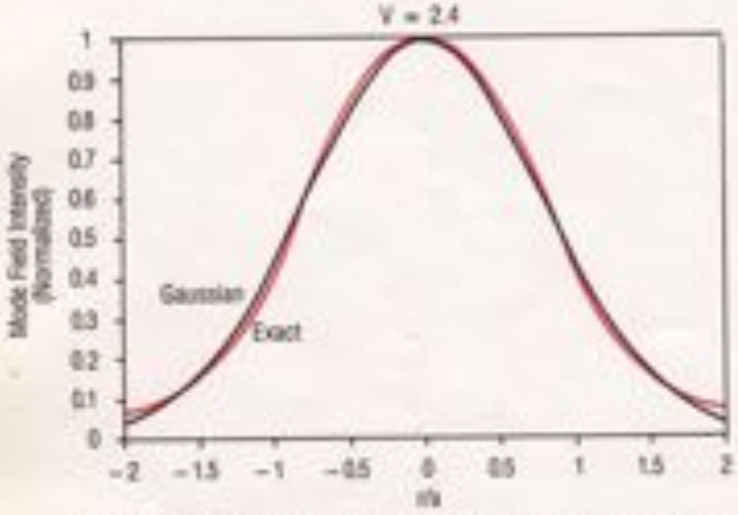

Figure 3.2. Comparison of the exact mode field intensity and its Gaussian approximation near the cut-off wavelength (V=2.4).

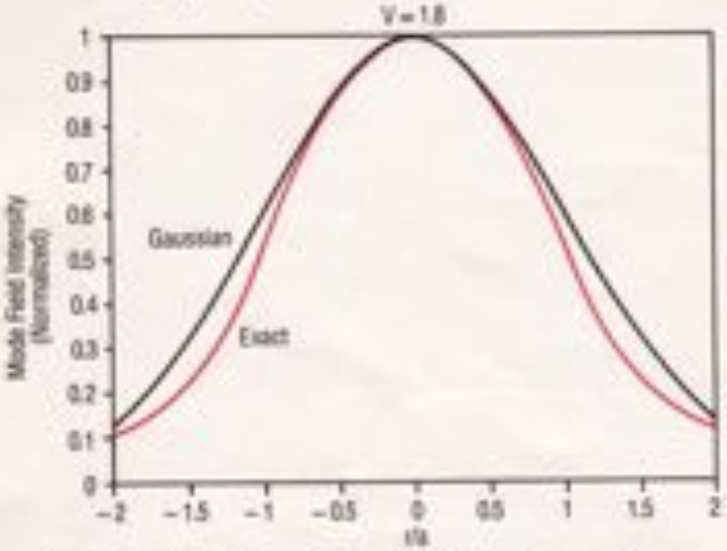

Figure 3.3. Comparison of the exact mode field intensity and its Gaussian approximation further from the cut-off wavelength (V=1.8).

(for example, the HeNe laser tube described in **Section 0.4.2** and **Fig. 0.27**), the lowest order mode has an irradiance pattern which is **Gaussian**. That is, the irradiance as a function of distance from the beam axis has the form

$$I(r) = I(0) \exp(-r/r_o)^2, \qquad (3\text{-}2)$$

where I(0) is the irradiance at the center of the beam and r_o is a measure of the radius of the beam, the radius at which the irradiance is $1/e^2$ of that at the center of the beam. **Fig. 3.1** shows the irradiance of a Gaussian beam.

The HE_{11} mode of a fiber is very close to a Gaussian mode when the light is near the cut-off wavelength.[1] **Fig. 3.2** shows the shape of the fundamental HE_{11} mode near the cutoff of the next-higher-order mode (that is, with V only slightly less than 2.405), as a function of r/a, where r is the radial position and a is the core radius. While the red line in the figure represents the actual distribution of the mode, the black line is a Gaussian. The two curves are quite similar and the exact solution near the cut-off wavelength is often approximated by a Gaussian. In the case of a parabolic profile fiber with an infinite core diameter, the Gaussian function is the exact solution for the fundamental mode.

Fig. 3.3 shows the exact modal distribution along with the Gaussian approximation for a longer wavelength, further from cutoff. It can be seen that the Gaussian approximation is not as good as one gets away from the cut-off wavelength. However, the qualitative shape of the exact solution curve is still not too far from Gaussian.

In this project, you will be exploring this Gaussian approximation for a single-mode fiber.

3.3 COUPLING TO A SINGLE-MODE FIBER

Coupling light into a multimode fiber is relatively easy. However, maximizing the coupling to a single-mode fiber is much more difficult. In addition to very precise alignment of the fiber to the incoming beam, it is necessary to match the incident electromagnetic field distribution to that of the mode which will be propagated by the fiber. The mode profile of the HE_{11} mode of a step-index single-mode fiber can be approximated by a Gaussian distribution with a $1/e^2$ spatial half-width given by[2]

$$w_o = a\,(0.65 + 1.619\,V^{-1.5} + 2.879\,V^{-6}), \qquad (3\text{-}3)$$

where a is the fiber core radius. For example, when V=2.405, the Gaussian spot size is approximately 10% larger than the core diameter. Therefore, in this case, the incident light should be focused to a spot size which is 1.1 times the fiber core diameter at the fiber end face. **Fig. 3.4** is a plot of the normalized radius of the Gaussian distribution as a function of the V-number. It can be seen that, for a fiber of given radius, as V becomes smaller (as λ becomes longer) the spot size increases. As the wavelength

increases, the electromagnetic field of the mode is less well confined within the waveguide. For this reason, single-mode fibers are designed so that the cutoff wavelength is not too far from the wavelength of the light intended for use with the fiber. Typically, λ_c will be about 80–90% of the wavelength at which the fiber is designed to be used.

3.4 REFERENCES

1. L. B. Jeunhomme, *Single-Mode Fiber Optics, Principles and Applications*, Marcel Dekker (New York) 1983, p. 16

2. ibid, p. 18, or D. Marcuse, "Loss analysis of single-mode fiber splices," Bell System Technical Journal *56*, 703 (1977)

3.5 PARTS LIST

Cat#	Description	Qty.
F-SV-20	4/125 SM fiber, 20 meters	1
XSN-22	2x2 Breadboard	1
U-1301P	1 mw HeNe laser	1
807	Laser mount	1
340C	Clamp	1
41	Short rod	1
815	Power meter	1
F-916	Fiber coupler (w/o lens)	1
M-20X	20X Objective lens	1
F-CL1	Fiber cleaver	1
FK-BLX	Balldriver set	1
SK-25	¼-20 Screw kit	1
SK-08	8-32 Screw kit	1
RSX-2	Rotation stage	1
MPH-1	Micro-series holder	1
MSP-1	Micro-series post	1
FP-1	Fiber positioner	1

Additional equipment required: Razor blades and tape to construct the slit mask for the power meter detector. Methylene chloride for stripping the F-SV fiber. (Many commercial paint strippers contain methylene chloride and work well for this purpose. Methylene chloride is toxic and can be absorbed through the skin. Any methylene chloride which gets on your skin should be washed off immediately.) Microscope slide cover glass for monitoring the positioning of the fiber in the F-916 Fiber Coupler.

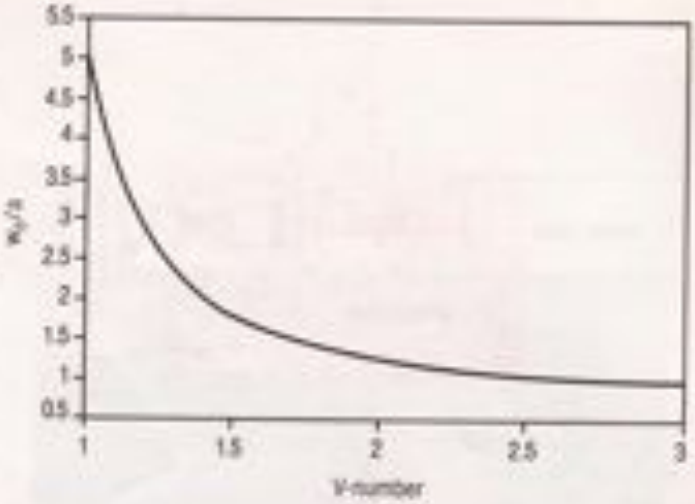

Figure 3.4. Mode field radius as a function of V-number.

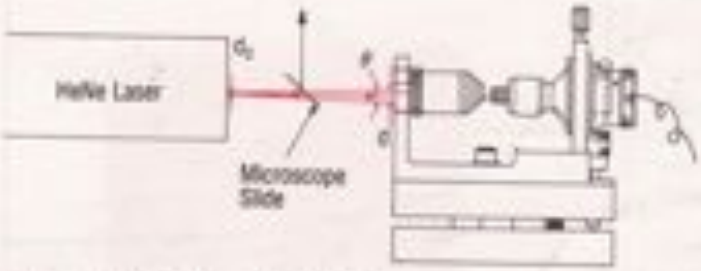

Figure 3.5. Coupling of HeNe laser light into a single-mode fiber.

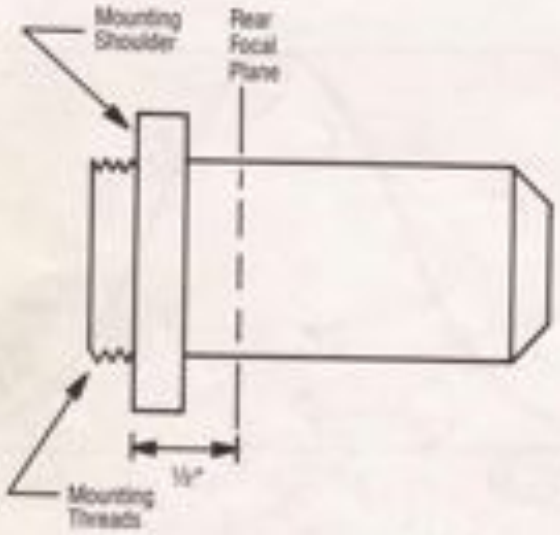

Figure 3.6. Microscope objective lens, showing the rear focal plane.

3.6 INSTRUCTION SET

3.6.1 OPTIMIZING SINGLE-MODE COUPLING

1. Using Eq. 3-1, confirm that V=2.19 at a wavelength of 633 nm for the F-SV fiber (NA=0.11). Use Eq. 3-3 to find the spot size of the fiber mode for this V-number. (Spot diameter = $2w_o = 1.2 \times 2a$.)

2. When coupling light into a single-mode fiber, one begins by using a microscope objective lens to focus the collimated beam from a laser to a small spot. The diameter, d_o, of the spot size at the waist of the focused laser beam can be determined from the local length, f = 8.3 mm, of the microscope objective lens, and the diameter, d, of the laser beam at the rear local plane of the objective lens, using $d_o = 4kf/\pi d$. (d may be found from the divergence of the laser, which is 1.3 mrad, and the distance from the laser to the objective lengths, using an equation from Gaussian optics, $d = d_0\sqrt{1+(z\theta/d_0)^2}$. In this equation, d_0 is the diameter of the laser beam at the output of the laser, 0.63 mm for the laser which you are using, z is the laser-to-lens distance, and θ is the beam divergence of 1.3 mrad or .0013 in the equation.)

3. If your calculations in Steps 1 and 2 show that $d_o = 2w_o$, then optimized coupling should be obtained when the input beam is focused on the fiber core, as shown in **Fig. 3.5**. If $d_o \neq 2w_o$, then the value of d_o must be adjusted by changing the distance between the F-916 coupler and the laser. For example, moving the laser further from the objective lens causes the input beam diameter, d, to become larger due to the beam divergence of the laser. This, in turn, causes d_o to become smaller.

4. Mount the HeNe laser and the F-916 Fiber Coupler, with the 20X objective lens, so that the laser beam is parallel to the lens axis and strikes the lens at its center, as is illustrated in **Fig. 3.5**. Be sure to place the lens/fiber-positioner assembly, which forms the top of the coupler, so that the rear local plane of the microscope objective lens is directly over the pivot of the tilt platform. The rear focal plane of the M-20X objective lens is ½" in front of the lens, as shown in **Fig. 3.6**.

5. Cut a segment of F-SV fiber of about two meters in length and cleave both ends as you did in Project #1 **(Section 1.6.1, Steps 1-3)**. (Chemical stripping in methylene chloride is recommended. You will not be able to strip this fiber with a razor blade, if you have been using that method.) Mount one end of the fiber in the fiber holder from the F-916 coupler and insert it into the F-916. Use the microscope slide cover glass to monitor the Fresnel reflection from the fiber end face, as you did in Project #2 **(Section 2.5, Step 3)**, and bring the end of the fiber into the focal plane of the objective lens by rotating the coarse adjustment knobs on the FP-1 positioner of the F-916 coupler. This will assure that the z-component of the fiber alignment is approximately correct and will assure that the laser beam is at least striking the fiber end face, if not the core.

6. Adjust the x and y components of the fiber alignment, using the fine adjustment knobs on the tilt stage of the F-916 Fiber Coupler, to achieve the maximum coupling of the laser beam into the fiber. You may wish to refer again to the F-916 instruction sheet to understand the principle of operation of the tilt stage adjustment. Monitor the output power using the Model 815 Power Meter. For someone who has never done single-mode coupling before, a total loss (from laser output to fiber output) of 3 dB (50% loss; see **Section 2.1**) would be considered to be a good result, but with experience one should be able to consistently achieve losses of less than 2 dB (< 37% loss).

3.6.2 GAUSSIAN APPROXIMATION

1. Mount the far end of the fiber on the RSX-2 rotation stage in exactly the same way that the front end of the fiber was mounted in Project #1 **(Section 1.6.2, Steps 3, 4)**. The experimental set-up is shown in **Fig. 3.7**. This time, however, you will actually be measuring the far-field distribution of the fiber output. (The far-field of a fiber is usually said to start at a distance $z_0 = (2a)^2/\lambda$ from the end of the fiber. The far field is, effectively, the region where the fact that the core diameter is non-zero plays no role in the energy distribution.)

2. Mask the detector head, as shown in **Fig. 3.8**, and post-mount it on the table a few inches away from the fiber end face. Two razor blades taped together with a spacing of about .040" between the blade edges makes a good mask. Be sure that the tape that is used is not transparent to the laser light.

3. When you rotate the tip of the fiber by turning the rotation stage, you will be scanning the far-field power distribution of the fiber across the detector. Measure the power received by the detector as a function of the angular position of the fiber. Use both positive and negative angular

Figure 3.7. Laboratory set-up for examining the Gaussian approximation for a single-mode fiber.

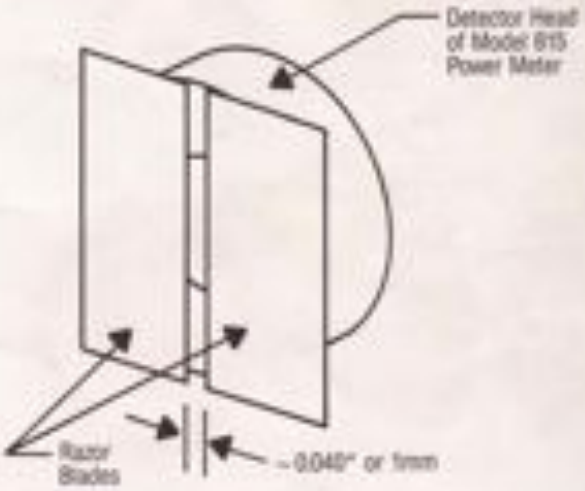

Figure 3.8. Masking of the detector with a slit made from two razor blades.

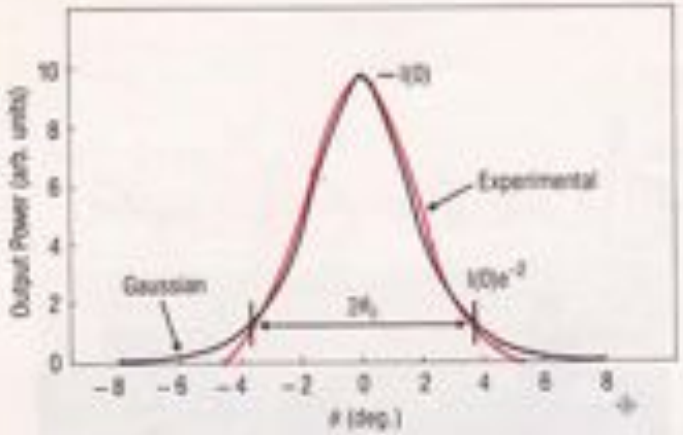

Figure 3.9. Plot of experimental data taken in Newport's laboratory. I(0) and θ_x found from this data are indicated.

deviations to compensate for any angular misalignment.

4. Plot the far-field distribution of the fiber as a function of angle. **Fig. 3.9** shows a plot of data taken in Newport's laboratory. Find the maximum recorded output power from your data. Call this value I(0). Now find the points where the output power is I(0)e^{-1}. Measure the full width between these two points as shown in **Fig. 3.9**. Take half of that full width and call it θ_x. Plot a Gaussian curve on the same graph with your experimental data. Use Eq. 3.2, substituting θ for r and θ_x for r_x. Compare the two plots and assess the validity of the Gaussian approximation for this fiber at this wavelength. (Most single-mode fibers have a step-index profile. In that case, the near-field distribution (scanning as a function of position across the end face of the fiber) and the far-field distribution (scanning as a function of angle far away from the fiber end face) will have the same form, with r/a and sinθ/NA substituting for each other as the scaling variables. We are then able to examine the Gaussian approximation by looking at the far-field distribution of the fiber output, since it will mimic the distribution as a function of position within the fiber.)

4.0 PROJECT #4: SINGLE-MODE FIBERS II

In Project #3 you had an introduction to single-mode fibers. In Project #4, you will continue to look at propagation in fibers which have a small V-number. This time you will start with a fiber which has a V-number which is slightly greater than 2.405. Such a fiber is a multimode fiber, but the number of allowed modes is small enough so that they may be individually identified when the output of the fiber is examined. Following that, you will look at a highly birefringent single-mode fiber, the polarization-preserving fiber, and measure its beat length.

4.1 FIBERS WITH V > 2.405

In **Section 0.3.1**, it was seen that if the V-number of a fiber is less than 2.405, then only a single mode may propagate in the fiber waveguide. This single mode is the HE_{11} mode, or, in the linearly-polarized mode theory for weakly-guiding waveguides (also discussed in **Section 0.3.1**), the LP_{01} linearly-polarized mode.

When V > 2.405, other modes may propagate in the fiber waveguide, as shown in **Fig. 4.1** (which is a repeat of **Fig. 0.15**). The first such linearly-polarized mode, which comes in at V=2.405, is the LP_{11} mode, the next-lowest order mode in the weakly-guiding approximation.

When V is just slightly greater than 2.405, only the LP_{01} and the LP_{11} modes may propagate. However, when V=3.832, two more linearly-polarized modes are now allowed to propagate. These are the LP_{21} mode and the LP_{02} mode.

The electromagnetic field distributions of these modes are shown in **Fig. 4.2** (which is a repeat of **Fig. 0.14**). If we have a fiber with the proper V-number, these modes can be selectively launched by varying the position and angle at which a tightly-focused beam of the proper wavelength is projected onto the fiber core. When this is done, the near-field of the fiber output can be inspected and the field distributions of the individual modes can be identified.

Newport's F-SS fiber is designed to be a single-mode fiber at a wavelength of 1300 nm. It has an NA of 0.11 and a core radius of 4 μm. At the 1300 nm wavelength, it has a V-number of 2.13. However, at a wavelength of 633 nm, it has a V-number of 4.39. These V-numbers can be verified by substituting a = 4 μm, NA = 0.11 and λ = 633 nm into Eq. 0-15. By examination of **Fig. 4.1**, it can be seen that this fiber should allow the LP_{01}, LP_{11}, LP_{21}, and LP_{02} linearly-polarized modes to propagate at the 633 nm HeNe laser wavelength.

In this project, you will use HeNe laser light to selectively launch different linearly-polarized modes in a length of Newport F-SS fiber.

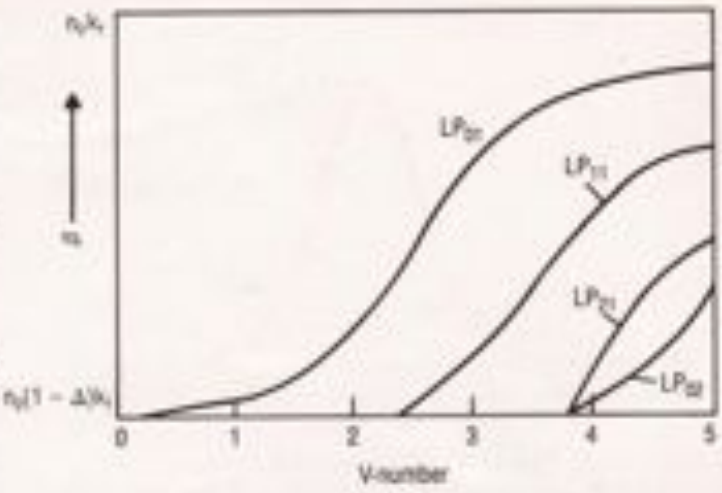

Figure 4.1. Low order linearly polarized modes of an optical fiber. Compare with Fig. 0.13. (This is a repeat of Fig. 0.15)

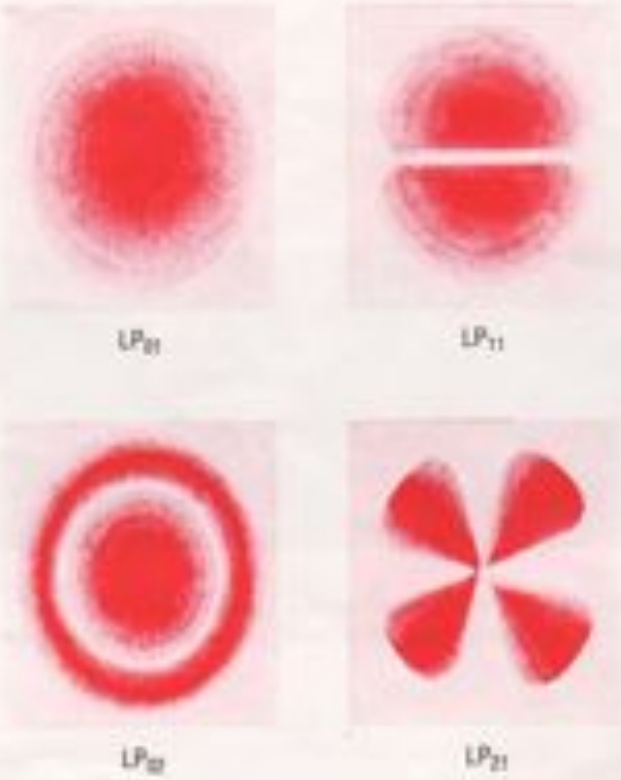

Figure 4.2. Irradiance pattern of some low order linearly polarized modes. (This is a repeat of Fig. 0.14)

4.2 POLARIZATION-PRESERVING FIBERS

The mode which propagates in a single-mode fiber, the fundamental HE_{11} mode, is actually a degenerate combination of two orthogonally-polarized components. In a perfectly symmetric, circular fiber, these components travel at the same velocity; that is, they have identical propagation constants. If the fiber is not perfectly symmetric, then the two polarization components have different propagation constants. The difference in their propagation constants, $\delta\beta$, is known as the birefringence of the fiber. The properties of birefringent fibers were discussed in detail in **Section 0.3.3**.

If light is launched with a linear component along each of the optical axes, the difference in propagation constants causes the net vector sum of the polarizations to vary periodically with distance along the fiber, as discussed in **Section 0.3.3**.

This sequence of alternating polarization states continues along the entire length of the fiber. The distance, L_p, over which the polarization rotates through an entire 360° is known as the beat length of the fiber. This is related to the birefringence by (repeating Eq. 0-16)

$$L_p = 2\pi/\delta\beta \qquad (4\text{-}1)$$

As was discussed in **Section 0.3.3**, this beat length can be observed visually when visible laser radiation is launched into a birefringent fiber with its direction of polarization oriented at an angle of 45° with respect to the principal axis of the fiber. Scattering centers in fibers emit dipole radiation. Since the radiation from a dipole is zero along its vibration axis, each time that the light becomes linearly polarized, there will be no scattering detectable when the fiber is observed with the line of sight along the vibration axis. This allows a direct measurement of L_p.

Polarization-preserving fibers have applications wherever the polarization of the transmitted light must be stable and well-defined. These applications include fiber interferometric sensors, fiber gyroscopes, and heterodyne detection systems.

4.3 PARTS LIST

Cat#	Description	Qty.
XSN-22	2x2 Breadboard	1
U-1301P	1 mw HeNe Laser	1
807	Laser mount	1
340C	Clamp	1
41	Short rod	1
F-916	Fiber coupler (w/o lens)	1
M-20X	20X Objective lens	1
F-CL1	Fiber cleaver	1
FK-BLX	Balldriver set	1
SK-25	¼-20 Screw kit	1
VPH-2	Post holder	2
SP-2	Post	2
FP-1	Fiber positioner	1
F-SS-20	8/125 SM fiber, 20 meters	1
F-SPV-10	Polar.-preserv. fiber, 10 m	1
M-40X	40X Objective lens	1
MH-2PM	Optics holder	1
FK-POL	Polarizer, sheet	1

missing 20X & 40X!

Additional equipment needed: Millimeter scale for measurement of beat length. Methylene chloride for chemical stripping of fibers. (Many commercial paint strippers contain methylene chloride and work well for this purpose. Methylene chloride is toxic and can be absorbed through the skin. Any methylene chloride which gets on your skin should be washed off immediately.)

4.4 INSTRUCTION SET

4.4.1 OBSERVING FIBER MODES

1. Prepare both ends of a segment of F-SS fiber approximately 2 meters in length as you did in Project #1 **(Section 1.6.1, Steps 1-3)**.

2. Couple the HeNe laser beam into the fiber using the F-916 coupler as described in Project #3 **(Section 3.6.1)**, optimizing the coupling efficiency.

3. Insert the far end of the fiber into a post-mounted FP-1 fiber positioner. Insert the 40X microscope objective into the MH-2PM Optics Holder and post mount this assembly. The laboratory set-up for this part of the project is shown in **Fig.4.3**.

4. Use the microscope objective to image the output end of the fiber on a convenient near-by wall. The farther the imaging distance, the larger the image will be. Three meters is a convenient working distance.

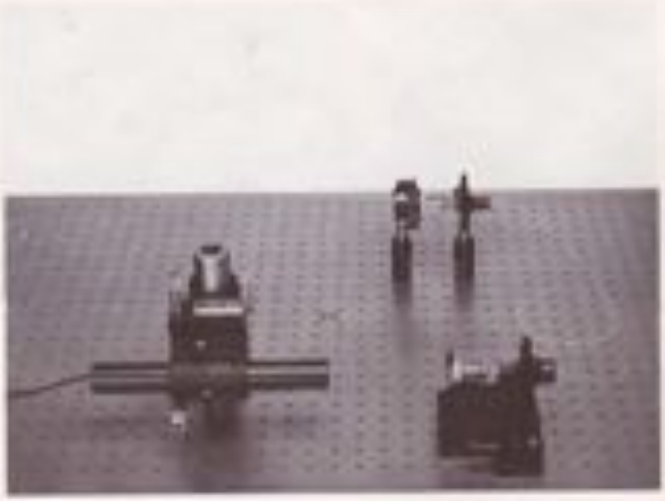

Figure 4.3. Laboratory set-up for observing low order modes in a multimode fiber with low V-number.

Figure 4.4. Laboratory set-up for orienting the polarization axes of the polarization fiber with the graduations on the chuck from the F-916 Fiber Coupler.

5. Examine this projection of the near-field distribution of the fiber. Change the x-y adjustment of the fiber position in the F-916. This has the effect of changing the position and angle of the launch of the focused laser beam into the fiber. Notice how this causes the projection of the near-field distribution of the fiber output to change.

6. Sketch the near-field images which you are able to obtain. Compare them with the LP_{lm} mode distributions shown in **Fig. 4.2**. Identify the patterns which appear to be pure LP_{lm} modes and those which are combinations of two or more LP_{lm} modes.

4.4.2 BEAT LENGTH OF A BIREFRINGENT FIBER

1. Cleave both ends of a ~1-2 meter segment of F-SPV fiber. This fiber requires chemical stripping in methylene chloride.

2. Be sure of the orientation of the polarization of the HeNe laser beam. Use the FK-POL Sheet Polarizer to check the laser's polarization axis. A method for determining the polarization axis of the sheet polarizer is given in **Section 9.6.2, Step 1**. Rotate the polarizer in front of the laser beam. When the power through the polarizer is a maximum, the plane of polarization of the laser is parallel to that of the sheet polarizer.

3. Substitute an FPH-S chuck from an FP-1 Fiber Positioner into the F-916 Fiber Coupler. Couple the HeNe laser light into the polarization-preserving fiber using the F-916 coupler, as you did in Project #3 **(Section 3.6.1)**.

4. Insert the far end of the fiber segment into the original chuck from the F-916. Loosen the set screw on the knob of the FPH-J and orient the chuck so that the major and minor axes of the slightly elliptical output spot are aligned with the 0° and 90° marks on the chuck. Tighten the set screw. The reason for doing this is so that you can now place this end of the fiber back into the F-916 coupler with the fiber axes at a known orientation with respect to the polarization of the laser beam. The arrangement of your equipment should be like that shown in **Fig. 4.4**.

5. Place the fiber end which you have just oriented in the chuck from the F-916 coupler back into the F-916. Orient the fiber at 45° with respect to the plane of polarization of the laser in the F-916 coupler.

6. Align the fiber to the laser beam as you did in Project #3 **(Section 3.6.1)**. Maximize the coupled power.

7. Chemically strip a section of the middle of the fiber. Use a magnifying lens in a darkened room to observe the beats in the fiber. You will be able to see alternating light and dark sections of the fiber. Measure the beat length. The beat length of this fiber is ~2 mm.

8. Calculate the birefringence, $\Delta\beta$. Calculate the refractive index difference between the fast and slow axes, $\Delta n = \Delta\beta(\lambda_o/2\pi)$.

9. Watch what happens if you change the orientation of the fiber axes to the plane of polarization of the laser beam. Give a qualitative description of the results.

5.0 PROJECT #5: COUPLING FIBERS TO SEMICONDUCTOR SOURCES

In this project, you will learn to couple semiconductor sources, i.e., injection laser diodes (ILD's) and light-emitting diodes (LED's), to optical fibers. ILD's and LED's are the sources generally used with optical fibers in communications and sensor applications. You will also experimentally determine the electrical and optical characteristics of these sources and learn the difference between them.

The coupling will be achieved using a 0.25-pitch graded-index (GRIN) rod lens. GRIN-rod lenses have become widely accepted for use in fiber optic applications because of their small size, convenient focal lengths and working distances, and high-quality images with low distortions.

The sources which you will be using are infrared devices, with the ILD emitting at approximately 780 nm and the LED centered at about 830 nm. Since these devices emit invisible radiation, proper safeguards must be used to ensure that the possibility of injury is eliminated. Never look directly into a laser beam or its reflection.

5.1 TYPES OF SOURCES

Two types of semiconductor light sources are used in fiber optic systems. These are light-emitting diodes (LED's) and injection laser diodes (ILD's). The theory of semiconductor devices was outlined in **Section 0.4.2** and is detailed elsewhere.[1,2] In this project, we will be concerned with the coupling of these devices to optical fibers.

A light source may be characterized by the distribution of power emitted from its surface among all of the possible ray directions. Sources are generally divided into two types, depending on the radiation distribution. These two types are Lambertian sources and collimated sources. A Lambertian source is one which emits light in all directions from each differential source element. A surface-emitting LED closely approximates a Lambertian source. A source which emits light only into a very narrow range of angles about the normal to its surface produces a collimated beam. The output of a HeNe laser approximates a collimated beam.

In general, the angular distribution of the source brightness can be expressed as (recalling Eq. 0-22)

$$B(\theta) = B_o (\cos \theta)^m, \quad \theta < \theta_{max} \qquad (5\text{-}1)$$

where θ_{max} is the maximum angle from the normal at which light is emitted and is determined by the geometry of the source. For a diffuse source, $m = 1$. For a collimated source, m is large. For intermediate cases, the source may be called a partially collimated source. The ILD is a special case. The far-field distribution of the radiation from an ILD diverges in a fan-shaped pattern with angles which are typically on the order of $15° \times 30°$. This is because the small emittance area of these devices (on the order of 1 μm on a side) causes the collimation of the far-field distribution of the

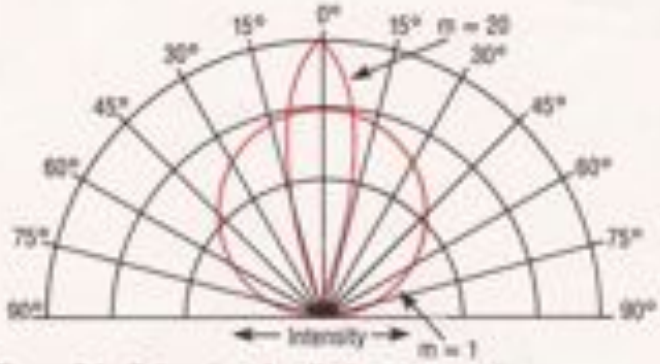

Figure 5.1. Polar plot of radiation patterns from typical ILD and LED sources.

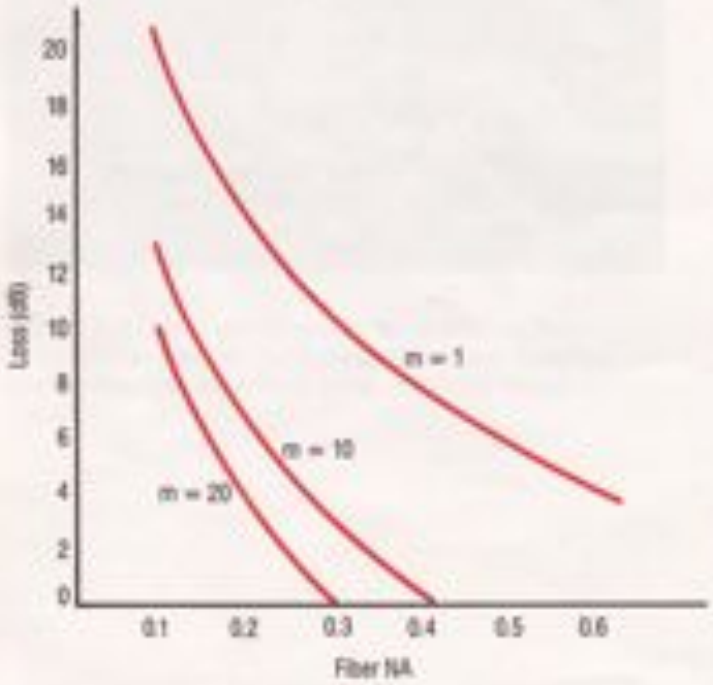

Figure 5.2. Plot of coupling loss as a function of fiber NA for various values of m, using Equation 5-2.

radiation to be limited by diffraction at the output. **Fig. 5.1** shows the output radiation characteristics, in polar coordinates, for two sources, one with m = 1 (typical of an LED) and one with m = 20 (typical of an ILD).

There are other properties which distinguish light-emitting diodes from laser diodes. These include the optical power-current curves which are characteristic of the devices and the polarization of the output beam. These properties were discussed in **Section 0.4.2.**

5.2 COUPLING EFFICIENCY

The amount of light energy which can be coupled into a fiber is dependent on the NA of the fiber. Since a fiber will accept only those light rays which are contained within a cone defined by the fiber's NA and core diameter, coupling loss will occur for sources which have an angular emission cone larger than the acceptance cone of the fiber's NA.

In some cases the fiber will be butt-coupled to the source. **Butt-coupling** is defined as coupling by placing the flat fiber end directly against the source, without the aid of any lens system. Butt-coupling cannot be achieved when the source is mounted in a package with a covering window glass. If the fiber is directly butt-coupled to the light source, the ratio of the power accepted by the fiber to the power emitted by the source can be shown to be[5]

$$P_c/P_s = 0.5\,[n + 1)(\alpha + (\alpha/2)]\,NA^2, \qquad (5\text{-}2)$$

where α is the index profile of the fiber. (In **Section 0.2.3**, it was stated that a parabolic graded-index would accept only one-half as much light as a step-index fiber. The factor $\alpha/\alpha + 2$ is a mathematical expression of this fact.) The coupling efficiency to either a graded-index ($\alpha = 2$) or a step-index ($\alpha = \infty$) fiber is proportional to the square of the numerical aperture and increases with increasing directionality (increasing m) of the source. The coupling loss in dB will be $-10 \log_{10} (P_c/P_s)$. **Fig. 5.2** shows the theoretical coupling loss as a function of fiber NA for some values of m.

For optimum coupling efficiency, one needs to match the source diameter-NA product to the fiber core diameter-NA product. This was discussed in detail in **Section 0.4.3.**

5.3 LENS COUPLING USING A GRIN-ROD LENS

This project uses a graded-index (GRIN)-rod lens to facilitate source-to-fiber coupling. Most optical devices used in fiber-optic systems employ lenses, and for most of these devices, GRIN-rod lenses have advantages over conventional lenses.

The GRIN-rod lens, which was described in **Section 0.2.4**, is a glass rod, 1.0 to 3.0 mm in diameter, with a radically-dependent index of refraction. This index of refraction is a maximum on the axis of the rod lens, and can be expressed as

$$n(r) = n_0(1-Ar^2/2), \qquad (5\text{-}3)$$

where n_0 is the index of refraction at the lens axis and $\sqrt{A}$ is referred to as the quadratic gradient constant. (This is really a restatement of Eq. 0-13, with $A = 2\Delta/a^2$.)

By far the most popular choice of GRIN-rod lens length is one-quarter pitch. This is because a beam travels exactly one quarter of a sinusoidal period in that distance. Therefore, a collimated beam incident on one end of the lens will be focused to a point on the opposite end of the lens. Conversely, any point source at the surface of a quarter-pitch lens will become a collimated beam at the far end, as was seen in **Fig. 0.11a**. The quarter-pitch lens will be used in **Projects #7, #9,** and **#10**.

Also widely used is the 0.29-pitch lens (which was illustrated in **Fig. 0.11b**), which is provided for use in this project. This lens is used to couple a laser diode to a fiber or a fiber to a detector. The lens which you will be using has $n_0 = 1.599$ and $\sqrt{A} = 0.332\ mm^{-1}$. Since the length of this lens is slightly more than one quarter pitch, the light from a point source will be converted to a converging beam, rather than a collimated beam.

Table 5-1 gives examples of the relationships between the working distances, l_1 and l_2, and the beam magnification, M, for the 0.29-pitch lens at a wavelength of 0.83 μm. l_1 is the working distance from the source to the lens, while l_2 is the working distance from the lens to the receiving fiber. The table may be used to optimize laser and fiber working distances. For example, a typical laser diode output may have a beam divergence cone with half-angle of about 15° at the half-power points in the direction perpendicular to the diode junction. Therefore, the e^{-1} power point for the Gaussian output beam will be at $\sin\Theta \approx 0.4$. Since the numerical aperture of a typical multimode communications fiber is ~ 0.2, a magnification of about 2 will optimize the laser-fiber coupling. If the physical dimensions of the device permit, l_1 and l_2 can now be adjusted to fit the required magnification. Note that the magnification in the table is the image size magnification; the beam divergence will be reduced by the same factor. The laser diode provided for use in this project has a diode-to-window distance of approximately 2.0 mm. Because of this, you will not be able to achieve a magnification of 2.0. The result is that the coupling loss will be about 4 dB when the laser-fiber coupling is optimized using the 0.29-pitch GRIN-rod lens.

TABLE 5-1

WORKING DISTANCES AND MAGNIFICATION OF THE 0.29-PITCH GRIN-ROD LENS

l_1 (mm)	l_2 (mm)	M
0.50	3.33	1.96
1.00	2.05	1.31
1.50	1.42	0.98
2.00	1.04	0.78

5.4 REFERENCES

1. H. Kressel and J. K. Butler, *Semiconductor Lasers and Heterojunction LED's*, Academic Press (New York), 1977

2. S. M. Sze, *Physics of Semiconductor Devices*, John Wiley & Sons (New York), 1969

3. M. K. Barnoski, in *Fundamentals of Optical Fiber Communications*, 2nd Edition, M. K. Barnoski, ed., Academic Press (New York), 1981, p. 158

5.5 PARTS LIST

Cat#	Description	Qty.
F-MLD-50	100/140 MM fiber, 50 meters	1
XSN-22	2x2 Breadboard	1
815	Power meter	1
F-CL1	Fiber cleaver	1
FK-BLX	Balldriver set	1
SK-25	¼-20 Screw kit	1
RS-05	¼-20 Thumbscrew kit	1
B-1	Base	2
VPH-2	Post holder	3
SP-2	Post	5
FP-1	Fiber positioner	1
F-925	GRIN-rod lens fiber coupler	2
FK-ILD	Laser diode assembly	1
FK-LED	Light-emitting diode assy.	1
FK-DRV	Driver circuit	1
FK-GR29	NSG SLW-1.8-0.29 lens	2
FK-POL	Polarizer, sheet	1
F-IRC1	IR phosphor card	1
CA-2	Universal clamp	2
MH-2PM	Optics holder	2

Additional equipment required: Digital voltmeter for monitoring ILD and LED currents. Methylene chloride for stripping the jacket from fibers. (Many commercially available paint strippers contain methylene chloride and work well for this purpose. Methylene chloride is toxic and can be absorbed through the skin. Any methylene chloride which gets on your skin should be washed off immediately.)

5.6 INSTRUCTION SET

CAUTION: READ THESE WARNINGS BEFORE PROCEEDING WITH THIS PROJECT.

The LED and ILD devices provided for use in this project are infrared devices which emit radiation which can damage the human eye even though it is invisible. Proper precautions must be taken to ensure that the beams cannot enter the eye. This means knowing exactly what the beam path is at all times, including the possibility of specular reflections. The laser output is current limited to meet Class I U.S. Federal Laser Safety Requirements. The output is limited so that not more than 35 μw of optical power will pass through a 7 mm diameter aperture at a distance of 20 cm from the source. Removal of the calibration labels on the FK-DRV driver circuit will invalidate the Class I certification.

CAUTION: Use of controls or adjustments or performance of procedures other than those specified herein may result in hazardous radiation exposure.

CAUTION: The use of optical instruments with this product will increase eye hazard.

The FK-ILD diode should be used only with the FK-DRV driver with the same serial number. They are not to be interchanged with other similar modules. Use of any other driver could destroy the laser and could cause hazardous radiation to be emitted. Use of any other driver will invalidate the Class I certification.

Also, it is important to remember that semiconductor infrared sources are highly sensitive devices. When going through the instruction set, check and double-check to be sure that all connections have been properly made, and carefully follow all directions for device operation. A wrong connection can cause the catastrophic failure of either the ILD or the LED. Before each use visually inspect the laser diode in the FK-ILD assembly to check for damage to the diode.

SERVICE: Do not attempt to replace the diode in the FK-ILD assembly. This will invalidate the Class I certification. Any repair to either the FK-ILD or FK-DRV must be performed at the factory by Newport Corporation.

5.6.1 INJECTION LASER DIODE

1. The FK-ILD Laser Diode Assembly is mounted in a threaded plate. Insert this plate into an MH-2PM Optics Holder. Post mount this assembly using two SP-2 Posts and the CA-1 Universal Clamp. Mount this on a B-1 Base. Secure the base to the table using two 1/4-20 thumbscrews from the BS-05 Thumbscrew Kit. The proper set-up can be seen in **Fig. 5.3.**

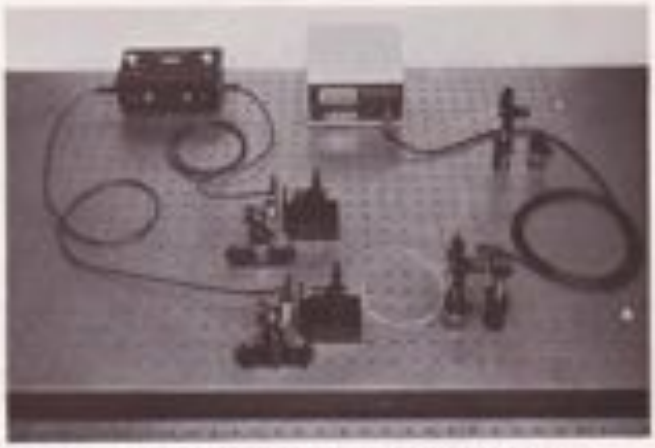

Figure 5.3. Laboratory set-up for coupling semiconductor sources to optical fibers.

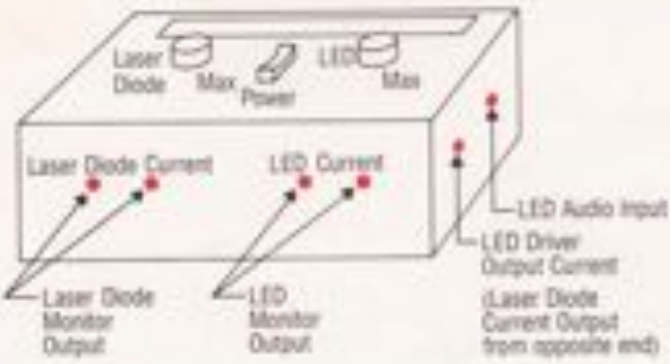

Figure 5.4. Laser Diode-LED Driver, Model FK-DRV.

Figure 5.5. Placing a 0.29-pitch GRIN-rod lens in the V-groove of the Model F-925 GRIN-Rod Lens Coupler.

2. **Make the following connections only when the diode power supply is off**. The driver which you will be using to power the ILD and LED is illustrated in **Fig. 5.4**. Connect the ILD to the driver circuit. Attach a voltmeter across the output monitor pins of the circuit, as shown in **Fig. 5.4**. The voltage measured at this point may be used to monitor the current through the ILD. The monitor voltage to laser current calibration is 70 mV per mA. The current in the diode should never exceed 100 mA. Typical operating current is 65 mA, with a typical threshold current of 50 mA. **It is very easy to blow out an ILD by exceeding current specifications.**

3. Place the detector head of the 815 power meter directly in front of the laser window. Increase the diode current to the operating current listed for the device. Monitor the output power as the current is increased. Make note of the power obtained when the listed optimum operating current is reached.

4. Reduce the current through the laser to zero. Now, slowly increase the current, recording the coupled output power as a function of diode current. Take data between current = zero and the listed operating current.

5. Plot the results. Draw a line along the rise in power above the onset of lasing. Extend this line down through the current axis. Compare the current at this point with the listed threshold current. This is the technique used to determine the laser's threshold current.

6. The F-IRC1 IR Phosphor Card may be used to view the laser output. Place the phosphor card in the path of the beam at a convenient viewing distance. Measure the widths of the beam parallel and perpendicular to the width of the diode junction. Using this and the distance from the device, calculate the divergence of the beam. The manufacturer specifies a divergence of about $15° \times 30°$ for this laser.

7. Place a polarizing sheet with a known polarization axis in the laser beam and determine the plane of polarization of the laser output.

8. Place the 0.29-pitch GRIN-rod lens into the groove of the F-925 coupler, as shown in **Fig. 5.5**. The lens should extend out of the coupler ~1 mm toward the ILD. Insert a cleaved segment of F-MLD fiber into the FP-1 of the coupler using the FPH-S holder and couple the laser output into the fiber through the GRIN-rod lens.

9. Optimize the coupling and determine the coupling loss, using the power coupled into the fiber and the power out of the ILD which you measured in Step 3. You will get the best coupling with the laser window as close to the lens as possible. With the Sharp LT020MC laser diode, which is used here, and the F-MLD fiber, a coupling loss of about 4 dB should be obtained.

10. **Reduce the laser current to zero. Disconnect the diode from the circuit before turning off any other part of the circuit.**

5.6.2 LIGHT-EMITTING DIODE

1. Post mount the FK-LED Light-Emitting Diode Assembly in the same way in which you mounted the ILD. (See **Fig. 5.3**)

2. Connect the LED to the driver circuit. Connect a voltmeter across the LED monitor pins. The monitor voltage to LED current calibration is 50 mV per mA. Turn the current up to 100 mA and record the power out of the device. The LED driver circuit has a current limiter at 120 mA.

3. Reduce the LED current to zero. Record the power out of the coupled LED as a function of current from zero to approximately 110 mA (10% over the optimum current). The data should provide a good fit to a straight line, a characteristic typical of LED's.

4. Place the F-IRC1 IR Phosphor Card in the path of the LED output. The LED has a microlens over the semiconductor chip; all of the output power will not be accepted by the lens, and the output will appear to be better collimated than might be expected from the discussion of **Section 5.1**. However, you will still see a marked contrast to the output of the ILD.

5. Place the polarizer used previously in the LED output beam. Confirm that the LED output is unpolarized.

6. Couple the LED to the fiber using the F-925 GRIN lens coupler as you did in Steps 8 and 9 of the previous section. Calculate the coupling loss using the power coupled into the fiber and the power out of the LED which you measured in Step 2.

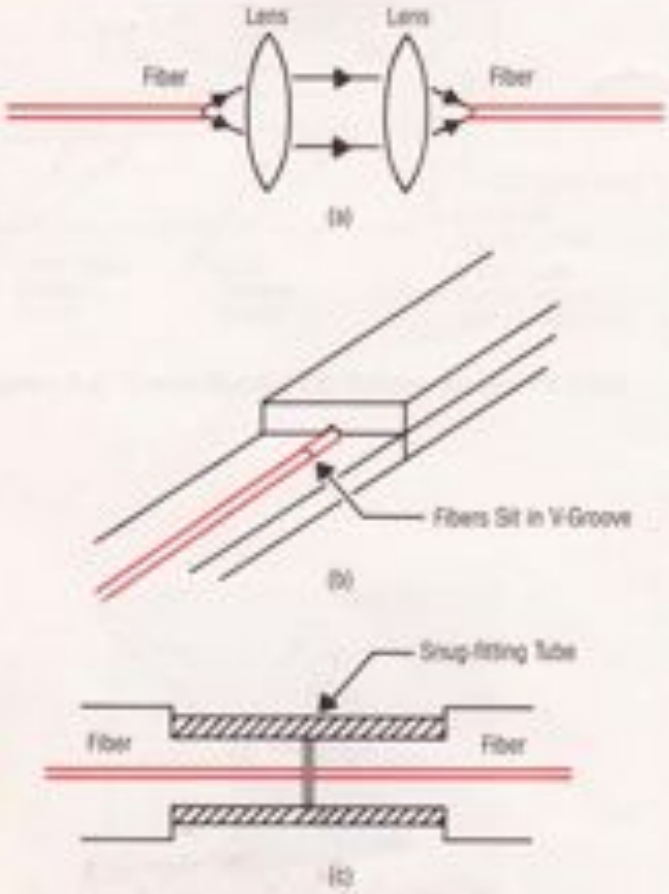

Figure 6.1 Schematic depiction of connector types. a) Lens type. b) Precision v-groove type. c) Snug-fitting tube type used in this project.

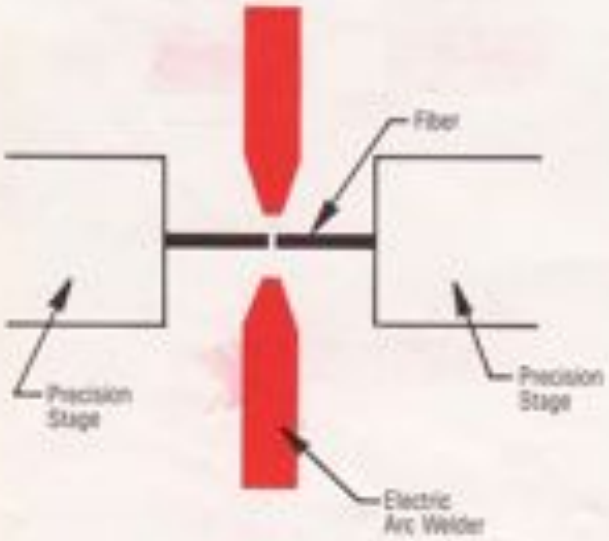

Figure 6.2. Fiber splices by thermal fusion. Fusion welder using electric arc. Microtorch may also be used.

6.0 PROJECT #6: CONNECTORS AND SPLICES

In addition to the need for coupling LED and ILD sources to fibers, as was explored in the previous project, we also need to look at the problem of connecting fibers to fibers. Both mateable-demateable connectors and permanent splices will be studied in this project.

You will begin this project by exploring the effects of misalignments on the coupling of two fibers. This will give you an understanding of the loss mechanisms seen in connectors and splices. You will then go on to couple fibers together using both connectors and splices.

6.1 FIBER COUPLING COMPONENTS

Both permanent splices and connectors which can be repeatedly coupled and uncoupled are used for coupling fibers to fibers. Each has its own area of applications. The connector finds application in the connection of fiber cables to transmitter and receiver modules, and in the connection to devices in optical communications systems. Permanent splices are required for joining sections of fiber in long distance communications links as well as for the construction of integrated fiber sensor systems.

Connectors use alignment techniques which fall into two general categories,[1] which are shown in **Fig. 6.1**. Lensed systems (**Fig. 6.1a**) image the core of one fiber onto the core of the second fiber. Other techniques use butt-coupling of fibers to achieve the connection. Butt-coupled connectors can be further divided into sub-categories. In some, precision grooves are used to align the fibers to each other (**Fig. 6.1b**). In others, including the connectors used in this project, snug-fitting tubes are used to align precision-machined ferrules with respect to each other (**Fig. 6.1c**). Typical insertion losses for connections between multimode fibers are less than 1.0 dB.

Fiber splicing is the permanent joining of two fibers to each other. The best results are obtained from thermal fusion of the two fibers. The fibers are aligned, either manually with precision stages under a microscope or with the aid of microprocessor control. The fibers are then heated and fused together as shown in **Fig. 6.2**. This fusion is typically done with a carefully regulated electric arc or with a microtorch. Skilled operators can achieve losses of less than 0.1 dB. The second method of splicing is a precision aligned groove technique which will be used in this project. The fibers are inserted in a groove formed by an arrangement of four glass rods which have been fused together as shown in **Fig. 6.3**. Index-matching epoxy is used to fix the splice in place. Untrained operators can routinely achieve splice losses on the order of 0.1–0.3 dB. When it is necessary to keep splice losses as low as possible, the thermal fusion splice technique is the best choice, but the epoxy splices are easier and can be made with little practice.

Permanent splices generally have lower losses than connectors since they do not need to be designed for repeated coupling and decoupling. Also, connectors require mating hardware attached to the fiber, making them more complicated. Both splices and connectors must be able to be done in the field by personnel who may not be highly trained. This dictates a design requiring a minimum of fiber handling. The resulting joints must be mechanically rugged, environmentally insensitive, and long lived.

6.2 ALIGNMENT LOSSES

The principal source of loss in both connectors and splices is fiber-to-fiber end face misalignment. There are three types of misalignment loss which may occur individually or in combination. These are lateral misalignment, axial separation, and angular misalignment. These misalignments are illustrated in **Fig. 6.4**. The design problem is to minimize these losses while making the devices, as far as possible, self-aligning.

The first of these loss mechanisms, lateral misalignment, is the largest contributor to the total loss in a fiber connection. Lateral misalignment is the failure of the cross sections of the two fiber cores to perfectly overlap (**Fig. 6.4a**). This may be due to tolerances on the fiber diameter, eccentricity of the fiber outside diameter or of the core with respect to the fiber axis, or machine tolerances in the construction of the connector.

Axial separation contributes to the connection loss when the end surfaces of the two fibers do not come into contact with each other (**Fig. 6.4b**). In connectors, a slight separation will generally be designed into the device so that the fibers are not damaged by butting against each other. This type of loss depends upon the numerical aperture of the fibers, since a large divergence will result in loss of the beam from the first fiber being accepted by the second.

The third loss mechanism, angular misalignment (**Fig. 6.4c**), generally does not contribute significantly to connection losses, both because manufacturing tolerances virtually eliminate this misalignment in connectors and splices and because the fiber connection itself is more tolerant of angular misalignments.

Theoretical loss curves for these three misalignments when graded-index fibers are coupled together are shown in **Fig. 6.5**, **6.6**, and **6.7**. In the case of step-index fibers, the loss from offset misalignment can be found by simply calculating the overlap area of the cores because the irradiance is constant over the face of a step-index fiber. In the case of graded-index fibers shown here (**Fig. 6.5**), the calculation is much more complicated because the irradiance varies as a function of position within the fiber core. The loss from the separation of two fiber ends (**Fig. 6.6**) is found by comparing the area of the receiving fiber with the area of the beam from the first fiber at a distance z from its end face. The loss from angular misalignment (**Fig. 6.7**) has the same form as the offset loss, with sin θ/NA replacing z/a as the scaling factor.

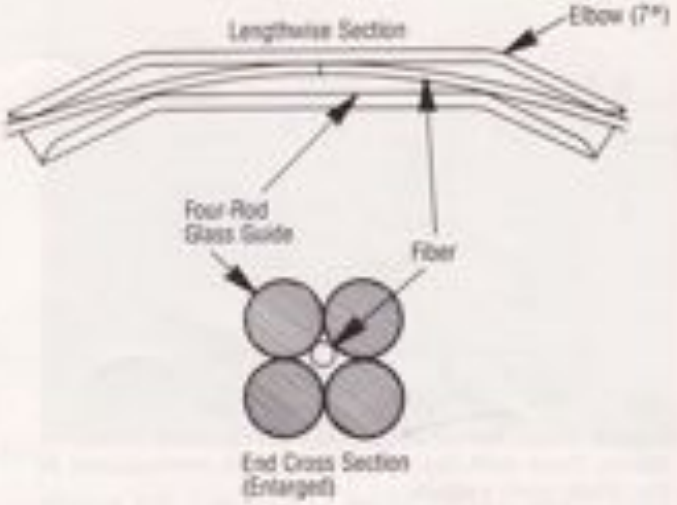

Figure 6.3. Precision groove splice used in this project.

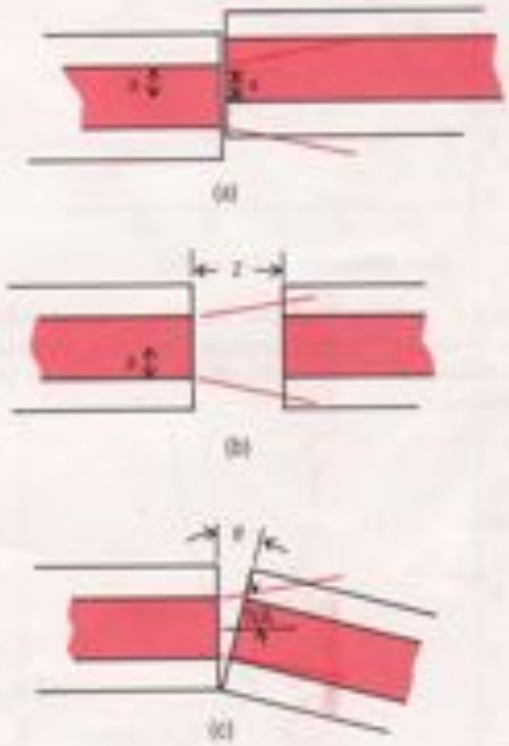

Figure 6.4. Misalignments of fiber cores in fiber-fiber connections. a) Lateral offset. b) Axial separation. c) Angular offset.

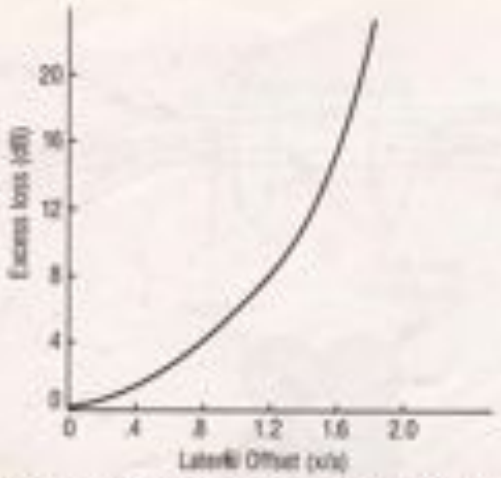

Figure 6.5. Lateral offset loss for graded-index fibers. Note that the offset has been normalized to the fiber core radius.

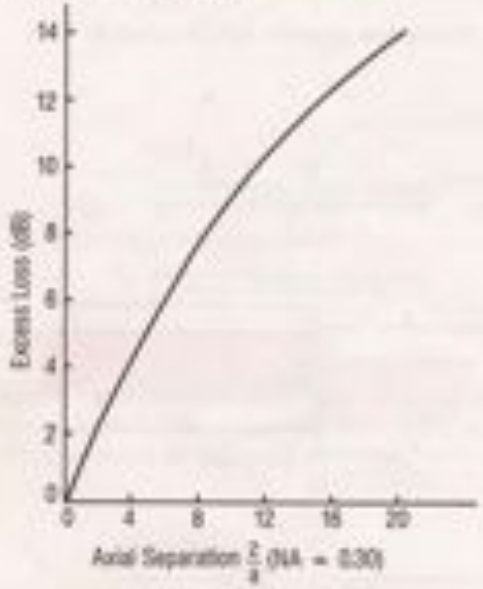

Figure 6.6. Axial separation loss for graded-index fibers. Note that the separation has been normalized to the fiber core radius. NA=0.30 was used in the calculation.

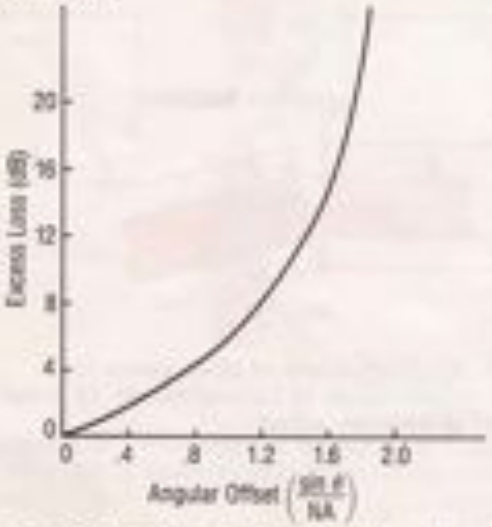

Figure 6.7. Angular misalignment loss for graded-index fibers. Note that the angle has been normalized to the fiber NA.

As an example of the tolerances which are allowable in making a fiber-to-fiber connection, consider a step-index fiber with core diameter = 50 μm and NA = 0.20. Losses of 0.1 dB occur for approximately 1 μm lateral offset, 4 μm axial separation, or 0.5° angular misalignment. The problem is much more difficult when single-mode fibers are used. If a single-mode fiber with core diameter = 4 μm and NA = 0.10 is used, then 0.1 dB losses occur for 0.1 μm lateral offset, 0.7 μm axial separation, and 0.2° angular misalignment. In each case, these are only the misalignment losses. Fresnel reflection losses will contribute about 0.2 dB loss per fiber face in dry connections. Imperfections in fiber end preparation may also contribute to the loss.

The losses which have been described here are for the butt-coupling types of connectors. Connectors which use lens systems to minimize the connection loss are useful in eliminating lateral offset and axial separation losses, but are very highly sensitive to angular misalignment.

6.3 REFERENCE

1. M. K. Barnoski, in *Fundamentals of Optical Fiber Communications*, 2nd Edition, M. K. Barnoski, ed., Academic Press (New York), 1981, p.177

6.4 PARTS LIST

Cat#	Description	Qty.
F-MLD-50	100/140 MM fiber, 50 meters	1
XSN-22	2x2 Breadboard	1
U-1301P	1 mw HeNe laser	1
807	Laser mount	1
340C	Clamp	1
41	Short rod	1
815	Power meter	1
F-916	Fiber coupler (w/o lens)	1
M-20X	20X Objective lens	1
F-CL1	Fiber cleaver	1
FK-BLX	Balldriver set	1
SK-25	¼-20 Screw kit	1
SK-08	8-32 Screw kit	1
RSX-2	Rotation stage	1
MPH-1	Micro-series holder	1
MSP-1	Micro-series post	1
VPH-2	Post holder	1
SP-2	Post	1
FP-1	Fiber positioner	3
FM-1	Mode scrambler	1
F-CC-140	Connector halves (F-MLD)	10
F-CA-001	In-line adapter	5
F-TK1E	20 pkgs. epoxy	1
F-TK1L	160 lapping sheets	1
F-TK1P	Polishing fixture	1
F-SK-C	Splice fixture	1
F-SK-S	10 PSI Lightlinker modules	1

Additional equipment required: Sheet of plate glass for use in polishing connectors. Methylene chloride for stripping jacket from fibers. (Many commercial paint strippers contain methylene chloride and work well for this purpose. Methylene chloride is toxic and may be absorbed through the skin. Any methylene chloride which gets on your skin should be washed off immediately.)

6.5 INSTRUCTION SET

6.5.1 FIBER ALIGNMENT LOSSES

1. Prepare two segments of F-MLD fiber, each about 1-2 meters in length, as you did in Project #1 (**Section 1.6.1, Steps 1-3**). Couple light from the HeNe laser into one of the fibers using the F-916 Fiber Coupler as you did in Project #2 (**Section 2.6, Step 3**). Insert the other end of this fiber into a post-mounted FP-1. Measure the output power from this fiber segment.

2. Insert one end of the second fiber segment into an FPH-S holder and place this in an FP-1 Fiber Positioner which has been post-mounted on the RSX-2 rotation stage, as you did in **Projects #1** and **#3**. (The laboratory set-up for this project is shown in **Fig. 6.8**.) Place the far end of this fiber in another post-mounted FP-1 so that the power coupled through the two fibers can be measured with the 815 Power Meter.

3. Extend the fiber ends so that the fibers can be butt-coupled over the center of the rotation stage. Centering of the fibers on the stage can be checked by rotating the stage and adjusting the fibers until the ends do not move relative to each other as the stage is turned. Adjust the x-y-z of the fibers to achieve maximum throughput in the butt coupling.

4. Measure the power transmitted through the second fiber segment. Calculate the loss of the butt coupling of the fibers, using the power out of the first fiber measured in Step 1 and the power coupled into the second fiber as measure in this step. A loss of less than 0.25 dB is excellent for this dry connection. A measurement in Newport's lab during the development of this project yielded a loss of 0.27 dB.

5. Measure the excess loss as a function of lateral misalignment as follows: Measure the power coupled into the second fiber and calculate the total coupling loss as a function of position. After finding this total coupling loss, subtract the loss measured in Step 4 from it. There is no direct calibration for measuring the offset from the FP-1, so it is best to calibrate from the rotation of the adjusting screws. These are 80 thread/inch screws, which means that one turn of the screw will give 0.0125 inch or 0.3175 mm of offset. (Be sure to move in one direction only so as to eliminate backlash in the movement. If you wish to go in

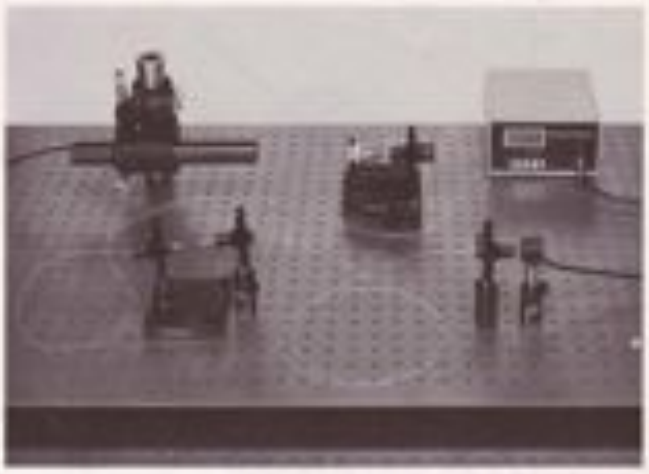

Figure 6.8. Laboratory set-up for measuring fiber alignment losses.

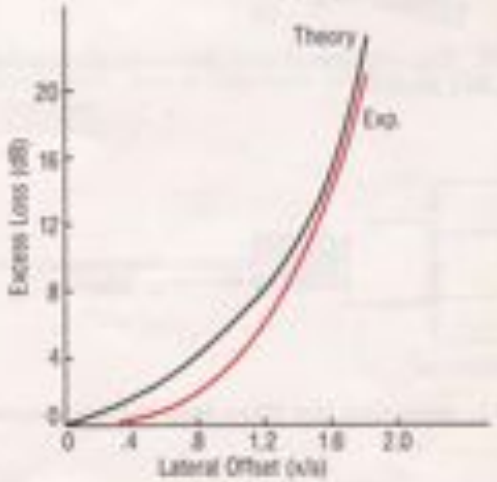

Figure 6.9. Experimental and theoretical lateral offset losses.

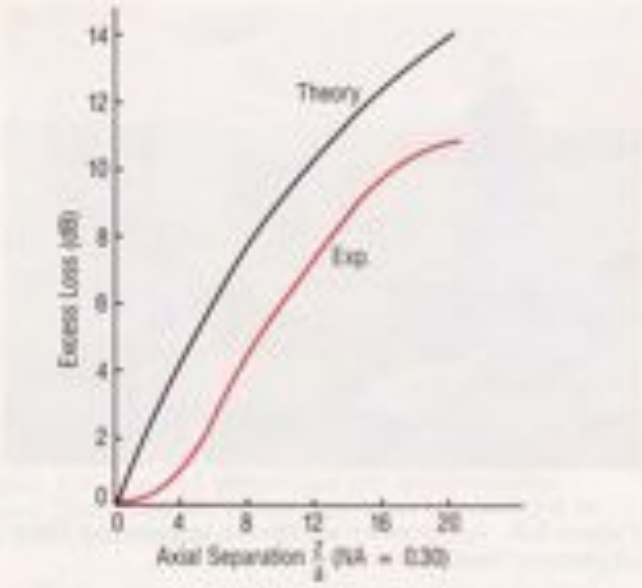

Figure 6.10. Experimental and theoretical fiber separation losses.

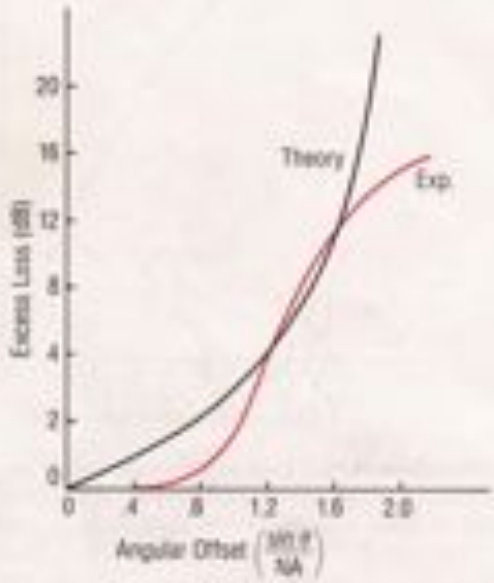

Figure 6.11. Experimental and theoretical angular misalignment losses.

Figure 6.12. Inserting the fiber into the connector half.

the other direction, reset the system and start over again.) Normalize the offset to the fiber core radius by dividing the offset by the fiber core radius. This will allow you to plot the loss as function of offset expressed in core radii. Plot the excess loss which you have obtained as a function of lateral offset. **Fig. 6.9** shows the loss, obtained in the Newport lab using the F-MLD fiber, plotted against the curve shown in **Fig. 6.5**. The deviation from the theoretical curve is due to the fact that the laser-fiber coupling underfills the fiber, as was discussed in **Section 0.3.2**. This causes more of the light to concentrated towards the center of the fiber core, reducing the misalignment loss.

6. Realign the fiber ends and measure the excess loss as a function of longitudinal separation. The screw at the back of the FP-1 which controls this separation is also an 80-pitch screw, which gives 0.0125 inch or 0.3175 mm per turn. Normalize the separation to the fiber core radius and plot the results. The results found in the Newport lab are shown in **Fig. 6.10**. They are plotted with the theoretical curve of **Fig. 6.6**. The deviation has the same origin as discussed in the previous step.

7. Realign the fiber ends once more and measure the excess loss as a function of angular misalignment using the RSX-2 Rotation Stage to change the angular orientation of the fiber ends. Normalize the sine of the angle of misalignment to the numerical aperture of the fiber. The results obtained in the Newport lab are shown in **Fig. 6.11**. The theoretical curve is from **Fig. 6.7**. The deviation at low angles is for the reason discussed above. At high angles, light is being launched into the cladding of the second fiber. Some of this light reaches the detector and decreases the apparent misalignment loss.

6.5.2 CONNECTOR ASSEMBLY AND TEST

1. You may use the two fiber segments which were used in the alignment loss study, above, for this exercise in connector assembly. Cleave the fibers so that there is about $^1/_{8}$–$^3/_{8}$ inch of bare fiber extending beyond the jacket at the end of each segment which will be inserted into the connector. End face inspection is not required; this step is simply to avoid having any jagged edge remain when the fiber is broken off to this particular length and will improve fiber insertion into the connector.

2. Remove the clip from the center of one of the packets of the F-TK1E Epoxy. Knead the epoxy until it is thoroughly mixed. Cut a corner from the packet and squeeze out the epoxy.

3. With a toothpick or other small probe, apply the epoxy to the length of the bared fiber.

4. Insert the fiber into each connector half (**Fig. 6.12**). A slight rotation of the connector may help "thread" the fiber through the precision hole in the connector. Use epoxy to fill the connector. (These connectors are designed to be used with cabled fibers. Filling of the connector halves with epoxy accommodates the use of bare fibers instead of the cabled fibers.)

5. Using the same small probe, place a small drop of epoxy onto the face of each of the connector halves where the fiber exits the precision hole. Allow the epoxy to fully cure. (This requires about 5 minutes. Check the unused remnant to tell when the epoxy is cured.)

6. Be sure that the polishing fixture is clean. If not, clean it with water and a lint-free wipe. Clean a sheet of plate glass with water and a lint-free cloth.

7. Place the 60 μm grit lapping sheet on the glass plate. (If a few drops of water are placed on the glass first, the surface tension will hold the sheet in place.) Screw the connector half onto the fixture until finger tight (**Fig. 6.13**). Do not overtighten.

8. Put a small puddle of water on the lapping film and begin the rough grind. Use a figure-8 motion (**Fig. 6.14**) in this and each of the subsequent grinding and polishing steps. Grind until the epoxy bead and excess metal are removed. Exert only light pressure on the fixture. You will feel a definite bottoming-out effect when the full face of the fixture comes into contact with the lapping film. This signifies that all of the excess material has been removed. About 20 to 30 strokes should complete the rough grind.

9. Rinse the polishing fixture with water and wipe dry. This is an important step which prevents carrying over contamination from the larger to the smaller grits. Most poor-quality finishes in the final fiber surface are due to lack of care in this step. Be sure to repeat this at each step of the grinding and polishing.

10. Next, use the 9 μm intermediate polish. Keep the lapping film wet and use a figure-8 stroke. Downward pressure may be required during this polish to overcome hydroplaning on the water. About 20 strokes should be sufficient. Don't forget to rinse thoroughly between steps.

11. Repeat step 10, using the 1 μm grit and then the 0.3 micron grit final polish. Rinse and clean the connector between each step.

12. Inspect the finished fiber using the F-MI.1 Inspection Microscope or other suitable high-power microscope.

13. When two connector halves have been completed, slip the full sleeve over the end of one of the halves. Screw the connector half onto the in-line adapter. Screw the second half onto the in-line adapter; the connector half will press fit into the full sleeve as you tighten the connector.

14. The testing of the connector to determine the connection loss is similar to the measurement used in the fiber attenuation project (**Project #2**). With the connector mated, couple the He-Ne laser output into the fiber. Measure the power through the connector. Demate the connector and measure the power from the first connector half. Determine the connector loss from this data. Mate and demate the connector several times to check the repeatability of the loss figure.

Figure 6.13. Screw the connector half onto the polishing fixture.

Figure 6.14. Use a Figure-8 motion in the polishing of the fiber.

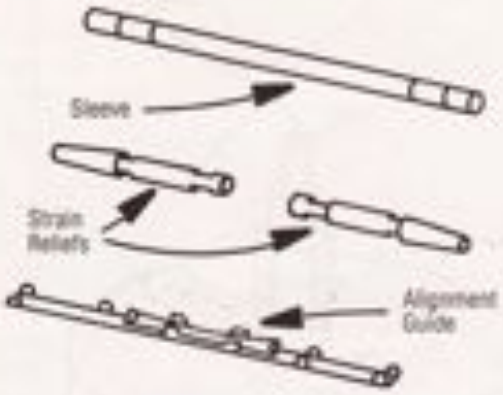

Figure 6.15. Contents of the TRW Optasplice™.

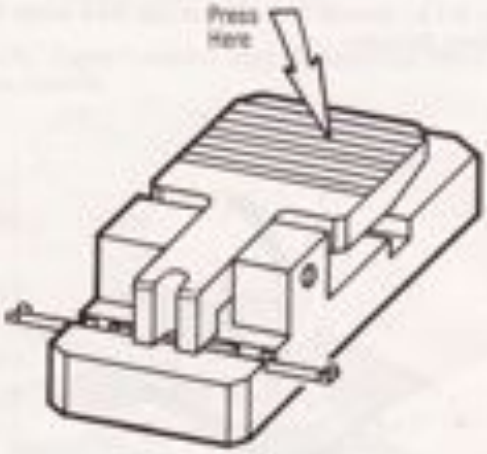

Figure 6.16. Placement of the alignment guide in the splice fixture.

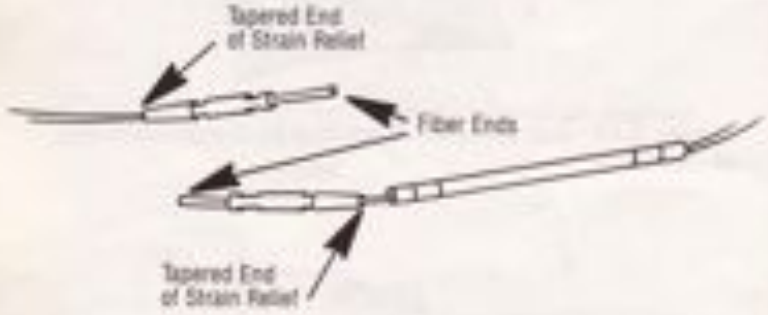

Figure 6.17. Positioning of the sleeve and strain relief on the fiber before splicing.

15. The loss in a connector is dependent on the modal distribution of light within the fiber core. If lower-order modes are preferentially launched, the power in a graded-index fiber will be concentrated toward the center of the core, giving lower connection losses. If higher-order modes are launched, the light will tend to be more toward the perimeter of the core, yielding more sensitivity to alignment losses. Use the FM-1 Mode Scrambler as was done in Project #2 (**Section 2.5, Steps 4** and **5**) to generate an approximation of a stable distribution. This will result in loss measurements which will better approximate those which would result in actual field practice.

6.5.3 SPLICE ASSEMBLY AND TEST

1. Prepare two segments of F-MLD fiber, each about 1 meter in length.

2. Identify the component parts of the TRW Optasplice™ module (Newport Model # F-SK-5). The parts contained in the plastic envelope are: one fiber alignment guide, which comes in a protective plastic tube, two silicone rubber strain reliefs, and one stainless steel sleeve (**Fig. 6.15**).

3. Place the alignment guide into the splice fixture (F-SK-C) (**Fig. 6.16**).

4. Slide the stainless steel sleeve onto one of the F-MLD fiber segments to be spliced. Slide one of the silicone rubber strain reliefs onto each of the fibers. The tapered end of the strain relief leads up the fiber, away from the fiber end to be spliced (**Fig. 6.17**).

5. Cleave both of the fiber ends which are to be joined together. When the cleave is completed, each fiber should have about 7/16-1/2 inch of bare fiber extending out of the fiber jacket. Couple one of the fibers to be spliced to the HeNe laser, using the F-916 Fiber Coupler as you did in Project #2 (**Section 2.6, Step 3**). Inspection of the cleaved fiber ends will not be necessary. Simply go on to Step 6.

6. Measure the optical power coming from the first fiber. Place the two fibers in the dry fiber alignment guide (no epoxy has yet been applied), one at each end of the guide, as in **Fig. 6.18**. Insert the fibers until they butt together at the middle of the guide. Measure the optical power coming from the far end of the second fiber. The loss which is now measured will be Fresnel-reflection limited, since the splice is still dry, but it will give you a good indication of the quality of the fiber ends. If the measured loss is not less than about 0.5 dB, it is a good indication that the fiber ends have not been properly cleaved. The other major contributor to splice loss is fiber eccentricity. If rotating the fiber changes the measured splice loss, then fiber eccentricity is a problem in this splice. If the splice loss is too high and eccentricity is not a problem, return to Step 5 and recleave the fibers.

7. Now is a good time to return to Step 6 and gain experience in handling fibers in this alignment guide before you make the permanent splice.

8. Remove the fibers from the alignment guide. Mix the epoxy to be used, as you did in Step 2 of the connector procedure, above.

9. Coat the bare ends of the fibers with epoxy. A toothpick or the end of a small paper clip makes a good applicator. The epoxy will both wick into the alignment guide and be carried into the guide by the fibers when they are inserted.

10. Again insert the fibers into the alignment guide as you did in Step 5. Minimize the splice loss by again rotating the fibers, if necessary. The epoxy will be cured and the splice may be handled in about 10 minutes. The curing of the epoxy can be checked by testing the remnant of the mixed epoxy which was not used in the splice.

11. After the epoxy is cured, remove the alignment guide from the splice fixture. Slide the rubber strain reliefs down the fiber and onto the alignment guide substrate. Note that the flat side of the strain relief sits on the alignment guide substrate and that the tabs on the substrate fit into the notches in the strain relief (**Fig. 6.19**).

12. Slide the stainless cover over the splice. Use the crimp tool on the back side of the splice fixture to complete the splice, as shown in **Fig. 6.20**. Crimp at the red bands on the cover. The permanently spliced fiber is now complete.

13. Measure the power through the completed splice. Calculate the splice loss again. Compare this with the value found in Step 6.

14. Losses in permanent splice are sensitive to the way in which light is launched into the fiber in the same way that connectors are, as discussed in Step 15 of the connector assembly procedure. Use the FM-1 Mode Scrambler to generate an approximation of a stable mode distribution as you did in Step 15 of the connector assembly and remeasure the splice loss.

15. When you find that you can make a good splice using the multimode F-MLD fiber, you may wish to try splicing the F-SV single-mode fiber which you used in Project #3. Typical high-quality splices will have ~0.5 dB loss for the single-mode fiber, compared to ~0.2 dB for the multimode fiber.

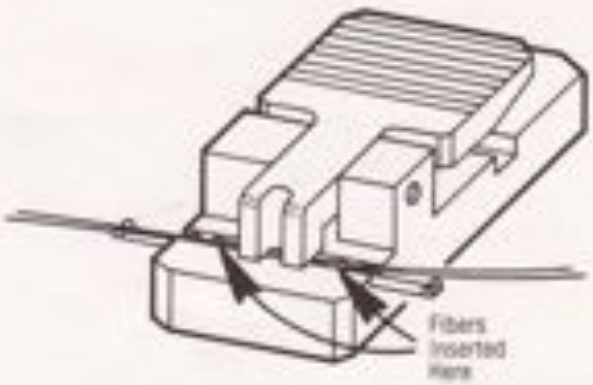

Figure 6.18. Insertion of the fiber ends into the alignment guide.

Figure 6.19. Placing strain reliefs on the alignment guide substrate.

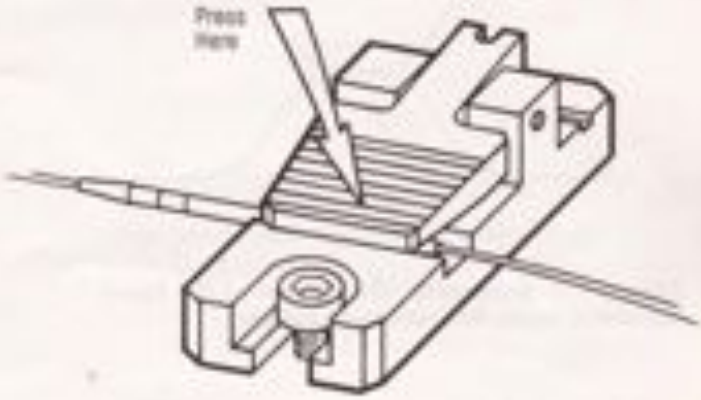

Figure 6.20. Crimping the completed splice in the crimp tool at the back of the splice fixture.

7.0 PROJECT #7: COMPONENTS FOR FIBER COMMUNICATION

In this project, the components which are needed to build a fiber data distribution system will be explored. Fiber optic components for data distribution are of importance in short-haul applications, such as local area networks (LANs), which provide information transfer within structures such as office buildings and manufacturing facilities, and in such vehicles as aircraft and ships. These components are also used in longer-haul systems in order to fully utilize the bandwidth of the optical fiber.

Current design trends are toward device miniaturization and integration at the system level. These result in smaller size, lower weight, lower power consumption, and higher reliability. Although a large number of components have been invented and used in fiber systems, this project will concentrate on two devices, the fused bidirectional coupler and the wavelength division multiplexer (WDM), which are representatives of this larger group. This will give you the opportunity to learn about parameters which are common to almost all fiber devices, such as excess loss, splitting ratio, directivity, and crosstalk.

7.1 MULTIMODE BIDIRECTIONAL COUPLERS

The need for devices to combine light from several fibers into a single fiber or to split the light from one fiber into two or more fibers has been recognized ever since optical fibers were first considered as a communications medium. A 2x2 (2 fibers in, 2 fibers out) **bidirectional coupler**,[1,2] which is a device for splitting the light in one input fiber into two output fibers, is illustrated schematically in **Fig. 7.1**. In fiber optic systems they play a role which is equivalent to that of beam splitters in conventional optics or T-taps in electronics. Bidirectional couplers play a critical role in fiber optic instrumentation, high-data-rate LANs, and communications systems. **Star couplers** are nxn (n fibers in, n fibers out) devices of the same basic construction.

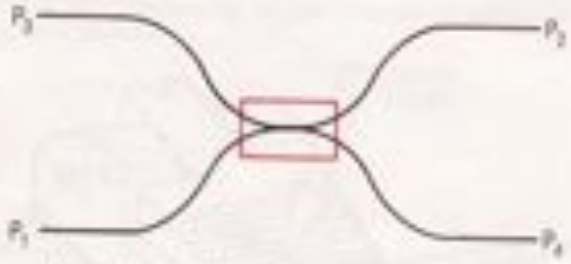

Figure 7.1. Schematic illustration of the fused biconical taper bidirectional coupler.

Bidirectional couplers can be classified into two broad categories, those that use conventional optical beam splitting techniques and those that couple energy between the two fibers using the overlap of the evanescent waves (**Section 0.2.2**) of the light in the cladding of the fibers. Several designs using beam splitting techniques have been developed. These have not found widespread use because of the problem of maintaining the alignment of discrete micro-optic components under extreme conditions. However, this type of device has an advantage over the evanescent wave coupler in that the modal content of the input fiber is preserved in the output fibers.

When the cores of two fibers are close together, the energy is shared between the two overlapping evanescent waves and energy is transferred from one fiber to the other. For this reason, energy coupling between two fibers by this technique is known as evanescent field coupling. The evanescent fields will penetrate significantly into the cladding

only for the highest-order rays, i.e., those nearest the critical angle for total internal reflection. Because of this, the coupling obtained using this technique is highly dependent on the modal content of the input fiber. If the light in the input fiber is carried in predominantly higher-order modes, more of the light will be coupled to the second fiber. If the light is in predominantly lower-order modes, less light will be coupled. Bidirectional couplers which use this technique actually achieve their specified coupling ratio when light is evenly distributed among the allowed modes of the input fiber.

Light which comes out of Port 2 (using the notation of **Fig. 7.1**) will be in mostly high-order modes, while the light remaining in the input fiber and coming out of Port 4 will be in mostly low-order modes. This will also have an effect on the performance of any other bidirectional couplers which are now connected in series with the first coupler since the distance between couplers is not likely to be great enough to allow the light to be redistributed among the modes. Couplers downstream from Port 2 will split off more than the specified power, while couplers downstream from Port 4 will split off less than the specified power.

[This discussion of the modal dependence of the evanescent wave coupling mechanism applies to multimode couplers. Although they are harder to fabricate, single-mode couplers are simpler to understand, because they have only a single mode involved in the coupling. You will have a chance to work with single-mode bidirectional couplers in Project #10.]

Because of the exponential decay of the evanescent field, the two fiber cores must be brought in close proximity for electric field overlap and optical power coupling to occur effectively. The most commonly employed technique for fabricating the coupler is called the **fused biconical taper technique**. In this technique, the two fibers are twisted together and then heated to about 1500°C. While the fibers are being heated they are subjected to a tension which causes them to stretch. This stretching increases the coupling between the two cores by two mechanisms. The first is due to the fact that when the fiber is stretched, the fiber cladding is tapered and becomes thinner, causing the two cores to come closer together, thereby increasing the evanescent field overlap. The second comes about because of the thinning of the core itself, which causes a decrease in the V-number of the fiber (see **Section 0.3.1**). This causes the fields' exponentially decreasing evanescent waves to decrease less rapidly as a function of radius, and this also increases the field overlap.

In practice, the stretching is continued until the desired coupling ratio is achieved. When the heating is stopped, the core separation is permanently locked in place. Couplers made by the fused biconical taper technique are extremely insensitive to temperature changes.

The bidirectional coupler which results was shown in **Fig. 7.1**. Light which is input at Port 1 may either come out of the same fiber at Port 4 or be coupled to the second fiber and emerge at Port 2. A small amount of light may be returned to the input port of the second fiber, Port 3,

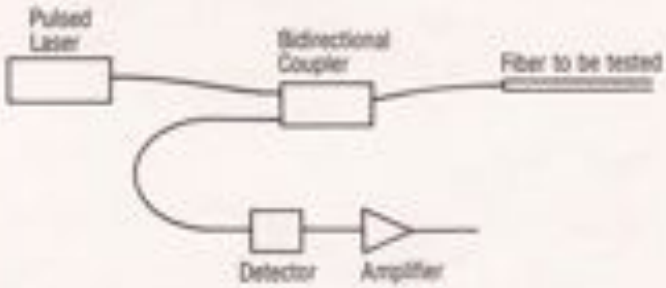

Figure 7.2. Schematic diagram of an Optical Time Domain Reflectometer.

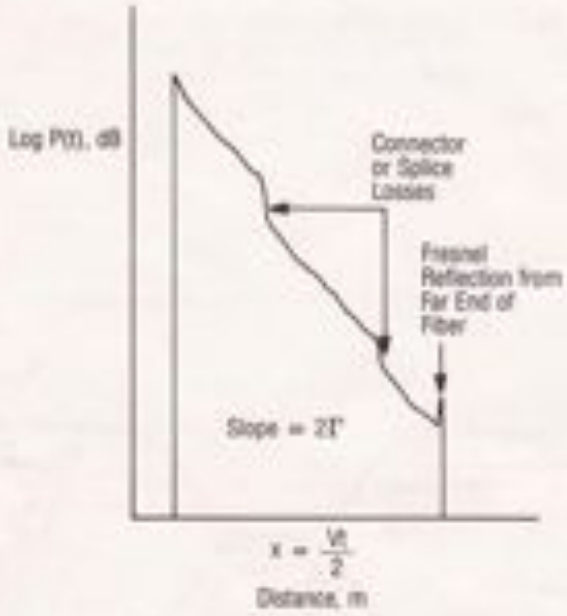

Figure 7.3. Logarithmic plot of an OTDR signal. When the optical power detected is plotted as a function of distance to the scattering center in the fiber, the slope of the signal will be twice the attenuation coefficient of the fiber. Also shown is the effect produced by a connector and the effect of the reflection at the far end of the fiber.

because of backscattering and reflections due to the constriction at the taper. The **coupling ratio**, or **splitting ratio**, is defined as the power coupled across to the second fiber divided by the total power through the coupler ($P_c/P_c + P_t$). Typical coupling ratios for commercially available devices are 3 (50%), 6 (25%), and 10 dB (10%). The **excess loss** is defined as the total output power divided by the total input power ($P_t + P_c/P_i$). Early couplers exhibited losses in the range of 2–3 dB. Most couplers today exhibit losses in the range of 0.5–1.0 dB. The **directivity** of the coupler is defined as the power returned to the input of the second fiber divided by the input power (P_r/P_i). This ratio is typically about –40 dB for good couplers.

In communications applications, the bidirectional coupler is more often used as a tap. Its application is in tapping information off of a main data bus or in inserting information onto the bus. In instrumentation applications, the major use is in **Optical Time Domain Reflectometers**[3] (OTDR's), which measure the losses in fiber optic systems. In essence, the OTDR is a one-dimensional optical radar which provides an echo scan of the entire length of an optical fiber (**Fig. 7.2**). It operates by periodically launching short-duration pulses from a laser diode into one end of the fiber being tested and measuring the time-dependent characteristics of the light which is reflected and/or backscattered to the same fiber end. The reflected signal, measured at the launch end of the fiber, is used to determine the location and magnitude of discontinuities in the fiber. A time-of-flight measurement allows the OTDR to determine the location of faults in the system. The bidirectional coupler directs the pulse into the fiber and directs the backscattered signal to the detector. A typical OTDR output is shown in **Fig. 7.3**. The slope is twice the attenuation coefficient of the fiber. Faults in the fiber, such as connectors, splices, or breaks are seen as abrupt changes in the amount of light returned to the detector.

7.2 WAVELENGTH DIVISION MULTIPLEXER

The **wavelength division multiplexer**[4] (WDM) provides the equivalent of multiple transmission lines in a single fiber by sending signals at various wavelengths in the same fiber. The WDM enables an optical fiber to be used more effectively. It allows a greater use of the bandwidth of the fiber, allows bidirectional communications, and allows the simultaneous transmission of different types of signals, such as analog and digital data.

A WDM device consists of two or more input fibers, each carrying a signal at a different wavelength, an output fiber which is connected to the transmission link, and wavelength-selective optical components, such as gratings, prisms, or thin-film filters, for combining the signals at different wavelengths onto the output fiber. A simple two-channel WDM, using two quarter-pitch graded-index (GRIN) rod lenses and a wavelength selective filter, is shown in **Fig. 7.4a**. (See **Sections 0.2.4** and **5.3** for an introduction to GRIN-rod lenses.) Signals carried on two different wavelengths, λ_1 and λ_2, are input from Fibers 1 and 2, respec-

tively. The quarter-pitch lens collimates the input beam at the point where it sees the fiber and the second lens refocuses the beam into the output fiber. The wavelength selective filter reflects λ_1 and passes λ_2 to be focused at the output. Fiber 3, which is placed symmetrically about the lens axis with respect to Fibers 1 and 2. Demultiplexing of the signals at the receiver is accomplished by simply reversing the path directions. Two-way transmission can be accomplished by replacing one of the sources, for example, Source #2, with a detector, as shown in **Fig. 7.4b**. The WDM then inserts λ_1 onto the transmission link and receives λ_2. The WDM at the far end will send λ_2 and receive λ_1.

In this project, you will construct a two-channel WDM of the type described above. The wavelength selective filter is not used in WDM's that have higher channel count, because an N-channel WDM would require N-1 filters. This WDM would require the cascading of several filters and this would greatly increase the losses in the device. WDM's of this type generally use a prism or a grating. A design for a five-channel WDM using a quarter-pitch GRIN-rod lens and a reflective diffraction grating is shown in **Fig. 7.5**. WDM devices of this type allow more of the total bandwidth of the optical fiber to be used (see **Section 8.1.2**). WDM's employing gratings are now available with more than ten channels.

The two most important parameters in characterizing a WDM are the insertion loss and the crosstalk. If the power to the device from the ith source is P_i and the total power from all sources combined on the output fiber is P_T, then the insertion loss is defined as $P_T/\Sigma P_i$. Typical insertion losses are about 1-2 dB, depending on the type of wavelength selection used, but may be as high as 8-10 dB when LED sources are used in a grating WDM device. The **crosstalk**, or **isolation**, is determined after the signals are demultiplexed at the receiver end. The crosstalk from channel i into channel j is defined as the power received from source i divided by the power received from source j when both are measured by the detector for channel j. Typical values for the crosstalk in available multiplexers is generally less than –20 to –30 dB.

7.3 REFERENCES

1. M. K. Barnoski, in *Fundamentals of Optical Fiber Communications*, 2nd Edition, M. K. Barnoski, ed. Academic Press (New York), 1981, p.334

2. S. D. Personick, *Fiber Optics, Technology and Applications*, Plenum Press (New York), 1985, p.107

3. ibid., p.236

4. ibid., p.110

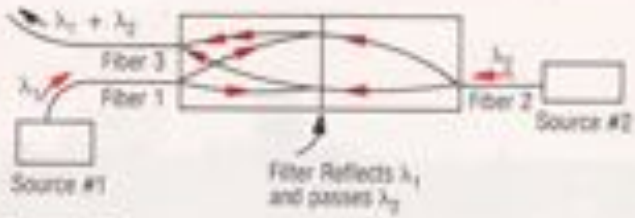

Figure 7.4a

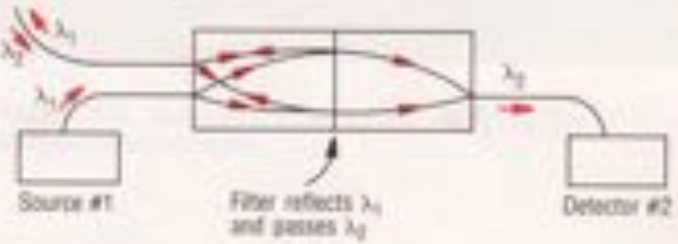

Figure 7.4b

Figure 7.4. Interference filter type wavelength division multiplexer (WDM). a) for two-channel transmission. b) for two-way transmission.

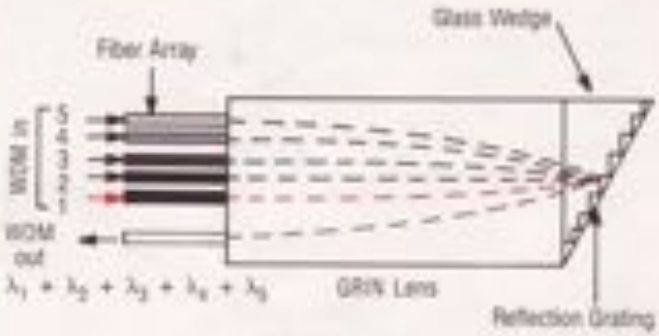

Figure 7.5. Five-channel grating WDM using a graded-index (GRIN) rod lens.

7.4 PARTS LIST

Cat#	Description	Qty.
F-MLD-50	100/140 MM fiber, 50 meters	1
XSN-22	2x2 Breadboard	1
U-1301P	1 mw HeNe laser	1
807	Laser mount	1
340C	Clamp	1
41	Short rod	1
815	Power meter	1
F-916	Fiber coupler (w/o lens)	1
M-20X	20X Objective lens	1
FK-BLX	Balldriver set	1
F-CL1	Fiber cleaver	1
SK-25	¼-20 Screw kit	1
BS-05	¼-20 Thumbscrew kit	1
B-1	Base	2
VPH-2	Post holder	10
SP-2	Post	10
SP-3	Post	2
CA-2	Universal clamp	2
FP-1	Fiber positioner	4
FM-1	Mode scrambler	1
F-925	GRIN-lens fiber coupler	2
FK-ILD	Laser Diode assembly	1
FK-LED	Light-emitting diode assy.	1
FK-DRV	ILD LED Driver circuit	1
FK-GR29	NSG SLW-1.8-0.29 lens	2
F-IRC1	IR phosphor card	1
MH-2PM	Optics holder	4
F-TK1E	20 pkgs. epoxy	1
F-SK-C	Splice fixture	1
F-SK-S	10 TRW Optasplice Modules	1
FK-BTC	ADC bidirectional coupler	1
FK-MUX	Multiplexer assy. base	2
FK-GR25F	NSG 0.25-p lens w/ filter	2
FK-GR25P	NSG 0.25-p lens w/o filter	2
FPH-S	Fiber chuck	2
MPC	Collar	2

Additional equipment required: Methylene chloride for stripping the jacket from fibers. (Many commercial paint strippers contain methylene chloride and work well for this purpose. Methylene chloride is toxic and can be absorbed through the skin. Any methylene chloride which gets on your skin should be washed off immediately.) Glycerin (glycerol) for index matching.

7.5 INSTRUCTION SET

7.5.1 BIDIRECTIONAL COUPLER

1. Remove a section of the outer jacket from the cabled fiber pigtail of the FK-BTC bidirectional coupler at Port 1. Cleave the end of the fiber. (You can actually use any of the four ports of the coupler, but using Port 1 will allow you to use the notation of the previous discussion.)

2. Splice a one-meter length of F-MLD fiber to the cleaved fiber as you learned to do in Project #6 (**Section 6.5.3**). This will make it much easier to handle the input to the coupler. However, the splice must be done properly, or there may be significant mode coupling at the splice and the following exercise will be meaningless.

3. Couple HeNe laser light to the fiber at Port #2 as you did in Project #2 (**Section 2.5, Step #3**). The laboratory set-up for this exercise is shown in **Fig. 7.6**. Arrange the input so that low-order modes are preferentially launched into the input fiber. You can check this by visually examining the output from Port #4. (Low-order modes will be confined to low output angles. Arrange the launch conditions so that the output cone at Port #4 is as narrow as possible.) Measure the outputs at Ports #2, #3, and #4.

4. Change the launch conditions so that high-order modes are preferentially launched (large output cone). Again, measure the output powers.

5. Return to the launch conditions of Step #3. Use the FM-1 mode scrambler as you did in Project #2 (**Section 2.5, Step 5**) to generate an approximation of a stable distribution in the launch fiber. Measure the output powers.

6. Put some index matching fluid such as glycerin on the fiber ends at Ports #2 and #4. Remeasure the returned light at Port #3. Index matching will reduce the light returned to Port #3 by Fresnel reflections from the far end of the fiber at Ports #2 and #4.

7. Compare the results of Steps #3-#6. What conditions are assumed when the manufacturer quotes a 3 dB splitting ratio and a directivity of –40 dB?

Figure 7.6. Laboratory set-up for studying the bidirectional coupler.

7.5.2 WAVELENGTH DIVISION MULTIPLEXER

1. Prepare four lengths of F-MLD fiber, each about 1 to 1½ meters long as you did in Project #1 (**Section 1.6.1, Steps 1–3**). Construct an array of two fibers as follows: Lay two lengths in a single FPH-S fiber chuck (**Fig. 7.7a**) so that they are parallel and so that the fiber end faces are co-planar (**Fig. 7.7b**). Mix some of the two-part epoxy (F-TK1E) and place a drop at both ends of the fiber chuck (**Fig. 7.7c**). Make sure that the epoxy does not run over the end faces of the fibers or over edge of the chuck, because this chuck will have to be inserted into an FP-1 fiber positioner. Allow the epoxy to fully cure.

2. Repeat Step 1 with the other two lengths of fiber and a second FPH-S chuck.

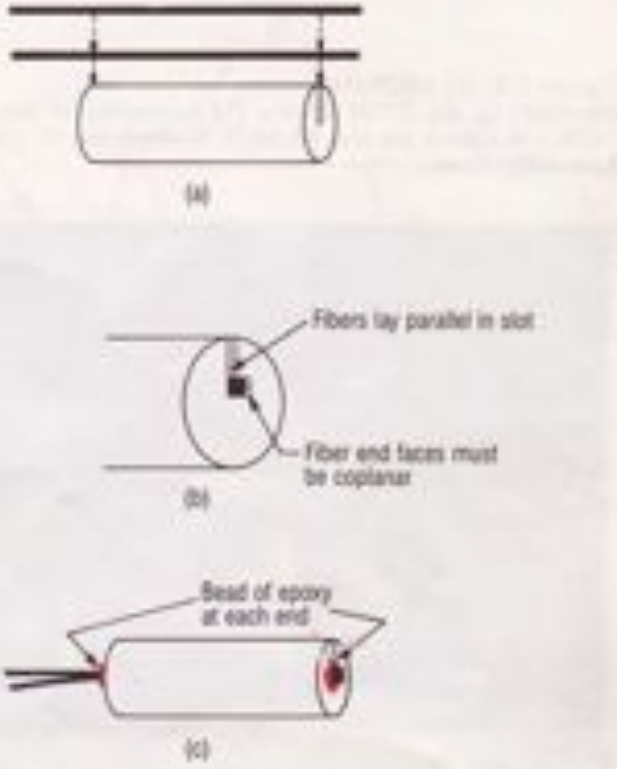

Figure 7.7. Construction of a two-fiber array. (a) Lay two cleaved fibers in an FPH-S Fiber Chuck. (b) Fibers must lay parallel in the chuck with co-planar end faces. (c) Apply a bead of epoxy at each end to hold fibers in place. Do not allow epoxy to run over the edge of the chuck or over the end faces of the fibers.

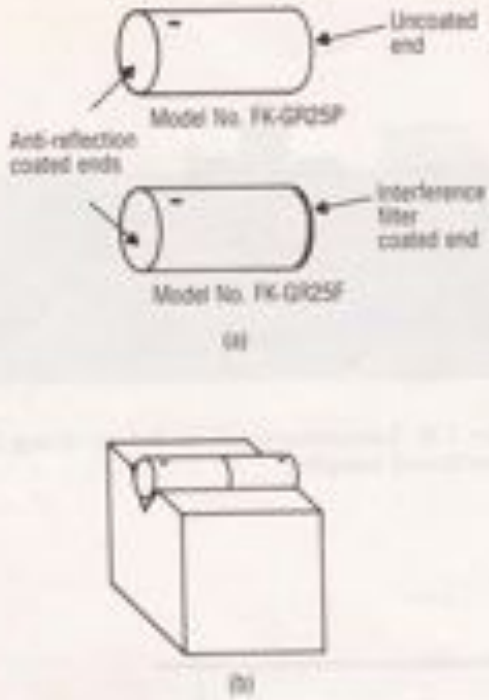

Figure 7.8. (a) GRIN-rod lenses used in the assembly of the WDM device. (b) Assembly of the GRIN-rod lenses on the FK-MUX Multiplexer Assembly Base.

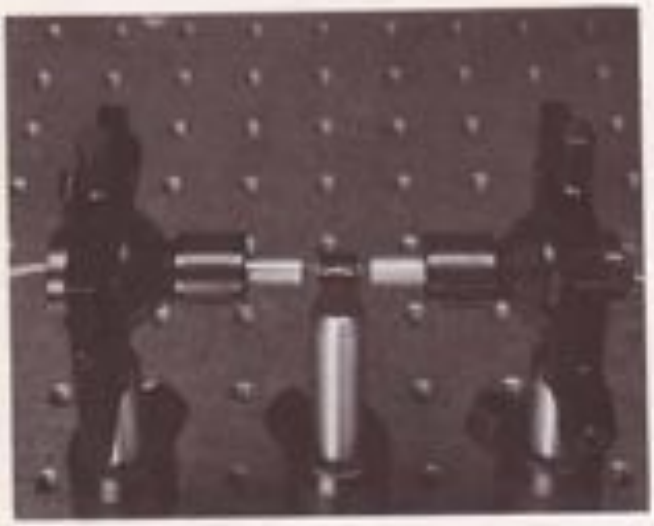

Figure 7.9. Construction of the WDM device. Arrangement of the components is in an orientation which agrees with that shown schematically in Fig. 7.4a.

3. You will now assemble the lenses for the WDM device. You will need two of the GRIN-rod lenses as shown in **Fig. 7.8a**. One is coated with an interference filter which passes the light from the ILD and reflects the light from the LED (Model No. FK-GR25F). The other does not have this interference filter (Model No. FK-GR25P). Both are coated on one end with an anti-reflection coating. Place one of each of these lenses on an FK-MUX Multiplexer Assembly Base, with the anti-reflection coated end (marked with a small black dot) toward the outside of the assembly base as in **Fig. 7.8b**. Epoxy these in place, making sure that there is a film of epoxy between the two lenses for index matching purposes.

4. The procedure listed in Step #3 for assembling the lenses of the WDM was quite involved. However, you now need to repeat the procedure of Step #3 in order to assemble the lenses for the wavelength demultiplexer device.

5. Prepare another 1 to 1-1/2 meter length of F-MLD fiber and couple the output of the ILD into it as you did in Project #5 (**Section 5.6.1**, **Steps 1**, **2**, **8**, and **9**). The precautions noted in that instruction set still apply here. This fiber will be fiber #2 of **Fig. 7.4a**. Use the 815 Power Meter to measure the amount of power coupled into this fiber.

6. Couple the light from the LED into one of the fibers which you have epoxied into one of the FPH-S Fiber Chucks as you did in Project #5 (**Section 5.6.2**, **Steps 1** and **6**). This fiber will be fiber #1 of **Fig. 7.4**. Use the 815 power meter to measure the amount of power coupled into fiber #1. The other fiber in the same chuck will be fiber #3.

7. Post mount one of the WDM assembly bases with the lenses epoxied in place. Use the SP-3 Post so that the lenses can be aligned at the proper height with respect to the fibers in the FP-1 Fiber Positioner. Place the chuck with fibers #1 and #3 in a post-mounted FP-1 Fiber Positioner (see **Fig. 7.9**).

8. Couple light from fiber #1 to fiber #3 by aligning the fibers with the lenses as shown schematically in **Fig. 7.10**. When the two fibers are located symmetrically about the center line of the lens, LED light from fiber #1 will be reflected from the interference filter, which is now located between the two GRIN-rod lenses, and will be focused into fiber #3.

9. Place fiber #3 in an FPH-S Fiber Chuck. Hold this chuck in an MPC Collar and post-mount the assembly. Position the 815 Power Meter so that you can measure the coupled power.

10. Measure the power in fiber #3 and calculate the insertion loss of the WDM for this channel.

11. Once Step 10 is completed, place the fiber into which you have coupled light from the ILD in an FPH-S chuck and place this in an FP-1 Fiber Positioner. Post mount this FP-1, completing the arrangement of equipment shown in **Fig. 7.9**.

12. Couple light from fiber #2 into fiber #3 as shown in **Fig. 7.11**. Adjust fiber #2 until the maximum coupling is achieved. Fiber #2 will be symmetrically across the lens center line from fiber #3 at the opposite end of the lens assembly. Do not move the position of fiber #3, as this will reduce the coupling from fiber #1 into fiber #3. Measure the ILD power coupled into fiber #3 and calculate the insertion loss for this channel.

NOTE: If you are also going to do Project #8 as part of this series, you may wish to leave off at this point and do the rest of the construction at the beginning of the next session.

13. Using one of the splices which you used in Project #6 (**Section 6.5.3**), dry splice (no epoxy) fiber #3 to one of the fibers which have been epoxied into the other FPH-S chuck. Measure the optical power for each channel coupled through the splice.

14. Repeat Steps 7 and 8 for this end of the link. You are now putting together the demultiplexer, so fiber #3 is the input, with channels 1 and 2, and fiber #1 is the output (the arrows indicating the light path are reversed in **Fig. 7.10**). Measure the LED power in fiber #1 and calculate the insertion loss of the demultiplexer for this channel.

15. Repeat Step 11 for the demultiplexer. The fibers with the demultiplexed signals may be placed in the remaining FPH-S Fiber Chucks. Hold these in two post-mounted MPC Collars to couple to the 815 Power Meter. Measure the ILD power in fiber #2 and calculate the demultiplexer loss for this channel. The arrows indicating the light path are reversed in **Fig. 7.11** for the demultiplexer. The completed multiplexer-demultiplexer system is shown in **Fig. 7.12**.

16. Measure the ILD power in fiber #1 and the LED power in fiber #2. Calculate the crosstalk in each channel using the definition given in **Section 7.2**.

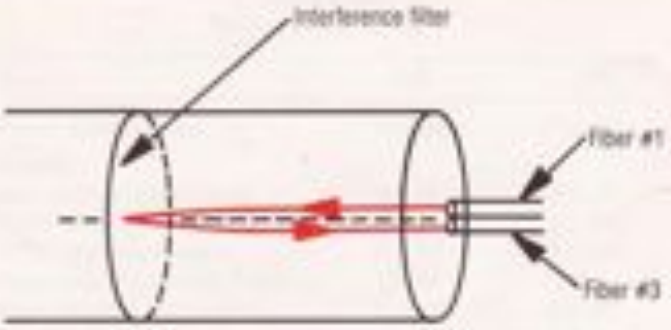

Figure 7.10. Coupling light from fiber #1 to fiber #3. When the fibers are placed symmetrically about the center line of the lens, light out of fiber #1 will be reflected by the interference filter and be focused into the core of fiber #3.

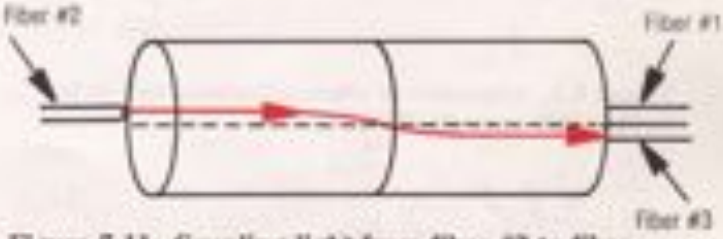

Figure 7.11. Coupling light from fiber #2 to fiber #3. Fiber #2 is placed symmetrically across the center line of the lens from fiber #3 at the opposite end of the lens assembly.

Figure 7.12. Completed multiplexer-demultiplexer system.

8.0 PROJECT #8: FIBER OPTIC COMMUNICATION LINK

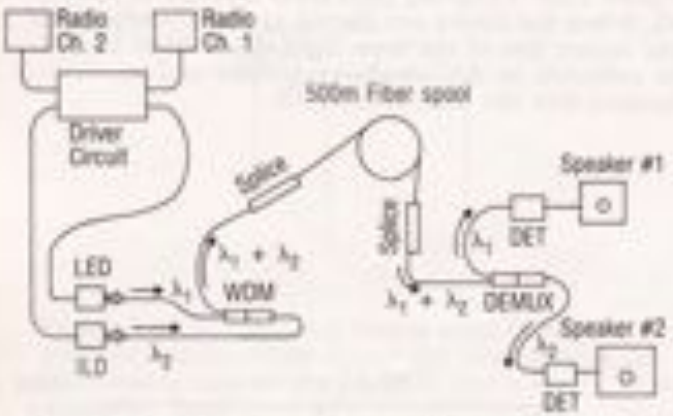

Figure 8.1. Schematic of communications link to be built in this project.

Previous projects have concentrated on the basic properties of fibers, the coupling of optical power into optical fibers, and fiber optic components. In this project, the techniques and devices examined in preceding projects will be utilized to construct a fiber optic communication link, as an illustration of the most important and widely used application of fiber optic technology. Communication links are constructed to accept data in either digital or analog form. This project will take two analog inputs, wavelength division multiplex them onto a single fiber, and demultiplex them at the receiver end of the link.

8.1 DATA COMMUNICATION LINKS

A schematic illustration of the analog communication link which will be constructed in this project is shown in **Fig. 8.1**. The outputs from a light-emitting diode (LED) and an injection laser diode (ILD) are both launched onto the same fiber using a wavelength division multiplexer (WDM), which was built during Project #7. The audio output signal of two radios, which are tuned to two different stations, will be the modulation sources (see **Section 0.5**) for the two diodes. At the receiver end of the link, a demultiplexer (DEMUX), which is a device identical to the WDM, but with light paths reversed, will separate the two signals and direct them to their respective detectors. The output of the two detectors will drive the speakers of the radios. In this way, you will be able to hear the results of sending two signals over a fiber optic communication link and will also be able to listen to the crosstalk to gain a qualitative as well as a quantitative appreciation of this important link parameter. Another option in building the link is to exchange positions of one of the sources with its detector to provide a two-way communication link.

8.1.1 SYSTEM LOSSES

In order to determine the performance characteristics of a fiber communications link, several factors must be taken into account. These include source power characteristics, intrinsic fiber transmission losses, coupling and connection losses (all of which have been treated in previous projects), and the receiver sensitivity. The source characteristics (**Project #5**) include total power output, wavelength dependence, and NA and area mismatch with the fiber. The fiber loss (**Project #2**) is the attenuation of the fiber in dB/km at the particular wavelength being used multiplied by the length of the link, in kilometers. At each fiber joint in the link, whether it be a connector or a splice (**Project #6**), there will be a loss which must be included. The total loss in the link will be the sum of all of these losses plus the loss due to the quantum efficiency of the photodetector. (The **quantum efficiency** of a detector is the fraction of incident photons at a given wavelength of light which produce electron-hole pairs.[1] The quantum efficiency is repre-

sented by η.) For the silicon detector used for this project, the quantum efficiency is 0.62 (representing a loss of -2 dB) at a wavelength of 900 nm.

When all of the losses in the link have been estimated, they are summed to give a total system loss and are then subtracted from the input power to find the received power at the end of the link. Such a calculation is called the power budget of the link. This is usually done in tabular form as part of the formal design of a fiber optic communication link. An estimate of the power budget for the data link described above is shown in **Table 8-1**. The estimated values in the table may be slightly different than those which you actually find in practice in this project. [The term dBm used in the table means "dB with respect to 1 mW of optical power," as was discussed in **Section 2.1**.]

TABLE 8-1
Power Loss Budget

Source:	ILD	LED
Power from source	0.0 dBm	+7.0 dBm
Losses:		
Source-fiber connection	4.0 dB	18.0 dB
WDM filter	0.5 dB	1.5 dB
WDM-fiber connection	0.5 dB	0.5 dB
Fiber transmission (0.5 km)	1.8 dB	1.8 dB
Fiber-DEMUX connection	0.5 dB	0.5 dB
DEMUX filter	0.5 dB	0.5 dB
Fiber-detector (η)	2.0 dB	2.0 dB
Total losses	9.8 dB	24.8 dB
Detected power	−9.8 dBm	−17.8 dBm

8.1.2 SYSTEM BANDWIDTH

When the modulation of the light transmitted by the link varies at a low rate, the detector can faithfully reproduce the signal. However, when the modulated light varies at a high rate, the detector may not be able to track the variations. This frequency response limitation may be due to ordinary circuit limitations (capacitance and inductance of the circuit) or to intrinsic electron-hole recombination times of the semiconductor device. The bandwidth of a detector is a measure of the modulation rate to which it can respond. The **3-dB bandwidth** is defined as the modulation rate at which the detector is only 50% efficient in responding to the variation in the modulated signal.[3] The detector bandwidth can be related to an equivalent **rise time**, which is the time it takes for the detector to go from zero current to maximum current when a pulse of light is incident on it. The rise time of the detector used in this project is less than 1 nsec.

We also need to calculate an equivalent rise time and bandwidth for the fiber. This rise time has two factors, the modal dispersion and the material dispersion of the fiber.

Modal dispersion is due to the differential time delay discussed in **Section 0.2.3**. Even when a graded-index fiber is used, small variances in the index profile from the ideal parabolic profile will result in some differential time delay. The modal dispersion term is found from the bandwidth-length product of the fiber. For the Newport F-MLD fiber, which is the fiber used here, this product is 300 MHz-km. The fiber bandwidth may be found by dividing the bandwidth product by the fiber link length. An equivalent rise time for the fiber is approximately 0.35 divided by the fiber bandwidth. For a 1 km link using the F-MLD fiber, this rise time is -1.2 nsec.

There is another type of dispersion which is due to the fact the index of refraction of the core of the fiber, n_{core}, of Eq. 0-12 is wavelength dependent. When the signal carried by the fiber has a spread of wavelengths, δt of Eq. 0-12 will be non-zero even for rays traveling the same path. This type of differential delay is due to the wavelength dispersion of the index of refraction, which was discussed in **Section 0.2.2**; it takes into account the wavelength dependent delays in the fiber. (You will also see this called

material dispersion in some fiber optics literature.) A typical value of the wavelength dispersion for fibers used in the 750-900 nm window is about 100 psec of delay difference per nanometer of spectral width per kilometer of fiber length. For an LED with a spectral width of 50 nm, this results in a delay of about 5 nsec/km. For laser sources, the delay is essentially zero, except when it is compared to the rise time required for the highest-speed data links.

In a cascade-connected system, the cumulative rise time is found by multiplying the square root of the sum of the squares of the individual rise times by 1.1. Thus, when the LED source is used, we have

$$1.1\times[(1\text{ nsec})^2+(1.2\text{ nsec})^2+(5\text{ nsec})^2]^{1/2} = 5.7\text{ nsec.} \quad (8\text{-}1)$$

In the case of the ILD source, we find a rise time of 1.7 nsec by replacing the 5 nsec term by zero. The 3 dB bandwidth of the system can then be found by dividing 0.35 by the resulting system rise time. This gives 61 MHz in the case of the LED source and 206 MHz in the case of the ILD source. From this, one can readily see why laser sources are used for high-speed data communication.

In the analog data link which you will be constructing, the bandwidth of the system will not be a limiting factor. The ILD and LED sources will be driven at audio frequencies, which have maximum frequencies on the order of tens of kilohertz. Therefore, the bandwidth required by the signal will be orders of magnitude less than the system bandwidth which we just calculated.

8.2 DATA TYPES

Data communications links use two data forms, as was discussed in **Section 0.5**. Digital communication sends data in the form of a binary code of 1's and 0's, and, after the signal is received, it is decoded. Analog communication, which is used in this project, sends data as a continuously varying signal, and the signal level itself is the message which is being transmitted.

8.2.1 DIGITAL SIGNALS

For many transmission applications, a binary signal is generated. That is, the optical power coupled into the fiber makes transitions only between two discrete levels, with those transitions occurring at only well-defined, periodically spaced, points in time. The signal source may also produce another periodic output, known as a clock, which is synchronous with the data signal.

The quality of the received signal is generally expressed in terms of error rates. In each time slot, there is a chance that the slot will contain a pulse when the signal did not, or vice versa. The most common approach to expressing the error rate is to state the average ratio of the number of errors to the number of transmitted pulses. This is the bit-error-rate (BER). State-of-the-art digital systems will have a BER of less than 10^{-9}.

8.2.2 ANALOG SIGNALS

Analog signals take on a continuum of levels. The signals which will be used in this project are analog signals with direct intensity modulation of the sources. Transmission fidelity requirements are generally much greater for analog signals than for digital signals. These requirements

are expressed in terms of the signal-to-noise ratio (SNR). Typical SNR requirements are 50-70 dB for analog signals. The SNR can be determined by comparing the power received in the message signal to the noise power generated in the detector and amplifier.

For a given noise level at the detector, there is a value of received power which gives SNR = 1. This power is defined as the **noise-equivalent power** (NEP),[3] which is an often quoted parameter characterizing receivers. Since the noise at the detector may be proportional to the system bandwidth, the NEP is usually expressed as watts per root hertz. A typical silicon p-i-n detector which would be used in a 0.8 micron communications link would have an NEP on the order of 10^{-13} watts/$Hz^{1/2}$ for a 10 MHz bandwidth system. This project does not require a detector with that low of an NEP value, because the message will be at audio frequencies and will require a bandwidth of only a few kilohertz.

8.3 REFERENCES

1. S. D. Personick, *Fiber Optics, Technology and Applications*, Plenum Press (New York), 1985, p.73
2. ibid., p.53
3. S. D. Personick, in *Fundamentals of Optical Fiber Communications*, 2nd Edition, M. K. Barnoski, ed., Academic Press (New York), 1981, p.281

8.4 PARTS LIST

Cat#	Description	Qty.	
F-MLD-50	100/140 MM fiber, 50 meters	1	
F-MLD-500	100/140 MM fiber, 500 meters	1	(optional)
XSN-22	2x2 Breadboard	1	
F-CLI	Fiber cleaver	1	
815	Power meter	1	
FK-BLX	Balldriver set	1	
SK-25	¼-20 Screw kit	1	
BS-05	¼-20 Thumbscrew kit	1	
B-1	Base	2	
VPH-2	Post holder	12	
SP-2	Post	12	
FP-1	Fiber positioner	4	
FPH-5	Fiber chuck	2	
MPC	Collar	2	
F-925	GRIN-lens fiber coupler	2	
FK-ILD	Laser diode assembly	1	
FK-LED	Light-emitting diode assy.	1	
FK-DRV	ILD LED Driver circuit	1	
FK-GR29	NSG W-1.8-0.29 lens	2	
F-IRC1	IR phosphor card	1	
CA-2	Universal clamp	2	
MH-2PM	Optics holder	4	
SP-3	Post	2	
FK-MUX	Multiplexer assy. base	2	
FK-GR25F	NSG 0.25-p lens w/ filter	2	
FK-GR25P	NSG 0.25-p lens w/o filter	2	
FK-DET	Detector assembly	2	
FK-SPKR	Speaker output	2	
F-TK1E	Epoxy	1	
F-SK-S	Splices	1	
F-SK-C	Splice fixture	1	

Additional equipment required: Methylene chloride for stripping fiber jackets. (Many commercial paint strippers contain methylene chloride and work well for this purpose. Methylene chloride is toxic and can be absorbed through the skin. Any methylene chloride which gets on your skin should be washed off immediately.)

8.5 INSTRUCTION SET

NOTE: Time constraints may dictate that part of the construction done as part of Project #7 be left until the start of this project. A convenient breaking point is indicated in that instruction set.

1. Disconnect the dry splice between the multiplexer and demultiplexer which you made as part of Project #7. Splice the 500 m spool of fiber which you used in Project #2 onto the output of the WDM. Make a permanent epoxy splice as you did in Project #6 (**Section 6.5.3**). (If you have chosen not to use the 500 meter spool of fiber, go on to Step 3, using the multiplexer output and demultiplexer input fibers.)

2. Measure the power out of the end of the spool of fiber and calculate the loss of the transmission fiber in your link. (Use an average value from other splices which you have made for the insertion loss of the splice.)

3. Splice the end of the fiber spool to the input fiber of the demultiplexer. Use the power out of the demultiplexer and the known demultiplexer losses, from Project #7, to find the insertion loss of this last splice.

4. Complete a power budget for your link similar to the one in the introduction.

5. Place a pre-recorded tape in each tape deck. The ear jack output of the tape deck runs directly to the modulation inputs of the driver circuit. The current of both laser and LED must be set so that the power output of each device is about half-way up the curves which you generated in Project #5 (**Section 5.6.1, Step #5 and Section 5.6.2, Step #3**). This will allow the tape deck input to modulate the outputs of the laser and LED without distortion.

6. Post mount each of the detectors. Run the output of the detectors to the two speakers.

7. Mount each of the demultiplexer outputs in an FPH-S Fiber Chuck. Hold each FPH-S in a post-mounted MPC Collar.

8. Mount each FK-DET Detector Assembly in a post-mounted MH-2PM Objective Lens Holder, in the same manner as the FK-ILD and FK-LED assemblies. Plug the output of each FK-DET assembly into an FK-SPKR Output Speaker.

9. Couple each fiber output to an FK-DET detector assembly. The completed laboratory set-up is shown in **Fig. 8.2**.

10. Power up the sources one at a time and listen to the sound from each of the speakers. Power up both sources together and listen to each speaker separately. How does what you hear correlate with the crosstalk figures calculated in Project #7?

11. Another project which you may wish to try is a two-way communications link. This can be accomplished by interchanging the fiber to one of the detectors with the corresponding fiber, which is the input fiber to the WDM for the same channel. [Changing the connections in this completed link to get two-way communication will be a project in itself.]

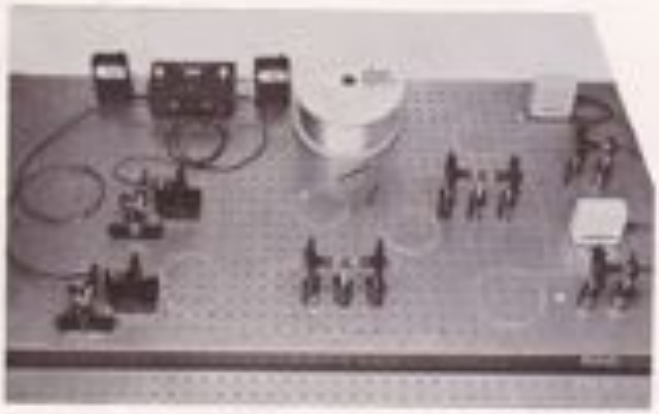

Figure 8.2. Photograph of laboratory set-up of the analog communications link. Compare with Fig. 8.1.

9.0 PROJECT #9: MULTIMODE INTENSITY SENSORS

The projects which you have undertaken up to this point have explored the basic properties of fibers, components for fiber communication, and an analog communication link. Another area of application in which fibers are being greatly used is the area of sensors. In this project, you will be looking at some examples of sensors which exploit the optical properties and light-guiding capabilities of multimode fibers. You will see examples of a variety of sensors, measuring a number of different physical parameters. What these fiber sensors have in common is that they all measure the intensity of the light returned by the fiber from a discrete sensor element. Single-mode fiber sensors, which measure the phase changes of the light carried by a single-mode fiber, will be studied in Project #10.

The multimode sensors which are illustrated in this project represent only a small sample of the many intensity sensors which have been designed or are in use. Instructors of advanced students may choose to design and construct sensors other than those presented here.

9.1 FIBER OPTIC SENSORS

The properties of optical fibers allow innovative approaches to the design of optical sensors. Because optical fibers are non-conducting, fiber optic sensors are immune to electromagnetic and radio frequency interference and are safe in explosive environments. The low attenuation coefficients of fibers allow sensitive electronic equipment to be remotely located. The availability of fiber optics gives the system engineer great flexibility in sensor design. Fiber optic sensors are used in applications ranging from simple counters and limit switches to measurements requiring high precision and accuracy.

Fiber optic sensors can be classified into two general categories, intensity sensors and phase sensors. These two classes of sensors differ not only in construction, but also in sensitivity, dynamic range, and signal transmission and detection schemes. Phase sensors use single-mode fibers and employ interferometric techniques to extract phase information from the sensor. They will be explored in Project #10, "Single-Mode Interferometric Sensors."

Intensity sensors generally use multimode fibers and small transducers which can make measurements at specific points along the light path. (A **transducer** is a device which converts one physical parameter into another, making the measurement of the first parameter easier. For example, the mercury in a thermometer is a transducer that converts temperature into a column height which can be more easily measured. The transducer in a fiber optic intensity sensor converts a physical parameter into a change in the amount of light which is transmitted.) Optical power is transmitted to the sensor, the physical parameter

Figure 9.1. Liquid level sensor. θ_c is the critical angle for total internal reflection at a glass-air interface in the glass fiber.

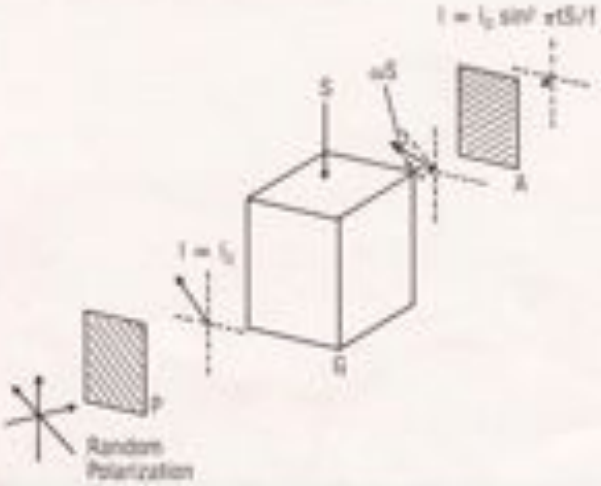

Figure 9.2. Pressure sensor using the photoelastic effect. Unpolarized light is polarized, at an angle of 45° with respect to the stress axis, S. Stress causes birefringence which causes the polarization of the light to change. Analyzer, A, selects the perpendicular component of the beam.

to be measured causes the transducer to change the amount of light passed by the sensor, and the power is then returned to the detector. Depending on the type of intensity modulation used, multimode intensity sensors may be further subdivided into two major groups, hybrid sensors and internal effect sensors. Hybrid sensors treat the fiber as a light pipe, transmitting the light to a remote sensor, which is generally a miniaturized device at the end of the fiber. Hybrid sensors allow a broad range of modulation schemes, which includes practically all conventional non-fiber optical sensors, limited only by the imagination of the system designer. Internal effect sensors, on the other hand, use the fiber itself as the transducer, with the parameter being measured causing a modulation of the light-guiding properties of the fiber.

The remainder of this discussion will focus on the fiber optic intensity sensors that will be examined in the laboratory project. The first three references which appear in the list following this introduction cite a large amount of recent developmental work in fiber optic sensors and further information can be gained from them.[1-3]

9.2 HYBRID SENSORS

The simplest of sensors acts as an on-off switch to detect the presence or absence of a stimulus at the sensor site. An example of this, shown in **Fig. 9.1**, is a liquid level sensor which detects the presence or absence of liquid in the gap between two fiber ends. As shown in the figure, the fiber ends are tapered so that the angle of the fiber end is greater than the critical angle for total internal reflection of the central ray of the beam transmitted by the fiber. When a liquid is present in the gap between the fiber ends, the glass-air interface at which total internal reflection occurs is eliminated and the index of the glass is nearly matched by the liquid. When this happens, the light is no longer totally internally reflected and optical power is transmitted from one fiber end to the other.

Another, more sophisticated hybrid sensor is the pressure sensor, illustrated in **Fig. 9.2**, which uses the photo-elastic effect to monitor the pressure in a glass transducer.[4] Pressure applied to the glass causes stress-induced birefringence, resulting in a change of the polarization of the beam transmitted through the transducer. The polarizer, P in the figure, causes the light incident on the glass to be polarized at an angle of 45° with respect to the applied stress, S. The stress-induced birefringence causes the plane of the polarization to change from linear to elliptical. A second polarizer, A, which acts as an analyzer selects the component of the transmitted beam perpendicular to the original linear polarization. For the configuration shown, the optical power transmitted by the sensor is[5]

$$I = I_o \sin^2(\pi t S/f). \qquad (9\text{-}1)$$

where t is the thickness of the glass transducer, S is the applied stress, and $f = 2S_0$, where S_0 is the stress required to make the transmitted power through the transducer go from a maximum to a minimum. It is called the material fringe value. Typical values for f are in the range of 0.2–0.3 MPa-m. This type of sensor has been used to measure pressures of up to 21 MPa (3,000 psi) with a resolution of better than $\Delta P/P = 10^{-4}$.

The previous two examples use high-quality low-loss multimode transmission fibers so that remote measurements can be made at long distances. Some other fiber sensors make use of lower-technology fiber bundles. An example of a proximity sensor which uses a bifurcated (Y-branched) fiber bundle is shown in **Fig. 9.3**. Optical power, which, in this case, can be from a white-light source, is launched in one arm of the fiber bundle. It is reflected from a surface at the output end of the fiber, and part of that reflected light is accepted by the second arm of the bundle and is transmitted to a detector. The amount of light returned to the detector depends on the distance between the end of the bundle and the surface being monitored.

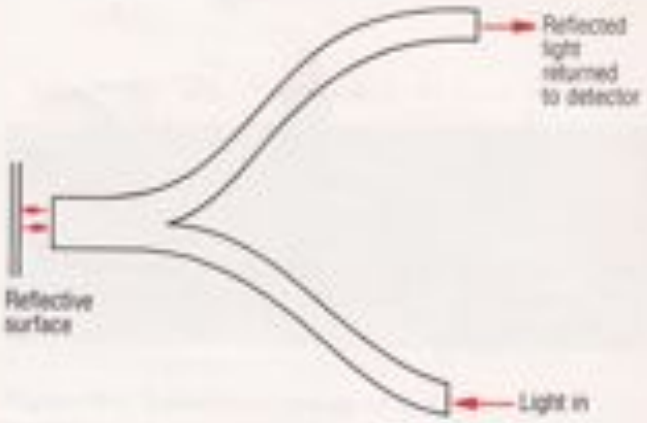

Figure 9.3. Proximity sensor using a bifurcated fiber bundle.

9.3 INTERNAL EFFECT SENSORS

Internal effect sensors make use of modulation schemes which perturb the fiber itself, so that the fiber is both the transmission medium and the transducer. The modulation effects which may be used in these sensors includes the microbending loss mechanism, the "fiberdyne" modal intensity modulation effect, in which mode filtering is used to detect redistribution of the optical power due to mode coupling caused by mechanical deformation of the fiber, and internally generated thermal radiation.[2]

As an example of the sensors which can be designed, **Fig. 9.4** shows a displacement sensor which makes use of the microbending phenomenon.[3] Optical power is coupled from guided modes to the cladding when the fiber is bent. The displacement sensor has a fiber placed between two corrugated plates and the optical loss is measured as a function of the displacement of the two corrugated plates with respect to each other.

The examples of multimode fiber optic intensity sensors which have been discussed here are, of course, only a small part of the large number of fiber optic sensors which have been investigated or developed.

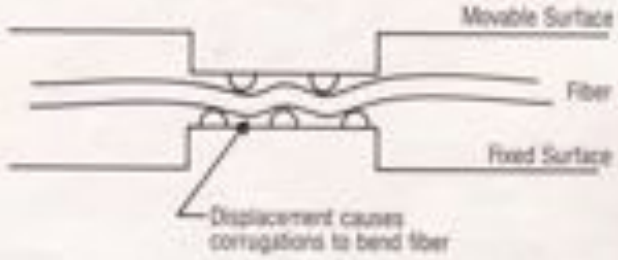

Figure 9.4. Microbend strain sensor. Structural strain causes corrugations to bend the fiber, causing loss.

9.4 REFERENCES

1. T. G. Giallorenzi, et al., "Optical fiber sensor technology," IEEE Journal on Quantum Electronics *QE-18*, 626 (1982)

2. S. K. Yao and C. K. Asawa, "Fiber optic intensity sensors," IEEE Journal on Selected Areas in Communications *SAC-1*, 562 (1983) and references therein.

3. Proceedings of the SPIE, *Fiber Optic and Laser Sensors*, Vol. 412 (1983), Vol. 478 (1984), Vol. 566 (1985), Vol. 586 (1985)

4. E. Hecht and A. Zajac, Optics, Addison-Wesley (Menlo Park), 1974, p.260

5. W. B. Spillman, Jr., "Multimode fiber-optic pressure sensor based on the photoelastic effect," Optics Letters *7*, 388 (1982)

6. C. K. Asawa, S. K. Yao, R. C. Stearns, N. L. Mota, and J. W. Downs, "High sensitivity fiber optic strain sensor for measuring structural distortion," Electronics Letters *18*, 362 (1982)

9.5 PARTS LIST

Cat#	Description	Qty.
F-MLD-50	100/140 MM fiber, 50 meters	1
XSN-22	2x2 Breadboard	1
U-1301P	1 mw HeNe laser	1
807	Laser mount	1
340C	Clamp	1
41	Short rod	1
815	Power meter	1
F-CL1	Fiber cleaver	1
F-916	Fiber coupler (w/o lens)	1
M-20X	20X Objective lens	1
FK-BLX	Balldriver set	1
SK-25	¼-20 Screw kit	1
VPH-2	Post holder	7
SP-2	Post	7
FP-1	Fiber positioner	3
FM-1	Mode scrambler	1
F-TK1E	20 pkgs. epoxy	1
F-TK1L	160 Lapping sheets	1
FK-LS	Liquid-level sensor assy.	1
FK-PS	Pressure sensor assy. base	1
FK-GT	Glass transducer	4
FK-GR25P	NSG 0.25-p lens w/o filter	2
FK-POL	Polarizer, sheet	1
421-0.5	Translation stage	1
MPC	Collar	3
777-1	Bifurcated fiber bundle	1

Additional equipment required: Laboratory weight set for the pressure sensor. Methylene chloride for stripping fiber jackets. (Many commercially available paint strippers contain methylene chloride and work well for this purpose. Methylene chloride is toxic and can be absorbed through the skin. Any methylene chloride which gets on your skin should be washed off immediately.)

9.6 INSTRUCTION SET

9.6.1 LIQUID-LEVEL SENSOR

1. Strip the jacket from the end of two lengths of F-MLD fiber. Lay the fiber in the grooves of the liquid-level sensor inserts. There is a recessed area at the end of the insert into which the jacketed end of the fiber may be set for strain relief.

2. Use the F-TK1E epoxy to mount the fibers in the grooves as shown in **Fig. 9.5**. Be sure that this includes part of the jacketed fiber in the recessed area.

3. When the epoxy is cured, polish the fiber ends. Use the same general technique you used to polish the fibers in the connector halves in Project #6 (**Section 6.5.2, Steps 6–11**); this time, however, you do not have a polishing fixture to hold the pieces.

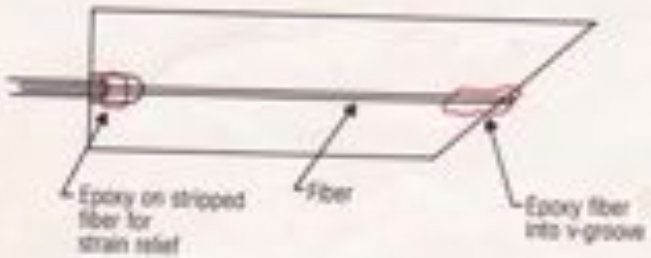

Figure 9.5. Epoxy the fibers into the v-groove of the angled pieces of the FK-LS Liquid Level Sensor.

4. When the polishing is complete, place the insert on the sensor assembly base. Slide the inserts against the rail so that the fibers will be aligned with each other. Adjust the spacing between the fiber ends to about ½ mm. The actual spacing required depends on the surface tension and viscosity of the liquid which you have chosen to use in your experiment. The trade-off is between the fact that the spacing must be large enough so that surface tension will not cause a bead of liquid to remain between the fiber ends when the liquid level subsides, and the fact that you also want to keep the spacing small to maximize the optical coupling between the fibers.

5. Couple light from the HeNe laser into one of the fibers. Record the optical power through the sensor. The complete laboratory set-up for this sensor is shown in **Fig. 9.6**.

6. Immerse the sensor in a liquid bath or place a drop of liquid between the fibers in the gap in the sensor. (Glycerin, water, or alcohol all work well. Acetone will eventually dissolve the epoxy.) Record the power through the sensor.

7. Calculate the ratio of power between the on and off states of the sensor.

9.6.2 PRESSURE SENSOR

1. Determine the optical axis of the FK-POL Polarizing Sheet. The following simple method can be used to determine the optical axis of a polarizer. When viewed at an angle of ~56°, the glare from a sheet of glass will be polarized in a plane parallel to the glass sheet. (See p.244 of Reference 4, above, for a description of this phenomenon.) When viewed through the polarizer, the glare will be a maximum when the optical axis is parallel to the plane of polarization (**Fig. 9.7a**) and the glare will be a minimum when the optical axis is perpendicular to the plane of polarization (**Fig. 9.7b**).

2. Cut two pieces from the FK-POL Polarizing Sheet so that the axis of polarization is at an angle of 45° to the sides of the rectangle which you cut and so that the pieces fit the ends of the FK-GT Glass Transducer.

3. Epoxy the polarizers to the glass transducer. Use a thin film of epoxy; be sure that there are no bubbles in the epoxy. If the polarization axes of the polarizer and analyzer are crossed with respect to each other, the sensor will give a $\sin^2$ stress dependence, as was seen in Eq. 9-1. If the polarization axes are parallel, the sensor will give a $\cos^2$ dependence. Crossed polarizers would be preferred in a commercial device, because the highest pressures would give the largest signals, and a large amplification could be used to detect small stresses in a dark background, but parallel polarizers are recommended for a student laboratory, because this makes the optical alignment of the sensor easier.

4. Glue two ¼-pitch GRIN-rod lenses (Model # FK-GR25P) into the grooves in the pressure sensor assembly base (see **Fig. 9.8**). Be sure that the ends of the lenses do not extend into the central portion of the sensor, which will be occupied by the glass transducer.

Figure 9.6. Laboratory set-up of the liquid-level sensor.

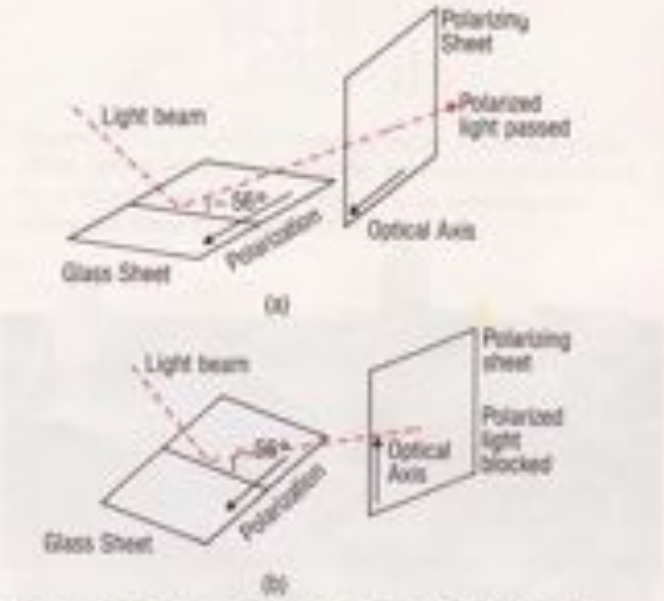

Figure 9.7. Determination of the optical axis of a polarizer. a) Optical axis parallel to the plane of polarization. b) Optical axis perpendicular to the plane of polarization.

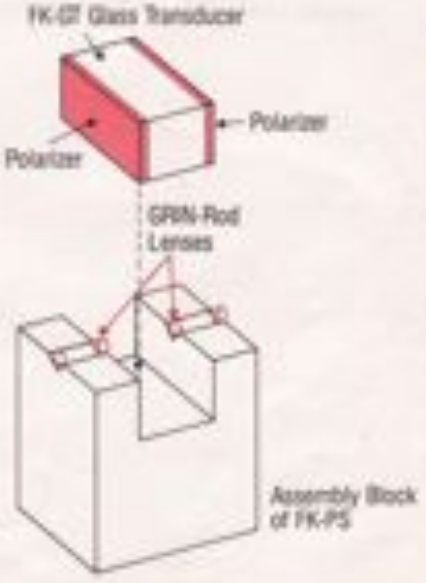

Figure 9.8. Placement of the two 1/4-pitch GRIN-rod lenses in the FK-PS Pressure Sensor Assembly.

Figure 9.9. Laboratory set-up of the pressure sensor.

Figure 9.10. Laboratory set-up of the proximity sensor.

5. Prepare two lengths of F-MLD fiber. Couple HeNe laser light into one of the fibers using the F-916 Fiber Coupler. Mount each fiber in an FP-1 Fiber Positioner, as shown in the laboratory set-up of **Fig. 9.9**. The sensor assembly should be mounted on posts to provide the proper height for coupling light through the sensor. Maximize the fiber-to-fiber coupling through the assembly.

6. Place the glass transducer in the assembly. Again maximize the fiber-to-fiber coupling.

7. Bring the lever arm down on top of the transducer. Adjust the set screw so that the lever arm is horizontal when it rests on the glass. Add weight to the end of the lever arm. Monitor the optical power through the sensor as a function of applied weight. Calculate the pressure in the glass from the applied force, the cross-sectional area of the glass, and the mechanical advantage of the lever arm.

8. Plot the power transmitted by the sensor as a function of applied pressure. Compare this with a cosine^2 curve (assuming that you used parallel polarizers). Find the pressure at which the transmitted power goes through a minimum. Use this to calculate the fringe constant of the glass from Eq. 9-1.

9.6.3 PROXIMITY SENSOR

1. Insert an 8-32 set screw into each of three SP-2 posts. Screw an MPC collar onto each set screw. Insert each of the three ends of the 777-1 dual fiber bundle into each collar. **Gently** tighten each set screw. Do not overtighten. The laboratory set-up for this sensor is shown in **Fig. 9.10**.

2. Mount one of the single ends in a VPH-2 post holder and illuminate this end with a HeNe laser. This sensor can also be constructed using a white-light source if you have a high-power lamp which can be focused onto the end of the fiber bundle.

3. Fix a VPH-2 post holder onto a 420-0.5 translation stage and place the post with the common end of the fiber bundle into this holder. Set up a card so that the HeNe output of the fiber bundle shines on the card or mount the translation stage so that the output shines on a wall. In either case, the fiber bundle needs to be mounted so that it is able to actually make contact with the surface to be measured.

4. Light reflected by the surface being monitored will be reflected back into the fiber bundle and will go to the second single end. Mount this end in a VPH-2 post holder and couple the output light onto the detector of the 815 Power Meter.

5. Measure the reflected output as a function of distance, d, of the surface of the common end of the bifurcated fiber bundle from the monitored surface. Also plot this power as a function of $1/d^2$.

6. Find the point where a linear $1/d^2$ dependence begins. This is the distance at which the finite diameter of

the fiber core is no longer significant in determining the amount of reflected light accepted by the fiber bundle. Why does the amount of reflected power accepted by the fiber bundle drop from a maximum as you get very close to the surface? (**HINT:** Draw the light cone from the fiber bundle incident on the surface being monitored and the cone of acceptance of the neighboring fiber which detects the light as in **Fig. 9.11**. Vary the distance between the fiber end faces and the reflecting surface.)

7. Estimate the positional resolution of this sensor.

9.6.4. MICROBEND DISPLACEMENT SENSOR

1. The FM-1 mode scrambler which you used in Projects #2 and #6 may be used as an example of a displacement sensor. Rotate the knob on the FM-1 to fully separate the corrugated surfaces.

2. Launch light into a segment of F-MLD fiber using the HeNe laser and the F-906 coupler. The laboratory set-up for this sensor is shown in **Fig. 9.12**.

3. Place the jacketed fiber in the slot between the corrugated surfaces.

4. Rotate the knob until the corrugated surfaces just contact the fiber. Note the knob position. Each major graduation on the knob represents a 25 micron displacement; the smaller graduations mark 12.5 micron displacements.

5. Record the output from the fiber as a function of displacement. The fiber has a soft buffer, so some period of stabilization may be needed after you set the displacement for the transmitted power to come to equilibrium. In an actual sensor system, the knob-controlled displacement would be replaced by having the corrugated surfaces attached to two surfaces whose relative position is to be measured.

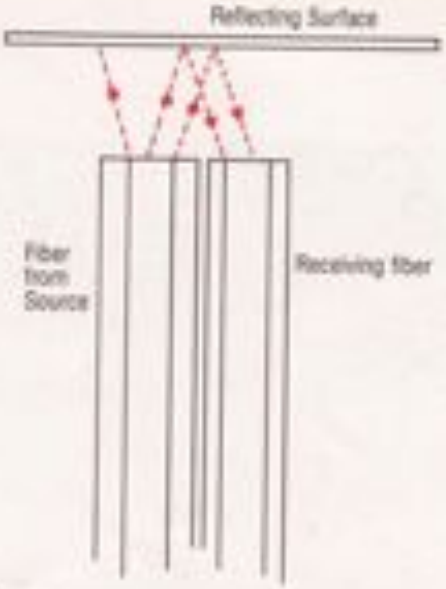

Figure 9.11. Drawing showing light emitted by one fiber, reflected by the near-by surface, and received by a neighboring fiber. Repeat this drawing for different fiber-to-surface distances.

Figure 9.12. Use of the FM-1 Mode Scrambler as a fiber optic microbend displacement sensor.

10.0 PROJECT #10: SINGLE-MODE INTERFEROMETRIC SENSORS

The previous project investigated multimode intensity sensors. This project will look at single-mode interferometric sensors. These sensors differ from multimode sensors, not only in the type of fiber used, but in the fact that they detect phase changes rather than the intensity of the transmitted light. These phase changes are caused by the effects which any of a variety of physical parameters may have on the fiber itself.

In the course of this project, you will construct a single-mode fiber interferometer and use it to measure changes in temperature and pressure. You will see that this technique allows for the construction of sensors which have high sensitivity and high resolution.

10.1 INTERFEROMETRIC SENSORS

Interferometric sensors are sophisticated sensors which detect the influence of physical perturbations on the phase of the light propagating in a single-mode fiber. These sensors offer the potential of extremely high sensitivity, but also require the best single-mode fiber technology available for their construction. The most common phase sensors use the Mach-Zehnder interferometer. The geometry of the Mach-Zehnder interferometer was described in **Section 0.3.5**. A fiber optics version is illustrated in **Fig. 10.1**. The first beamsplitter of **Fig. 0.24** is replaced by a bidirectional coupler and the light is launched into two single-mode fibers of equal lengths. These two fibers replace paths #1 and #2 and the mirrors of **Fig. 0.24**. One of the fibers serves as the reference arm, which is kept isolated from external perturbations, while the other fiber serves as the sensor arm of the interferometer, which is exposed to the perturbation to be measured. The external perturbation induces the phase shift in the sensing arm by means of a change in the optical path length, which is caused by a change in the index of refraction of the glass of the fiber and/or a change in the length of the fiber. The phase shift is detected when the two beams are recombined at the receiver end of the sensor. This results in fringes which can be detected and counted. Sensors using the Mach-Zehnder configuration can be constructed to measure a wide variety of physical parameters, including stress, strain, acoustic waves, magnetic field, and temperature. Single-mode optical fibers are employed in sensors using other types of interferometers, also. The best known of these is probably the fiber gyroscope for measuring rotation rates, which uses a Sagnac interferometer.[1]

When the Mach-Zehnder interferometer has been constructed, the light from the two fibers interferes to form a series of bright and dark fringes. A change in the phase of the light in the sensor fiber with respect to the phase of the light in the reference fiber appears as a displacement of the fringe pattern; a phase change of 2π radians causes a

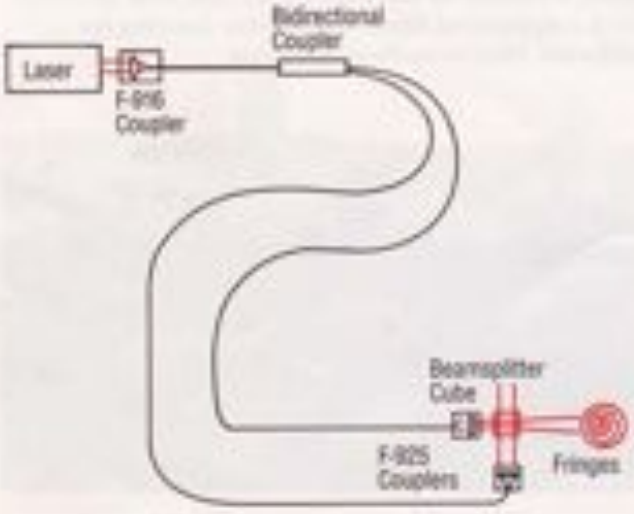

Figure 10.1. Mach-Zehnder fiber optic interferometer configuration.

displacement of one fringe. The magnitude of the change in the physical parameter to be measured can be determined directly by counting the fringe displacement.

The phase of a light wave which travels a distance, L, in an optical fiber is given by $\phi = \beta L$, where β is the propagation constant of the light in the fiber. Changing any physical parameter of the fiber's environment causes a phase change given by

$$\delta\phi = \beta\delta L + L\delta\beta. \tag{10-1}$$

The first term on the right hand side of the equation is due to a change in the length of the fiber, while the second term is due to a change in the propagation constant. The length, L, now represents the length over which the physical change affects the fiber. The quantity which we actually wish to determine is the phase change per unit fiber length per unit of physical stimulus, $(\delta\phi)/SL$, where S is the stimulus. The magnitude of the stimulus can then be measured by counting the shift of the fringes for a fiber of known interaction length.

10.2 INTERFEROMETRIC TEMPERATURE SENSOR

As an example, consider the effect of a temperature change, δT, which affects a length, L, of the fiber in the sensor arm of the interferometer. There are two effects which occur: the change of length due to thermal expansion or contraction, and the change of the propagation constant due to the temperature dependence of the index of refraction. Thus, Eq. 10-1 becomes[2]

$$\delta\phi/(\delta TL) = (2\pi/\lambda)\,[(n/L)(\delta L/\delta T) + (\delta n/\delta T)]. \tag{10-2}$$

where

$$\delta L/\delta T = [L(T_1) - L(T_2)]/[T_1 - T_2]$$

and

$$\delta n/\delta T = [n(T_1) - n(T_2)]/[T_1 - T_2].$$

For the case of a fused silica fiber and a HeNe laser source, the following values for pure silica might be used:

$$1/L\,(\delta L/\delta T) = 5 \times 10^{-7}/°C,$$
$$\delta n/\delta T = 10 \times 10^{-6}/°C,$$
$$n = 1.456,$$

and

$$\lambda = 632.8 \times 10^{-9}\ m.$$

This gives

$$\delta\phi/(\delta TL) = 107\ \text{radians}/°C\text{-m}, \tag{10-3}$$

which corresponds to 17 fringes per °C per meter of fiber.

This final value must be taken as an order of magnitude calculation, since both the thermal expansion coefficient and the temperature dependence of the index of refraction can vary greatly for multi-component glasses such as those in optical fibers ($\delta n/\delta T$ may even be negative

in some cases). However, this does show that even using a resolution of one fringe as a very conservative estimate yields a resolution of ~0.06 °C-m for a single-mode interferometric temperature sensor.

10.3 INTERFEROMETRIC PRESSURE SENSOR

As a second example, consider the effect of a pressure, P, on a length of fiber, L. [The following derivation[2] is quite involved. Students who have not had an upper-division course in solid-state physics at the level of Kittel[3] should proceed to Eq. 10-9.] If the pressure is isotropic, then any component of the stress can be written as $\sigma_i = -P$. The z-component of the strain can then be written as

$$\epsilon_z = -P(1-2\mu)/E, \tag{10-4}$$

where μ is Poisson's ratio and E is Young's modulus. The first term of Eq. 10.1 becomes

$$\beta\delta L = \beta\epsilon_z L = -\beta(1-2\mu)LP/E. \tag{10-5}$$

The second term of Eq. 10-1 reflects the strain-optic effect where the strain changes the refractive index of the fiber. (There is also a contribution from the change of diameter of the fiber due to the pressure, but this term is negligible compared to the others.)

$$L\Delta\beta = L(d\beta/dn)\,\delta n. \tag{10-6}$$

The change in the index of refraction may be calculated from the change in the optical indicatrix, $\delta(1/n^2)$. This change in the refractive index is found to be

$$\delta n = -\tfrac{1}{2}n^3\delta(1/n^2) = -\tfrac{1}{2}n^3\epsilon_z[2p_{12} + p_{11}]. \tag{10-7}$$

where p_{11} and p_{12} are elements of the strain-optic tensor. Combining these last three equations yields

$$\delta\phi/(\delta PL) = (-2\pi/\lambda)\,(1-2\mu)/E\,[n - \tfrac{1}{2}n^3[2p_{12} + p_{11}]] \tag{10-8}$$

Again assuming a HeNe source and a pure silica fiber, we have

$$n = 1.456,$$
$$E = 7 \times 10^{7}\ N/m^2,$$
$$p_{11} = 0.121,$$
$$p_{12} = 0.270,$$
$$\mu = 0.17,$$

and

$$\lambda = 632.8 \times 10^{-9}\ m.$$

This results in

$$\delta\phi/(\delta PL) = -4.09 \times 10^{-1} \text{ radian/Pa-m}. \quad (10\text{-}9)$$

which corresponds to a fringe shift for each 154 kPa-m or 22.3 psi-m. Again, this is really an order of magnitude calculation, since, for multi-component glasses, Young's modulus may vary by more than 20%, and Poisson's ratio may vary by a factor of 2 from that used in this example.

10.4 POLARIZATION PROBLEMS

The polarization of the light traveling in the interferometric sensor is important because if the polarizations of the two output beams are not plane parallel, sharp fringes will not be seen. In the worst case, when the two polarizations are orthogonal to each other, no interference will occur at all (**Section 0.3.5**).

When long lengths of fiber are used in the interferometer, polarization-preserving fiber of the type investigated in Project #4 is used. This assures that the output beam will be plane polarized in the same direction as at the input and that sharp fringes will be obtained. When short lengths of fiber, such as the approximately two meters required for this project, are used in the interferometer, standard single-mode fiber may be used. If plane-polarized light is launched in the fiber, the light will stay pretty well in its original plane-polarized mode as long as the perturbations which would cause mode coupling are kept to a minimum. The output ends of the fibers can then be manipulated to cause the polarizations of the output beams to be parallel.

This last statement may sound highly qualitative, but this approach works well for shorter fiber lengths, and avoids the need for handling and aligning the polarization-preserving fibers.

10.5 REFERENCES

1. L. B. Jeunhomme, *Single-Mode Fiber Optics, Principles and Applications*, Marcel Dekker (New York), 1983 p.251

2. G. B. Hocker, "Fiber-optic sensing of pressure and temperature," Applied Optics *18*, 1445 (1979)

3. C. Kittel, *Introduction to Solid State Physics, Fourth Edition*, John Wiley & Sons (New York), 1971

10.6 PARTS LIST

Cat#	Description	Qty.
F-SV-20	4/125 SM fiber, 20 meters	1
XSN-22	2x2 Breadboard	1
U-1303P	1 mw HeNe laser	1
807	Laser mount	1
340C	Clamp	1
41	Short rod	1
F-916	Fiber coupler (w/o lens)	1
M-20X	20X Objective lens	1
FK-BLX	Baldriver set	1
F-CL1	Fiber cleaver	1
SK-25	¼-20 Screw kit	1
MPH-1	Micro-series post holder	1

MSP-1	Micro-series post	1
MM-1	Mirror mount	1
FK-BSC	Beamsplitter cube	1
F-925	GRIN-rod lens coupler	2
FK-GR25P	GRIN-rod lens 0.25-pitch	2
FK-PS	Pressure sensor assy. base	1
FK-GT	Glass transducer	2
F-506B	SM Directional Coupler	1

Additional equipment required: Methylene chloride for stripping fibers. (Many commercial paint strippers contain methylene chloride and work well for this purpose. Methylene chloride is toxic and can be absorbed through the skin. Any methylene chloride which gets on your skin should be washed off immediately.) Laboratory weight set for pressure sensor.

10.7 INSTRUCTION SET

10.7.1 SETTING UP THE INTERFEROMETER

1. Couple the output of a polarized HeNe laser to any one of the four fibers of an F-506B single-mode bidirectional coupler, using the F-916 coupler as you learned to do in Project #3 (**Section 3.6.1**). The fibers used in this project may be stripped using methylene chloride.

2. Cleave the two output ends coming from the bidirectional coupler.

3. Cleave the two pigtails of the output end of the F-506B Bidirectional Coupler so that the two pigtails are of equal length. [Remember, in order to obtain sharp fringes, the total optical path lengths of the two arms of the interferometer, from the point where the sensor and reference beams are split to the point where they are recombined, need to be equal to within the coherence length of the laser (**Section 0.3.4**). The coherence length of the U-1301P HeNe laser is 20 cm.]

4. Mount the MM-1 Mirror Mount on the MSP-1 Micro-Series Post and place this in the MPH-1 Micro-Series Post Holder. Place the FK-BSC Beamsplitter Cube on top of the MM-1. The beamsplitter can be held in place with double-sided tape. Adjust the height of the beamsplitter so that it matches the height of the F-925 GRIN-Rod Lens Coupler.

5. Place an FK-GR25P GRIN-rod lens in each of the F-925 couplers. (This was shown in **Fig. 5.5**.) Insert one of the fibers of the interferometer into each of the F-925 couplers and adjust the fiber position so that the beam out of the GRIN-rod lens is well collimated. Arrange the F-925 couplers so that the beams cross at the center of the beamsplitter. Adjust the beamsplitter so that the output beams from the two arms of the interferometer overlap. The laboratory set-up of the interferometer is shown in **Fig. 10.2**.

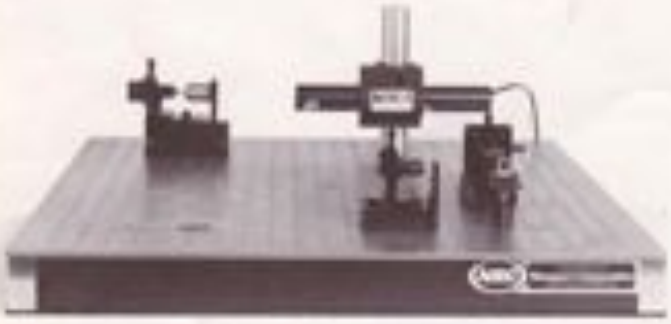

Figure 10.2. Laboratory set-up of the Mach-Zehnder interferometer.

6. Two beams will be coming from the beamsplitter at right angles to each other. Either of these beams may be used for viewing fringes. Block the unwanted beam and place a card in the path of the beam which you will be using at a distance which gives convenient viewing of the interference fringes. Back the fibers in the F-925 couplers away from the GRIN-rod lenses. This will give an adequate beam expansion so that the interference fringes can be viewed easily.

7. If fringes with good contrast are not obtained, recheck your alignment of Step 5. If the beams do not coincide properly at both the point where they cross at the center of the beamsplitter and where they overlap at the card, fringes will be difficult to observe. If you see many fine fringes instead of a bull's-eye pattern, you are off to the side of the interference pattern. Adjust the fiber in one of the F-925 couplers to find the center of the pattern.

10.7.2 TEMPERATURE SENSOR

1. In the discussion above, it was found that the fringe displacement of the interferometer is highly temperature dependent. You can get a good feeling for this by trying a simple qualitative demonstration. After the interferometer has been set up, place your hand around one of the fibers without touching it. The heat from your hand will cause a rapid displacement of the fringes, even though you are not in direct contact with the fiber. As you perform this and the following exercise, be aware of the environmental conditions of your interferometer, especially if there is an air-conditioner outlet near your apparatus.

2. A simple quantitative experiment to calibrate the temperature sensitivity of the interferometer can be done using ice. Before doing the experiment, use the data from Eq. 10-3 to calculate the expected fringe displacement between a typical room temperature and 0°C. You should get a value of about 9 fringes for an interaction length of about 1 inch (about 2½ cm).

3. Get some ice cubes and allow them to stand until they have become wet to the touch. If they feel dry, they may be at a temperature which is significantly less than 0°C. If they feel wet, then their surface should be right at 0°C.

4. Lay one of the ice cubes on a straight section of one of the fibers on the breadboard. Because of the large thermal mass of the breadboard, it may take 30-60 seconds for the fiber to come into thermal equilibrium with the ice. This will ensure that you have plenty of time to count the fringes as they change.

5. Compare the number of fringes which you counted with the value that you got when you did the calculation in Step 2. How good is the "order of magnitude" calculation leading to Eq. 10-3?

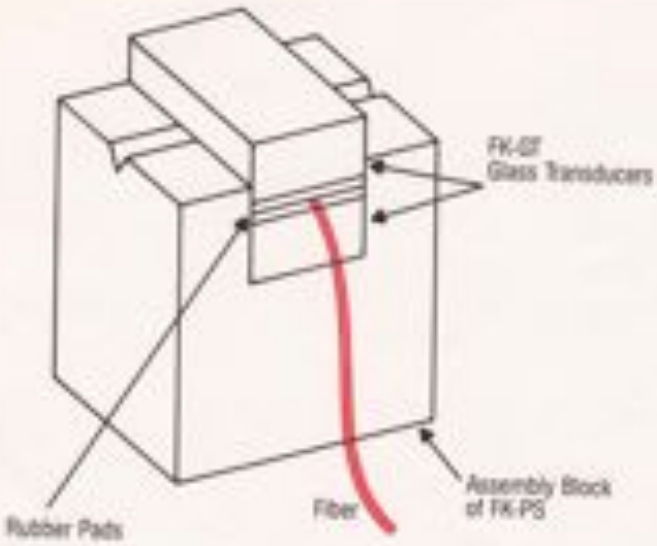

Figure 10.3. Assembling the pressure sensor for this experiment.

10.7.3 PRESSURE SENSOR

1. Set up the FK-PS pressure sensor assembly (which you used in Project #9) at the edge of the breadboard. Since you will not be coupling light through it, you will not need to raise it up on posts as you did before.

2. You will use two pieces of the glass transducer, FK-GT, from the supplies for Project #9. However, this time you will not be passing light through them to measure pressure. Lay one of the pieces of glass on its side in the assembly, as shown in **Fig. 10.3**. Cut two thin slices from a soft eraser. Lay one on top of the glass. Place one of the fibers over this. Lay the second piece of eraser on top of the fiber and then place the second piece of glass on top of the whole assembly.

3. Bring the lever arm of the FK-PS down on top of this stack and adjust the screw so that the arm is level.

4. Now add weight to the lever arm and measure the fringe displacement as a function of added weight.

5. Calculate, using Eq. 10-9, the expected fringe displacement for the amount of weight which you added. Even though you are using a soft rubber material around the fiber, you will probably find that the best agreement between your calculation from Eq. 10-9 and your experimental result is obtained when you assume that the force is concentrated on the fiber and not distributed over the full area of the glass transducer.

REFERENCES

The lists of references which are included in this section are representative of materials that are available but are not intended to be complete.

The following are books which you may wish to consider as texts for a fiber optics course:

M. K. Barnoski, ed., *Fundamentals of Optical Fiber Communications*, 2nd Edition, Academic Press (New York), 1981

S. D. Personick, *Fiber Optics, Technology and Applications*, Plenum Press (New York), 1985

The following are texts which you may wish to use as optics reference books in a fiber optics course:

F. A. Jenkins and H. E. White, *Fundamentals of Optics*, Fourth Edition, McGraw-Hill (New York), 1976

E. Hecht and A. Zajac, *Optics*, Addison-Wesley (New York), 1974

M. Born and E. Wolf, *Principles of Optics*, 6th Edition, Pergamon Press (Oxford), 1980

You may wish to use the following as supplementary references in a fiber optics course:

L. B. Jeunhomme, *Single-Mode Fiber Optics, Principles and Applications*, Marcel Dekker (New York), 1983

H. Kressel and J. K. Butler, *Semiconductor Lasers and Heterojunction LED's*, Academic Press (New York), 1977

D. Marcuse, *Theory of Dielectric Waveguides*, Academic Press (New York), 1974

D. Marcuse, *Principles of Optical Fiber Measurement*, Academic Press (New York), 1981

J. E. Midwinter, *Optical Fibers for Transmission*, John Wiley and Sons (New York), 1979

S. D. Personick, *Optical Fiber Transmission Systems*, Plenum Press (New York), 1981

A. W. Snyder and J. D. Love, *Optical Waveguide Theory*, Chapman and Hall (New York), 1983

S. M. Sze, *Physics of Semiconductor Devices*, John Wiley & Sons (New York), 1969

S. K. Yao and C. K. Asawa, "Fiber optic intensity sensors," IEEE Journal on Selected Areas in Communications *SAC-1*, 562 (1983), and references there-in.

Projects in Fiber Optics (FKP-STD)
Equipment List

Model #	Description	Qty.
B-1	Base	2
BS-05	Kit, thumbscrew, 1/4-20	1
CA-2	Clamp, universal	2
F-506B	Coupler, directional, SM	1
F-916	Coupler, fiber, w/o lens	1
F-925	Coupler, fiber, GRIN-lens	2
F-CA-001	Adapter, in-line	5
F-CC-140	Connector halves, (for F-MLD)	10
F-CL1	Cleaver, fiber	1
F-IRC1	Card, IR phosphor	1
F-MLD-50	Fiber, 100/140 MM, 50 m	1
F-MLD-500	Fiber, 100/140 MM, 500 m	1
F-SK-C	Fixture, splice	1
F-SK-S	Splice, fiber, 10 count	1
F-SPV-10	Fiber, pol.-preserving, 10 m	1
F-SS-20	Fiber, 8/125 SM, 20 m	1
F-SV-20	Fiber, 4/125 SM, 20 m	1
F-TK1E	Epoxy, 20 pkgs.	1
F-TK1L	Lapping Sheets, 160 count	1
F-TK1P	Fixture, polishing	1
FK-BLX	Set, balldriver	1
FK-BSC	Cube, beamsplitter	1
FK-BTC	Coupler, biconical, MM	1
FK-DET	Assy., detector	2
FK-DRV	Driver, ILD-LED, + laser	1
FK-GR25F	Lens, GRIN, w/ filter (2 count)	1
FK-GR25P	Lens, GRIN, w/o filter (2 count)	2
FK-GR29	Lens, GRIN, 0.29-pitch (2 count)	1
FK-GT	Transducer, glass	2
FK-LED	Assy., light-emitting diode	1
FK-LS	Assy., sensor, liquid-level	1
FK-MUX	Base, assy., multiplexer	2
FK-POL	Polarizer, sheet	1
FK-PS	Base, assy., pressure sensor	1
FK-SPKR	Speaker, output	2
FK-TAPE	Tape deck, multiplexer	2
FM-1	Mode scrambler, fiber optic	1
FP-1	Positioner, fiber	4
FPH-S	Chuck, fiber	2
XSN-22	Breadboard, 2x2	1
M-20X	Lens, objective, 20x	1
M-40X	Lens, objective, 40x	1
MH-2PM	Holder, lens, objective	4
MM-1	Mount, mirror	1
MPC	Collar	3
MPH-1	Holder, micro-series	1
MSP-1	Post, micro-series	1
RSX-2	Stage, rotation	1
SK-08	Kit, screw, 8-32	1
SK-25	Kit, screw, 1/4-20	1
SP-2	Post	12
SP-3	Post	2
U-1301P	Laser, HeNe, 1 mw, polarized	1
VPH-2	Holder, post	12
340C	Clamp	1
41	Rod, short	1
421-0.5	Stage, translation	1
777-1	Bundle, fiber, bifurcated	1
807	Mount, laser	1
815	Meter, power	1
FKP-TEXT	Applications Handbook	1

Options

F-ML1	Microscope, inspection	1
FP3-FH1	Adapter, bare fiber (for F-ML1)	1
FP3-FPH	Adapter, fiber chuck (for F-ML1)	1
FP3-CA3	Adapter, SMA (for F-ML1)	1
F-BK2	Breaker, fiber	1

NOTE: Model numbers with FK-prefix are available only with Projects in Fiber Optics. They are not listed in Newport's General Catalog.

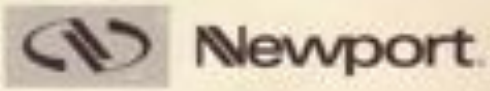

U.S. Headquarters:
Newport Corporation
P.O. Box 8020 / 18235 Mt. Baldy Circle
Fountain Valley, CA 92728-8020
Telephone: 714-963-0811
Facsimile: 714-963-2013

European Headquarters:
Federal Republic of Germany
Newport GmbH
Telephone: 06151-1540
Facsimile: 06151-15450

United Kingdom:
Newport Ltd
Telephone: 0583-398995
Facsimile: 0583-762035

Switzerland:
Newport Instruments AG
Telephone: 01-740-2203
Facsimile: 01-740-2205

Netherlands:
Newport B.V.
Telephone: 03402-50588
Facsimile: 03402-50577

Canada:
Newport Instruments Canada
Telephone: 416-567-0399
Facsimile: 416-567-0302

Japan:
K. K. Newport
Telephone: 06-359-0270
Facsimile: 06-359-0280